
# The Energy Yield Impacts of Wind Farm Design and Location

A Thesis Submitted for the Degree of Doctor of Philosophy

by

**Danial Gavin Sturge**

The University of Sheffield
Department of Mechanical Engineering
August 2015

# SUMMARY

It is notoriously difficult to improve the accuracy of predicting energy yield for wind farms due to the balance between computational power, time, and accuracy. This is a real world problem for wind farm developers, society, and the environment, because it leads to less than optimal energy yield from a site and may lead to some sites not being developed. This thesis addresses this problem by experimenting with the development of a new hybrid computational fluid dynamics approach to wind farm design based on combining established engineering theory. Actuator disc theory used for replicating the far wake of a wind turbine is validated using wind tunnel experiments and computational fluid dynamics simulations. The technique is then combined with a high fidelity full rotor model to produce a novel hybrid methodology for efficiently analysing wind turbine performance while in the wake of another. Using the new hybrid technique a set of reference cases was completed to produce an understanding of how the layout of multiple wind turbines affects performance. The wider contribution to engineering is that detailed turbine blade analysis while in the wake of another wind turbine is possible without having to intrinsically model multiple high fidelity rotors, which reduces computational cost and time.

A novel feature of the PhD was to develop the theoretical method with an understanding of the importance of real-world application. This was gained through investigation of the approach currently taken by wind farm developers and the ways in which better information about siting decisions might work with the details of the planning consent regime. Using the knowledge gained from studying energy policy and the computer simulated reference cases, a case study was performed on an existing wind farm. Suggestions are made to improve the power output from the site and a discussion of the potential policy implications of the results are considered. Improved predictive capacity can lead to significant improvements in a context where the location of wind turbines is fixed in planning consent. The Blackstone Edge wind farm case study reveals that marginal changes in wind turbine siting as a result of novel simulation techniques yielded a 3% improvement in energy yield, which equates to an increase of over 600 MWh or £55,000 per year.

# DECLARATION

Described in this thesis is work performed in the Department of Mechanical Engineering, the University of Sheffield between October 2012 and August 2015. I hereby declare that no part of this work has been submitted as an exercise for a degree at this or any other university. This thesis is entirely the result of my own work and includes nothing which is the outcome of collaboration, except when stated otherwise. This thesis contains 96 figures and approximately 38,000 words.

Danial Sturge

# ACKNOWLEDGEMENTS

Firstly, I would like to begin by thanking my supervisors, Dr. Rob Howell and Dr. Aidan While. Rob offered and convinced me to do the PhD and has since provided the enthusiasm, guidance, and availability for a chat whenever I have needed it. Aidan opened up a new world of academia and has never failed to be patient with explaining complex social science ideas to a simple engineer.

Next I must thank my mother Noni, my father Gavin, and my little sister Natasha, for without their love and support I would not be where I am today. I am particularly appreciative of my fiancé Liz, who has had to endure my daily ramblings about wind turbines, aerodynamics, CFD, and energy policy. Despite the 8 hour time difference and the 5000 miles distance between us, I've always felt that I could share the ups and downs throughout my PhD.

I'd also like to thank my fellow PhDers who have been both teachers and friends to me. Special thanks go to Oke for teaching me how to use the wind tunnel, Jason and Dorit for going above and beyond in helping me develop my CFD skills, Jon for being the other guy who isn't just an engineer, and the rest of the Howell group for sharing ideas, knowledge and lunches at Fagan's.

Finally, I would like to acknowledge the WindNet research group for the project and funding, and Infinis for providing expertise and data.

*Dedicated to the ones I love, for without them I would not be who I am today.*

# NOMENCLATURE

## Symbol

| | |
|---|---|
| $A$ | Axial induction factor, coefficient for atmospheric stability |
| $A$ | Rotor area, hot-wire anemometry constant 1 |
| $B$ | Hot-wire anemometry constant 2 |
| $c$ | Blade chord length |
| $CP$ | Power coefficient |
| $CT$ | Torque coefficient |
| $C_p$ | Pressure coefficient |
| $CT_h$ | Thrust coefficient |
| $D$ | Turbine diameter |
| $F_D$ | Drag force |
| $F_L$ | Lift force |
| $F_z$ | Axial force |
| $F_\theta$ | Tangential force |
| $\dot{m}$ | Mass flow rate |
| $n$ | Hot-wire anemometry constant 3 |
| $p$ | Pressure |
| $p_{atm}$ | Atmospheric pressure |
| $P$ | Power |
| $P_{max}$ | Maximum available power |
| $R$ | Turbine rotor radius |
| $Re$ | Reynolds number |
| $s$ | Seconds |
| $t$ | Time |
| $T$ | Torque |
| $T_h$ | Thrust |
| $T_{ab}$ | Absolute temperature |
| $T_u$ | Turbulence intensity |
| $r, \theta, z$ | Polar coordinates |
| $u$ | Velocity at the actuator disc |
| $u_1$ | Far wake velocity |
| $U$ | Wind speed |
| $U_r$ | Reference velocity |
| $V$ | Velocity, hot-wire voltage |
| $V_o$ | Undisturbed freestream velocity |
| $V_{rel}$ | Relative velocity |
| $W$ | Induced velocity |
| $W_z$ | Induced axial velocity |
| $W_\theta$ | Induced tangential velocity |
| $x, y, z$ | Cartesian coordinates |
| $Y^+$ | Dimensionless wall distance |

| | |
|---|---|
| $Z$ | Height |
| $Z_r$ | Reference height |

## Greek Symbol

| | |
|---|---|
| $\alpha$ | Angle of attack |
| $\gamma$ | Pitch angle |
| $\lambda$ | Tip speed ratio |
| $\mu$ | Dynamic viscosity |
| $\rho$ | Density |
| $\phi$ | Flow angle |
| $\omega$ | Angular velocity |

## Abbreviations

| | |
|---|---|
| ABL | Atmospheric Boundary Layer |
| AD | Actuator Disc |
| AL | Actuator Line |
| AS | Actuator Surface |
| AoA | Angle of Attack |
| BEM | Blade Element Momentum |
| CFD | Computational Fluid Dynamics |
| DECC | Department for Energy and Climate Change |
| DES | Detached Eddy Simulations |
| DNS | Direct Numerical Simulations |
| EIA | Environmental Impact Analysis |
| FiT | Feed in Tariff |
| FSI | Fluid Structure Interaction |
| GIS | Geographical Information System |
| HAWT | Horizontal Axis Wind Turbine |
| LES | Large Eddy Simulation |
| NPPF | National Planning Police Framework |
| PIV | Particle Image Velocimetry |
| PPS | Planning Policy Statement |
| RANS | Reynolds Averaged Navier-Stokes |
| STL | Stereolithography |
| TSR | Tip Speed Ratio |
| UDF | User Defined Function |
| WT | Wind Turbine |

# CONTENTS

# LIST OF FIGURES

# LIST OF TABLES

# 1 INTRODUCTION

## 1.1 Energy Security

From the perspective of the UK, renewable energy is important for energy security. 57% of the fuel for power stations and nuclear power plants is imported [1] from places such as Australia, Canada, South America, Middle East, USA, Poland, and Russia. Many of these countries are politically sensitive and result in a risk of reduced supply and fluctuations of fuel prices. Even if the UK were to extract fossil fuels from its own territories, the fact is that supply is finite and the long-term financial and environmental cost is high. As the UK has reportedly the best onshore and offshore wind energy resource in Europe [2] there is interest in the potential for renewable energy generation from wind.

## 1.2 Wind Energy

Humans have harnessed the wind for thousands of years for propelling ships, grinding grain, pumping water and more recently, generating electricity. There is debate about who should be credited for first using wind to produce electricity, either an American named Charles F. Brush or a Scottish Academic, Professor James Blyth [3]. Both experimented with wind-powered machines in 1887, marking the start of electricity generation using the wind. Arguably, Brush's windmill (Figure 1.1) was more sophisticated with a 17 m diameter rotor and rated at 12 kW, but all windmills from this period to what we now know as wind turbines use the same principle of lift to provide rotational energy to generate electricity.

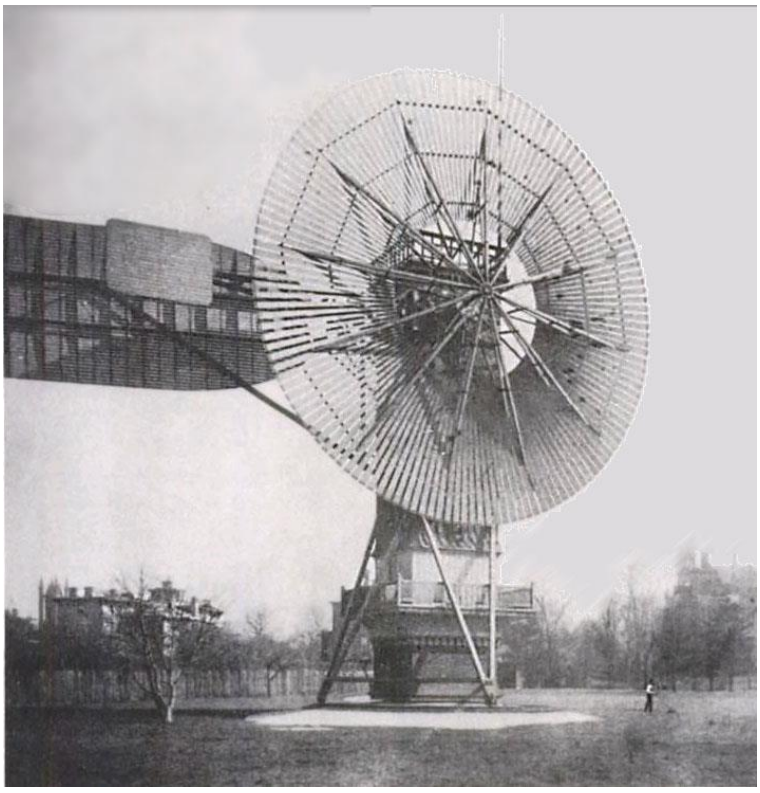

**Figure 1.1 Charles F. Brush's wind turbine built in 1888, from** [4]

The maximum available energy in the wind, $P_{max}$, can be obtained if the wind speed could be theoretically reduced to zero [5] using the following equation:

$$P_{max} = \frac{1}{2}\rho A V_o^3 \quad (1.1)$$

Where $\rho$ is the density of air, $V_o$ is the wind speed and $A$ the area of the wind turbine rotor. This reveals that the available power in the wind increases cubically with wind speed and linearly with density and area, which means that a small rise in wind speed yields a large power increase. However, as reducing the wind speed to zero is only theoretical, therefore, a ratio between power obtained and the theoretical maximum available in the form of a power coefficient, CP, is used. There is a theoretical limit of CP known as the Betz limit, CP = 0.593 [6] and modern wind turbines have been optimised to a point of operating with a CP up to 0.5 [5].

**The Wind Turbine**

A wind turbine uses the kinetic energy in the wind to produce lift along the blades; this process converts that energy into mechanical energy and in turn rotates the shaft. The shaft goes into a gearbox, which increases the rotational speed where a generator converts the rotational energy into electrical energy. Over recent decades wind turbines have increased in size, during the 1980s small rotor diameters of around 20 m were prevalent and were rated at 50 kW. Today, wind turbines can have rotors over 160 m in diameter and currently are rated up to 8 MW. Figure 1.2 illustrates all the major components of a wind turbine; below is a brief description of each part:

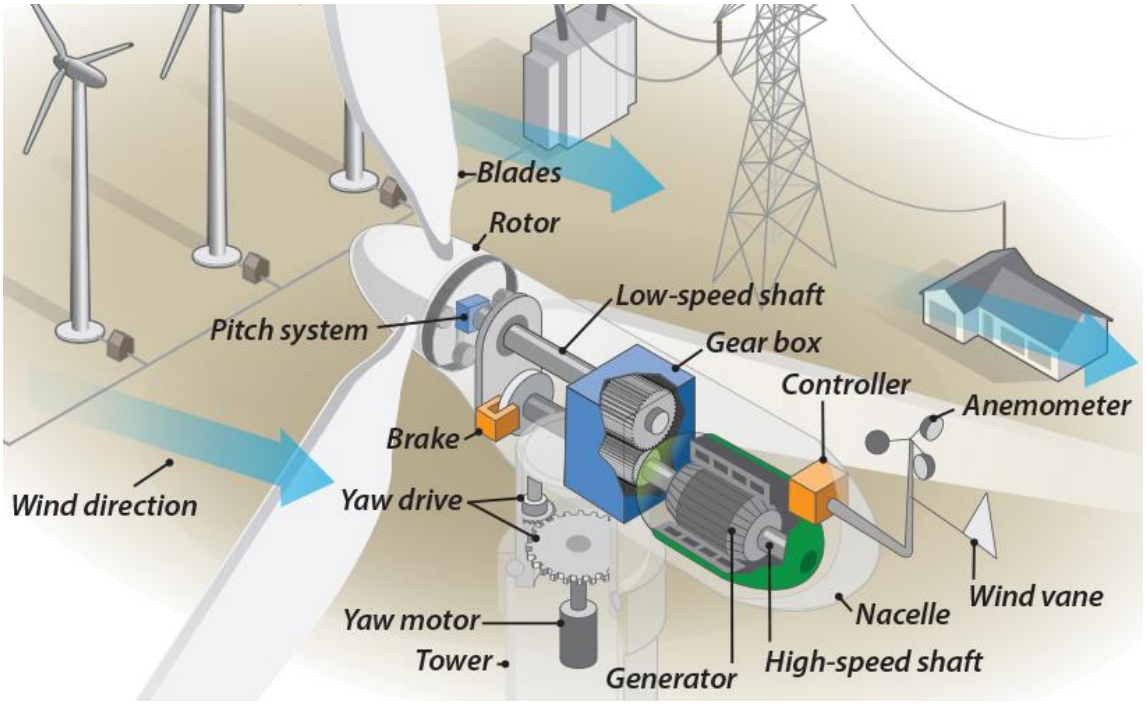


Figure 1.2 The components of a wind turbine, reproduced from [7]

- Anemometer – measures the wind speed, which is recorded and relayed to the controller.
- Blades – when air moves over the blades it produces lift causing them to rotate.
- Brake – used in emergencies to stop the rotor from continuing to spin.
- Controller – controls the pitch of the blades, which can be used to optimise the relative angle of attack, or to start up the machine and shut it off depending upon operating wind speeds.
- Gearbox – this connects the low-speed shaft to the high-speed shaft, increasing the rotational speed that is required by the generator to produce electricity.
- Generator – converts the mechanical energy from the gearbox to electrical energy.
- Nacelle – this is located at the top of the tower behind the rotor and is used to house all the equipment required for a wind turbine to run.
- Pitch system – the blades are angled for optimal angle of attack.

- Rotor – the hub and blades are collectively known as the rotor and this is connected to the nacelle.
- Tower – a hollow structure that the nacelle and rotor sits on, which also allows access to the major components for maintenance.
- Wind vane – measures the wind direction.
- Yaw drive – using the measured wind direction from the wind vane, the wind turbine is orientated to face the prevailing wind direction for maximum efficiency.
- Yaw motor – used to power the yaw drive.

The description above is a representation of the features found on most horizontal axis wind turbines (HAWT), but systems vary and are optimised according to the conditions they are designed for. A wind farm is a collection of wind turbines in relatively near proximity to one another, which introduce further design constraints due to potential turbine-turbine wake interactions.

## 1.3 Regulation of Onshore Wind Locations

The requirement for sustainable renewable energy sources as a move to replacing fossil fuels has become an important aspect of energy policies in many of the world's governments with at least 144 countries, with renewable energy targets [8]. As of 2012 renewable energy provided an estimated 19% of the global final energy consumption and continues to grow each year. Modern renewables account for 10% of the total, including wind energy which has added more capacity than other forms of renewable energy in recent years [8].

Increased pressure to reduce greenhouse gas emissions and investment returns has led to growing interest in optimising energy yield from wind turbines prior to

development [9]. Whilst the likely yield of a single turbine can be predicted with sufficient accuracy by using prior experience and wind measurements, anticipating the cumulative impact of multiple wind turbines in a wind farm is more complicated. This is because of the complex aerodynamic interactions between wind turbines due to disturbance of the flow in the wake of a rotor. In order to maximise the power output from a given site, the majority of developments are in farms of more than one turbine in relatively close proximity to one another. However, predicting and optimising layouts is complicated due to the detailed understanding of turbine-turbine aerodynamics required. Currently, approximations have to be made to reduce cost and time of simulation of multiple layouts, these include limiting the level of detailed included in aerodynamic simulations and choosing the prevailing wind direction as an overriding factor rather than considering all directions equally.

The importance of being able to calculate energy yield prior to development is also important in the context of UK policy and regulation of wind farms [10]. First, siting decisions have been strongly opposed by local residents and influential groups of national politicians predominantly because of the visual impact on the landscape. Under the land-use planning system the precise location of each turbine needs to be identified at the point of the planning application. Allowing for flexibility in siting post-development is not allowed, partly because it might have led to a different outcome in the granting of planning consent. Informed decisions to optimise energy yield are important for developers given the regulatory context. Moreover, there are provisions in both Environmental Impact Assessment and land-use planning for decisions to take into account the environmental benefits of renewable generation as material considerations when weighing up the positive and negative impacts of wind

farms. Although the energy yield of a wind farm has tended to be given limited weight in decision making, it is possible that it could be of more significance in the future.

However, despite the technological advances surrounding wind energy there is still often public backlash against such developments; a result of which has led to an unpredictable planning process and reduction in potential energy yield.

Wind developments are often contested in the UK, the following summarises the key reasons for rejected planning approval:

**Visual Impact**

The most prominent reason for developers failing to gain planning permission for siting wind turbines in their ideal locations is that of the visual impact it has on its surroundings. The 'visual impact' itself can take a number of forms, be it diminishing the visual dominance of a local landmark, undermining the character of the landscape or causing harm to the setting of historic instalments [11]. There is no statutory minimum distance separation between turbines and dwellings in the UK and merely a guidance of 2 km and 0.5 km in Scotland and Wales, respectively and so making it a very subjective issue [12]. Residents may argue that the value of their property will fall if a wind turbine is erected within sight; however, there is no evidence for this in the UK. A study carried out in the United States of America even suggests the polar opposite and states that property prices within a five mile radius of a wind farm actually increase above the regional average [13]. The shadow that is cast by the moving blades causes an effect, called shadow flicker, which may also determine where wind turbines are sited.

**Noise**

Noise is the second largest cause for contention, however, it affects less people as sound from the wind turbines can only travel so far before being lost in the background noise of everyday life. The noises experienced by affected residents are described as, “doof-doof”, “whooshing”, a jet rumble and the sound of a generator [14]. There is guidance on noise levels that state the sound a wind farm makes should not exceed 5 dB above of the background noise for both day and night time and a fixed limit of 43 dB is recommended for night [12]. However, background noise varies depending on location making the acceptable noise levels difficult to standardise [15].

**Ecological Effect**

A less common reason for dismissal is the effect a wind turbine or farm may have on the ecology of its surrounding areas. Most dismissals linked to ecological impacts are for the fear of the detrimental impact it will have on local bat populations and bird migrations, however, the National Wind Coordinating Collaborative concluded that these impacts are relatively low and do not pose a threat to species [16].

**Health and Safety**

The most controversial of all the categories revolves around health and safety. Despite the high level of safety that manufactures abide by, there is still much dispute surrounding the safety risks that wind turbines impose. Issues such as ice build-up on the blades and reports of sheets flying off [17] are one of the main concerns that opposition has. There have been reported incidents of blades flying off [18] and generators catching fire [19] when the brakes fail and consequently the turbine is allowed to spin freely. Shadow flicker which is caused by the sun casting a shadow of the rotating blades, can affect nearby residents and in some cases cause headaches and

other health related issues. “Wind turbine syndrome” is an on-going debate between ‘sufferers’ and professionals. Symptoms exhibited are similar to those seen in the general population as a result of daily stresses and come in the form of headaches, insomnia etc. As of 2012 there have been ten independent reviews on the evidence of the effect wind farms have on health; all have come back with the same findings stating that the perceived stress is simply annoyance and it is not a recognised disease. An expert panel carried out the most comprehensive of these reviews in 2009 [20] and found that the annoyance experienced is linked more with the psychological effect that a wind farm has on a person above the sound produced. This is especially the case when the media coverage is particularly negative and the power of suggestion increases anxiety above rational levels.

Much of the above is very much subjective (visual and noise impacts) and in many cases, such as “wind turbine syndrome”, heavily disputed by experts [20]. Others like failure are rare and often exaggerated by the media. Nonetheless, energy policy and the planning process place these as priorities above power generation, but how does this affect the economic viability of wind developments?

## 1.4 Multidisciplinary Research Objectives

A multidisciplinary approach to research allows for a more holistic understanding of the engineering and social aspects that are indicative of wind energy developments (Figure 1.3). As will be discussed, there is a vast amount of knowledge and research on the utilising wind energy, especially in aerodynamics. However, the cohesion between the technical knowledge and its use by developers and application in wind farms is currently limited by the energy policy [9] and developers not maximising the energy generating potential of sites because of the limitations of the planning process.

Using mixed-methods from mechanical engineering and social science disciplines, there are three primary research objectives:

1. To research the effect of wind turbine placement on performance due to wake interactions.
2. To develop a novel technique that can benefit developers and regulators using wind tunnel experiments and computational fluid dynamics (CFD) simulations that offer greater accuracy of aerodynamic interactions between wind turbines in a farm situation.
3. To highlight potential areas of improvement in terms of energy policy by investigating where improved energy yield assessment might help support better decision making from developers and also in the planning consent regime.

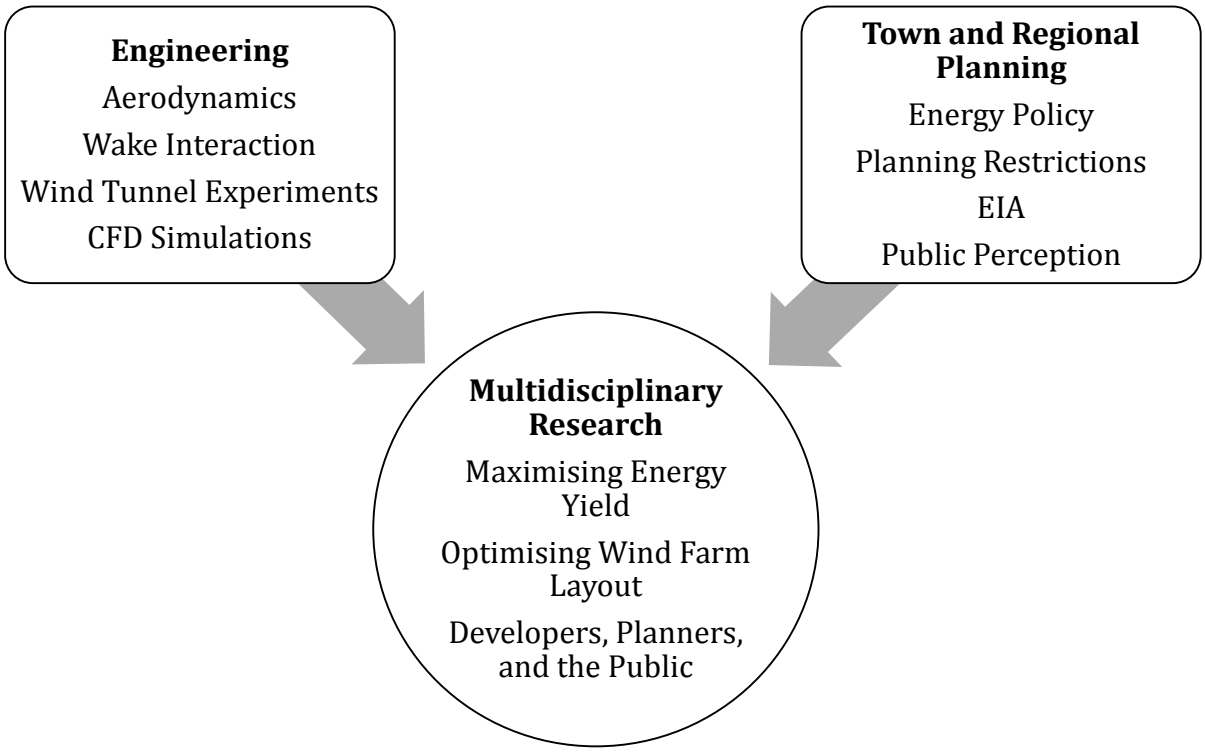


**Figure 1.3 A multidisciplinary approach to research.**

## 1.5 Thesis Outline

The thesis is divided into eight chapters; a brief summary of each is given below:

Chapter 1 has introduced the need for renewable energy, provided an account of the history of wind energy, and highlighted the necessity for a multidisciplinary approach to research.

Chapter 2 presents a current state of the art literature review in the field of horizontal axis wind turbines. The aerodynamics fundamentals of individual wind turbines and wind farms are provided to provide the background theory for this thesis. Modelling techniques, both experimental and numerical, along with the research that applies them are reviewed in order to inform potential areas for improvement in this body of research.

Chapter 3 puts into context the current energy policy in the UK in relation to wind energy. The planning process is investigated to determine how the priorities in determining approval for wind developments affect viability. Developer interaction is touched on by outlining the development process and potential difficulties met. Introducing the 'engineering dimension' into the procedure and drawing on international comparisons opens up areas requiring improvement.

Chapter 4 outlines the experimental methods used for validating the actuator disc theory for use in computational fluid dynamics (CFD) simulations. It then details the development of various numerical models; beginning with the validation of the actuator disc technique using data from the wind tunnel experiments. A full rotor model is introduced and a hybrid technique, which combines it and the actuator disc method is described and validated.

Chapter 5 analyses the results of a set of reference cases that have been simulated in CFD using the techniques developed in Chapter 4. The reference cases begin with an ideal situation in which a wind turbine is simulated in undisturbed air for which all other cases can be compared to. A set of turbine-turbine interactions are modelled and simulated at a range of distances apart and offset locations, these are then analysed to determine aerodynamic characteristics often found in wind farms.

Chapter 6 investigates, through the use of a case study, the potential changes that can be made to a current wind farm in order to improve its energy yield. The suggestions are solely based on engineering knowledge gained from Chapter 6 and aerodynamic understanding of wind turbines, terrain, and the atmospheric boundary layer (ABL).

Chapter 7 discusses the implications of Chapter 6 on the developer, planners and, the general public involved. As well as how policy change and better informing the public can be beneficial for wind energy developments.

Chapter 8 describes the conclusions from the analysis of wind turbine assessment during the planning process, the simulations, and case study suggestions and implications conducted in the thesis. Finally, suggestions for further work as a result of this research are identified.

## 1.6 Publications

During the course of the research in this thesis, various aspects have been published in journals. The following is a list of journal articles co-written by the author in chronological order:

D. Sturge, A. While, and R. Howell, “Engineering and energy yield: The missing dimension of wind turbine assessment,” *Energy Policy*, vol. 65, pp. 245–250, Nov. 2014.

C.R. Jones, E. Lange, J. King, A. Tsuchiya, R. Howell, A. While, R.J. Crisp, J. Steel, K. Meade, F. Qu, D. Sturge, and A. Bray, “WindNet: Improving the impact assessment of wind power projects,” *AIMS Energy*, vol. 2(4), pp. 461-484, Dec. 2014.

D. Sturge, D. Sobotta, R. Howell A. While, and J. Lou, “A hybrid actuator disc – Full rotor CFD methodology for modelling the effect of wind turbine wake interactions on performance,” *Renewable Energy*, vol. 80, pp. 525-537, Aug. 2015.

# 2 LITERATURE REVIEW

## 2.1 Introduction

The aim of this chapter is to help form the direction of this thesis and place the research presented into perspective by examining the relevant literature. The aerodynamics of horizontal axis wind turbines (HAWT) and its research are extensive. The following literature review identifies those aspects of HAWT aerodynamics that are relevant to the aims of the thesis, but is predominantly focused on wind farms with respect to the aerodynamic interactions between individual wind turbines and the effects terrain and layout have on energy yield.

## 2.2 Fundamental Aerodynamics

To begin the literature review, the fundamentals of wind turbine aerodynamics are established in order to form a strong foundation of knowledge for the complex aspects of turbine-turbine interactions.

### 2.2.1 Aerofoil Flow Physics

**Lift**

An aerofoil designed for use on a wind turbine has the sole purpose of generating lift. Figure 2.1 is a simple schematic of the streamlines around the simplest form of aerofoil, which is a curved plate. Beyond the region represented within the figure the streamlines are straight and horizontal because at this point the air is undisturbed. Following the line from A to B the streamlines become curved representing a pressure gradient, in this case the pressure drops while moving towards the surface. Similarly, observing the change in curvature along the streamlines from C to D there is seen a pressure increase towards the surface. Therefore, the pressure at D is greater than at B, and this generates a resultant pressure force acting upwards known as lift.

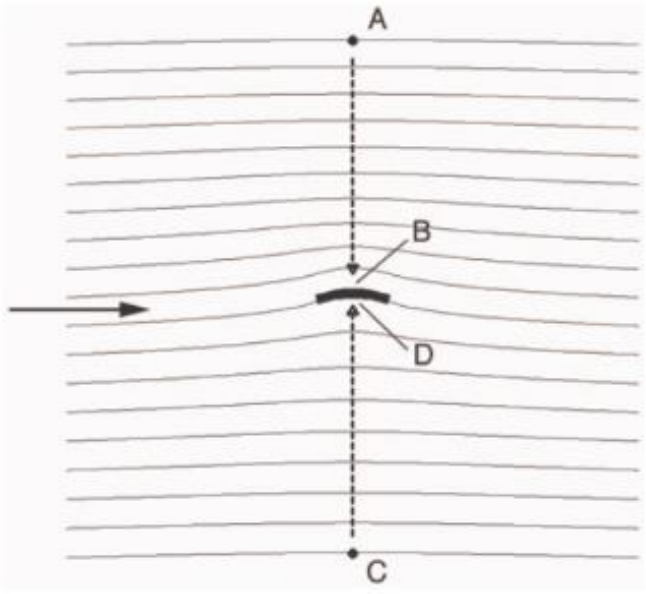


**Figure 2.1 Streamlines around a lifting curved plate representing an aerofoil, from** [21]

**Drag**

The opposite to lift is drag, which is the force that opposes the forward motion of the aerofoil. Induced drag is the result of when an aerofoil generates lift and forms

trailing edge vortices, this type of drag increase with an increase in the angle of attack (AoA). Form drag which is caused by the movement of the aerofoil through the air and is linked to the shape of the aerofoil, this results in a wake behind the aerofoil due to turbulence and opposes the forward motion. There is also skin friction caused by viscous drag in the boundary layer around the aerofoil.

**Boundary Layer**

Figure 2.2 illustrates the air flow over an aerofoil, the flow will form a laminar boundary layer at the leading edge and eventually this will transition to a turbulent boundary layer as it thickens and becomes less stable along the surface. A laminar flow occurs when the fluid flows with distinct parallel layers. At low velocities these layers do not often mix, resulting in smooth streamlines and high momentum diffusion, which means that the drag caused by skin friction is low. A turbulent boundary layer has no slip at the surface and the total thickness is greater when compared to laminar. Toward the trailing edge the flow stalls and separates due to the increasing thickness of the boundary layer and formation of adverse pressure gradients. This is the beginning of the wake forming behind the aerofoil which is detrimental for the production of lift (discussed further in Section 2.4.1).

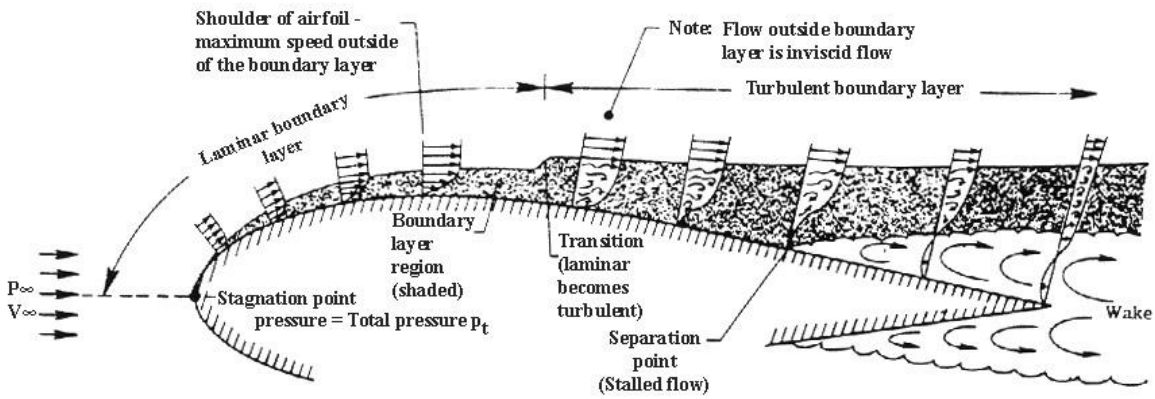


**Figure 2.2 An example of the flow and boundary layer along an aerofoil,** [22].

### 2.2.2 Reynolds Number

Reynolds number is a dimensionless number that describes the ratio of inertial to viscous forces within a fluid. The Reynolds number is key but not absolute in determining whether the flow is laminar or turbulent. In general, laminar flow occurs at low Reynolds numbers where the viscous forces dominate and turbulent flow is seen at higher numbers because of prevailing inertial forces. The ratio of Reynolds number, *Re*, is given as the following [23]:

$$Re = \frac{\rho U L}{\mu} \tag{2.1}$$

Where $\rho$ is the density of the fluid, U is the wind speed and μ is the dynamic viscosity of the fluid. L is the characteristic length and is chosen based on what the flow is moving over, for example the chord length of an aerofoil or the diameter of a wind turbine rotor. The Reynolds number also allows for the ability to perform scaling of fluids by determining dynamic similitude between different cases of fluid flow. This is particularly useful when it comes to designing experiments as there is no wind tunnel that can house, for example, a full size 100 m tall 2.5 MW wind turbine. This is discussed further in Section 2.5.2.

## 2.3 Main Features of HAWT Operation

Research into the area of HAWT aerodynamics gained momentum in 1920 with the publication of the Betz limit [24]. This set a precedent for the field of wind turbine aerodynamics with the discovery that, theoretically, no more than 59.3% of the kinetic energy of a fluid contained in a stream tube with the same cross sectional area as a rotor disc may be converted into useful work. Since then the aerodynamics of wind turbines

have been studied extensively and Vermeer et al. [25] suggests that the efficiency has improved from 40% to 50%.

**Solidity**

Due to the limitation of available power in the wind an increase in the number of blades means that each one is able to extract less kinetic energy. The solidity is the total blade area as a fraction of the total swept disc area, and in order to optimise the solidity for a given tip speed, the more blades a wind turbine has the narrower each must be. Three blades are common for large wind turbines, which is a fine balance between structural integrity, cost, turbine stability, aerodynamic efficiency, and aesthetics.

**Aerodynamic Blade Forces**

The diagram presented in Figure 2.3 shows the velocity and force vectors acting on a cross-sectional aerofoil element of a wind turbine blade at radius (r) in the ($\theta$,$z$) plane. The relative velocity ($V_{rel}$) to the element is determined using velocity triangles such as:

$$V_{rel}^2 = (V_o - W_z)^2 + (\omega + W_\theta)^2 \quad (2.2)$$

Where ω is the angular velocity. The flow angle (ϕ) between $V_{rel}$ and the rotor plane is given by:

$$\phi = \tan^{-1}\left(\frac{V_o - W_z}{\omega + W_\theta}\right) \quad (2.3)$$

The force per span wise unit length is defined as the vector sum $F_{Total} = F_L + F_D$. This results in the components of the axial and tangential force per unit span:

$$F_z = L\cos\phi + D\sin\phi \quad (2.4)$$

$$F_\theta = L\sin\phi - D\cos\phi$$

The blade forces balance the momentim changes in the axial and tangential directions, therefore the torque (T) is:

$$T = F_\theta r \Delta r \tag{2.5}$$

Where $r$ is the difference in streamsurface radii.

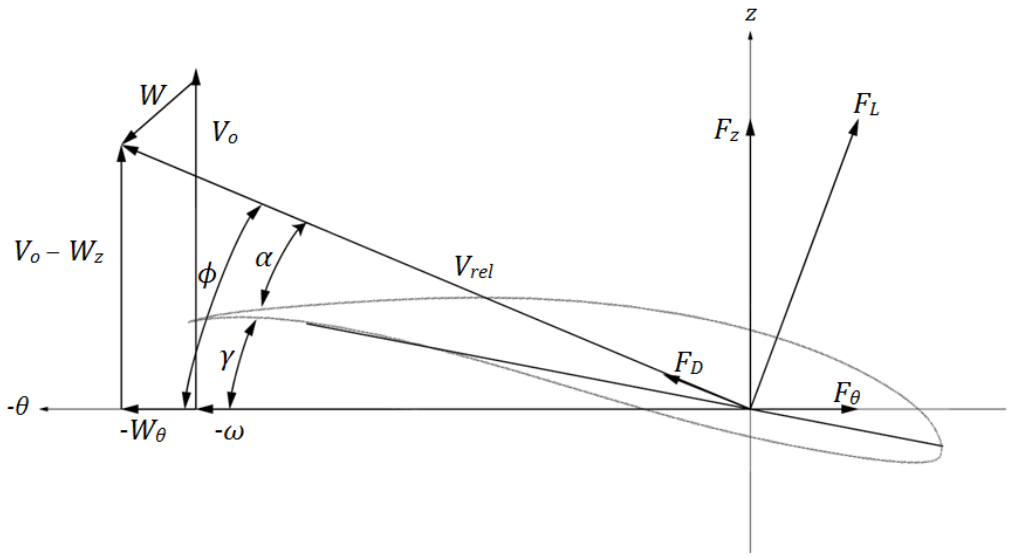


Figure 2.3 Cross-sectional aerofoil element showing the velocity and force vectors.

A wind turbine blade divided into elements will result in each of the elements experiencing a slightly different flow due to their unique: angular velocity (ω), chord length (c), and local pitch angle (γ). These elements can be used to provide a model for a complete wind turbine blade through the use of the blade element momentum method (BEM). The local forces on the wind turbine blade are calculated and combined with momentum theory (or actuator disc theory) so that it is possible to account for the induced velocities that result from the angular momentum of a rotor. It is still the most used aerodynamic model for wind turbines due to its efficient use of computational power, however, it requires accurate tabulated aerofoil data [26].

**Power and Tip Speed Ratio**

The tip speed ratio (λ or TSR) is the ratio between the tangential speed of the tip of the blade and the velocity of the wind:

$$\lambda = \frac{\omega R}{V} \tag{2.6}$$

TSR is used to determine the most efficient rotational speed of a wind turbine to maximise power output. While a blade of a wind turbine rotates through the air, as seen by the blade, the wind is approaching from a different direction, known as relative wind or velocity (Figure 2.4). If the wind speed, for example, increases while the rotor's rotational speed remains constant, then this relative wind direction vector moves toward the true wind direction. The result of this is that the effective angle of attack (AoA) also changes, and in order to optimise the turbine's performance the TSR must remain constant for a given Reynolds number. In order to keep the AoA optimised along the length of the blade, a twist must be introduced, because the tip of the blade is moving through the air faster than towards the root.

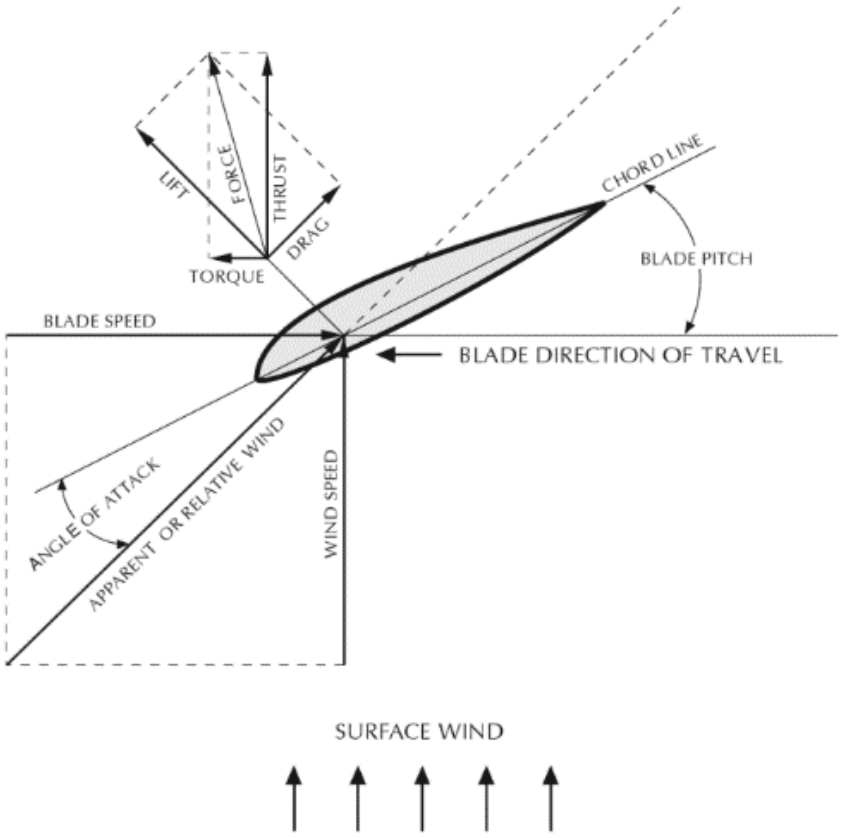


**Figure 2.4 Relative wind and the resulting angle of attack, from** [27].

The coefficient of power (CP) is extremely useful in wind turbine aerodynamics as it provides a non-dimensional measure of performance:

$$CP = \frac{P}{\frac{1}{2}\rho A V^3} \tag{2.7}$$

Plotting CP against TSR describes the performance of a wind turbine at varying rotational speeds and allows for the optimal conditions to be determined for a particular wind speed. In the example shown in Figure 2.5 the optimal TSR is seen to be around 6, up to this point as the rotational speed of the wind turbine increases so does the CP. However, after it peaks at TSR = 6, the increasing rotational speed will result in a reduction of CP and thus it is crucial that a wind turbine is kept within its most efficient TSR region so as to maximise the power extraction from the wind.

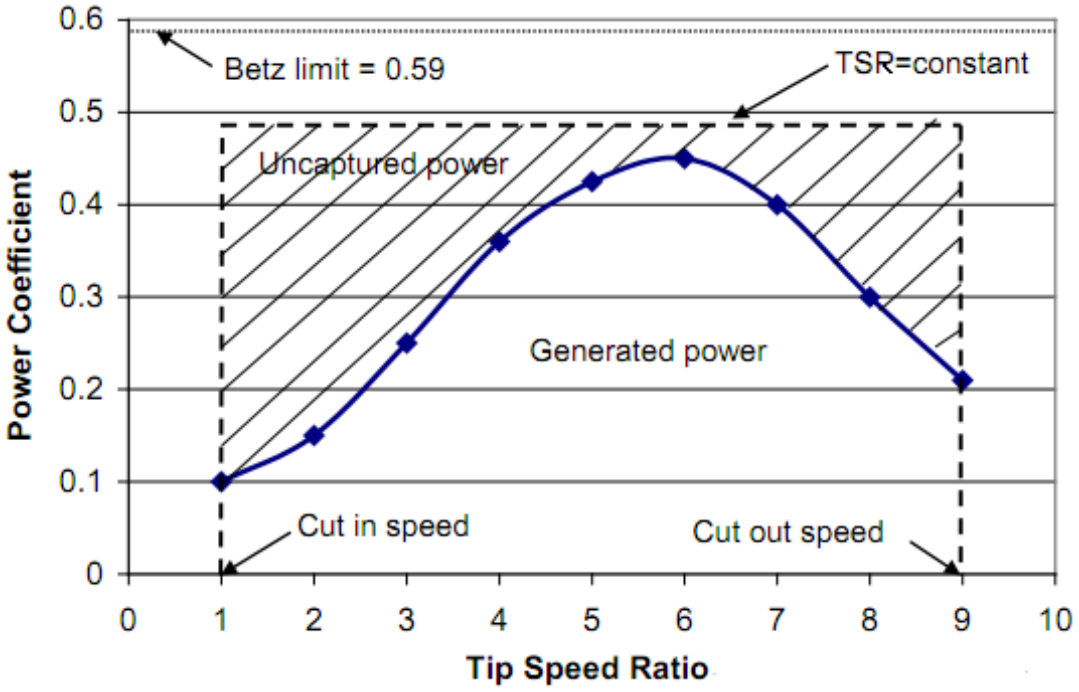


**Figure 2.5 An example of a power coefficient vs. tip speed ratio curve, from** [28].

The aerodynamics of the individual blades is still a key research area for wind energy. Optimising the shape of the blade to maximise the power production must be finely balanced with producing a product that can survive the 25-year life span expected for a wind turbine. There are two aspects to wind turbine blade aerodynamics [29], when at zero to low yaw angles, lift production determines design. Conversely, at moderate to high yaw angles, blade aerodynamics is dominated by dynamic stall.

**Dynamic Stall**

Stall occurs when the critical angle of attack of an airfoil is exceeded, which results in the flow separation regions on the blade to increase in size and impede the ability for the aerofoil to produce life. Conversely, dynamic stall occurs when an aerofoil rapidly changes the angles of attack, causing a subsequent unsteady boundary layer separation [30]. This occurs in the presence of an adverse pressure gradient where the velocity of the boundary layer falls to zero before reversing at which point the flow

detaches from the surface. Laminar flow is particularly susceptible to adverse pressure gradients due to high momentum diffusion. The flow on the surface has zero velocity, known as no-slip condition and shear stresses within the fluid slow down the layer above; this continues through the boundary layer. The result is that a stall vortex is created, which appears near the leading edge and begins to promptly grow as the vortex is swept downstream before eventually shedding at the trailing edge (illustrated in Figure 2.6). The net effect of this process is an initial increase in lift, and then deep stall when the vortex sheds. The shedding contributes to the formation of a wake behind the rotor, this is discussed in detail in Section 2.4.1.

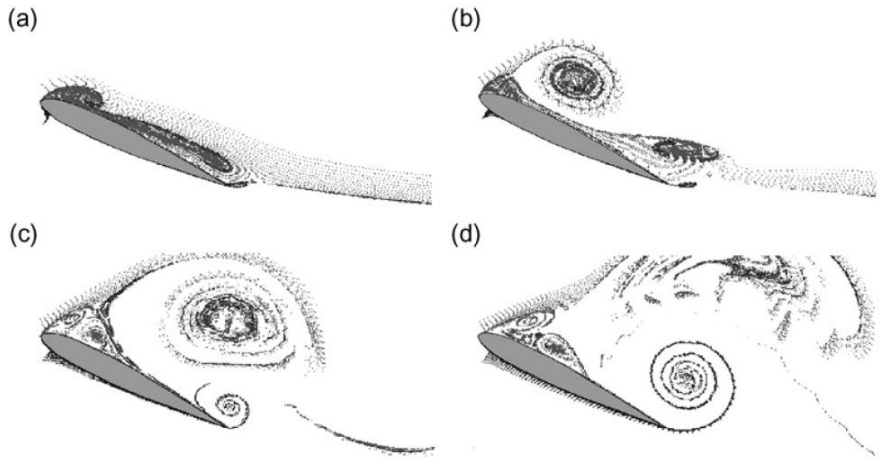


**Figure 2.6 Flow visualisation of a wing section during dynamic stall. (a) Leading edge separation begins. (b) Vortex build-up at the leading edge. (c) Detachment of leading edge vortex and build-up of trailing edge vortex. (d) Detachment of trailing vortex and breakdown of leading edge vortex. Adapted from** [30]

### Tip Vortices

Another aspect of importance in blade aerodynamic is the formation of tip vortices. These are the culmination of the pressure differences between the top and bottom surfaces of a blade when it is producing lift. The air flows from below and out around the tip of the blade in a circular motion, as visualised in Figure 2.7. The tip

vortices are associated with induced drag and reduce the ability for the blade to produce optimal lift.

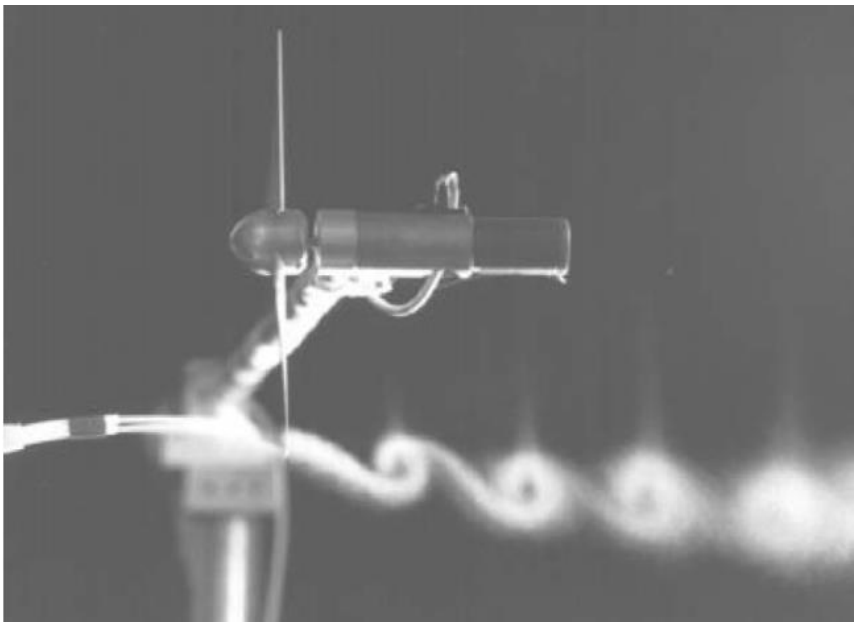

**Figure 2.7 Flow visualisation experiment at TU Delft, showing tip vortices, from** [25].

The blade tip vortices eventually mix out and affect the overall development of the near wake formed downstream of a wind turbine, which ultimately influences the far wake; these regions are discussed in more detail in Section 2.4.1.

## 2.4 Wind Farm Aerodynamics

Despite extensive research into the aerodynamics of horizontal axis wind turbines, much of the flow physics within a wind farm is still not fully understood. For example, the interactions of wakes between wind turbines and the effect the atmospheric boundary layer (ABL) and terrain have on wind farms. Simulating such interactions is difficult and complex because the difference between the smallest (aerofoil boundary layer) and largest (atmospheric boundary layer) lengths scales in the flow are up to six orders of magnitude.

### 2.4.1 Wake

In a wind farm made up of multiple rows, the downstream wind turbines see the combined effects of the incoming flow and the disturbance caused by the upstream turbines. This latter flow is known as the wake, which is a region of low velocity fluid coupled with high turbulence. As a result, a wind turbine sitting in the wake of another potentially has a greatly reduced energy yield due to a diminished wind speed [31]. The turbulence in the wake causes the low velocity fluid in the wake to mix with the high velocity fluid outside of it, this way momentum is transferred into the wake causing it to expand and the velocity deficit to recover [31]. The wake itself can be divided into two separate regions known as the near and far wake regions [25], as illustrated in Figure 2.8. The near wake region is found within the distance of three rotor diameters (3D) downstream of the wind turbine; in this, the properties of the turbine (number of blades and blade aerodynamics, as discussed in Section 2.3) are of importance. For example, the tip vortices produced by a wind turbine blade directly impacts the characteristics of the near wake. Beyond this region is known as the far wake, where the finer details of the flow have been mixed out with the free stream air flow, but the velocity deficit still remains. These two regions are of course related because the characteristics of the far wake are dependent on the near wake and the wind turbine rotor. However, the focus of this thesis will be on the far wake region as it is this area that determines the aerodynamics of a wind farm.

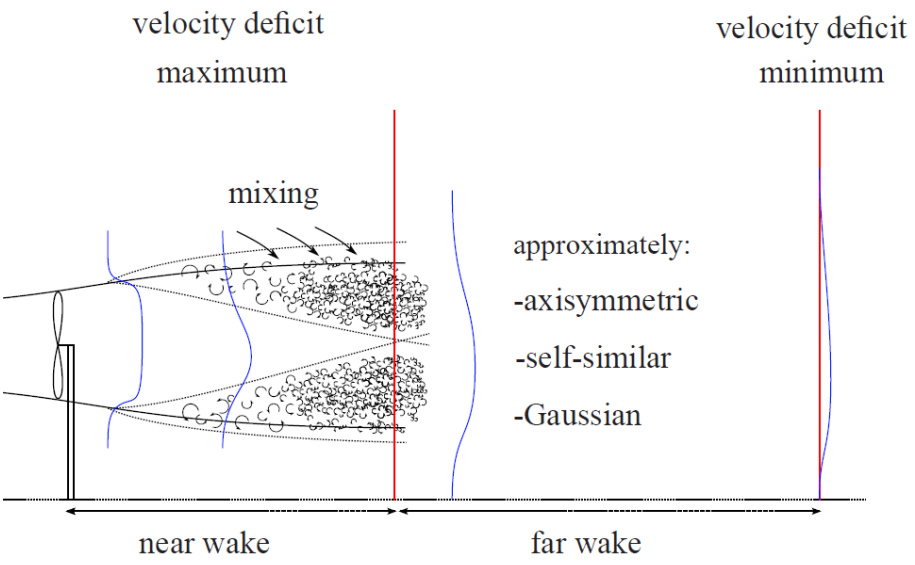


**Figure 2.8 Velocity profile in the near and far wake of a wind turbine, from** [31]

The effect of a wind turbine wake on other turbines is essential in determining the efficiency of a large-scale wind development. Zervos et al. [32] developed a numerical method in 1988 using the vortex particle concept in which vorticity is discretised into a set of vortex carrying particles. The method was applied for the calculation of wake characteristics and compared to experimental data for validation. The technique described a developed wake well, however, due to the computing limitations at the time calculations for a complete wind farm were demanding. Since then, more detailed techniques that take into account other factors such as the ABL and surrounding terrain have been developed [33].

Wakes produced behind a wind turbine means that the layout of a wind farm is crucial for optimising the overall energy yield. For example, a wind turbine placed directly behind another at 5D will see a reduced incoming wind velocity when compared with turbines at 10D apart. This phenomenon is shown by Chamorro et al. [34], the authors simulated numerically a perfectly staggered wind farm consisting of 10 rows by 2-3 columns in a wind tunnel. Cross-wire anemometry was used to measure

the streamwise and vertical velocity components and it was shown that the staggered layout yields a 10% increase in overall power output when compared to an aligned wind farm array. The cause of this power increase is a result of the net effect of more efficient momentum transfer, which can be inferred indirectly through the angular velocity, Figure 2.9 illustrates the results when comparing the two layouts. This is an important finding as it provides a basis for how wind farms should be laid out, however, not all sites allow for such positioning especially onshore where space is limited.

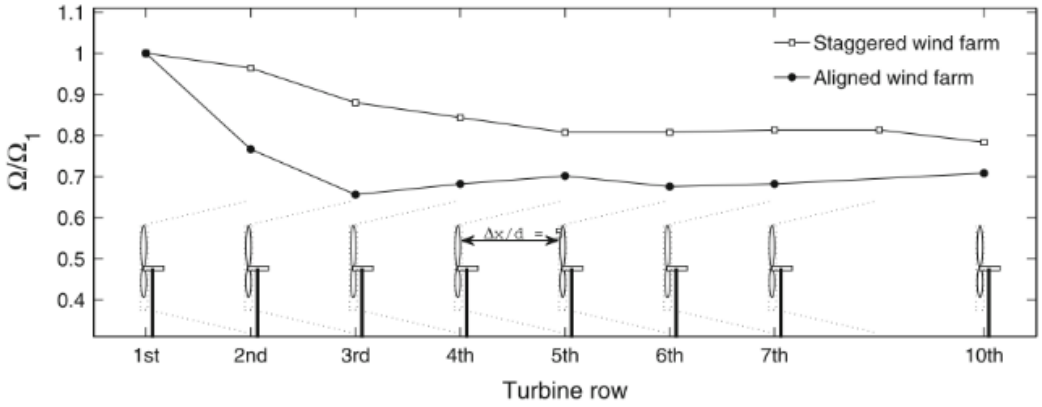


**Figure 2.9 Normalised angular velocity in the staggered and aligned wind farms, from** [34].

In another study, Chamorro et al. [35] carried out a wind tunnel experiment to quantify the Reynolds number dependence of mean velocity, turbulence intensity, kinematic shear stress, and velocity skewness in the wake of a model wind turbine. The experiments used the wind turbine rotor diameter and velocity at hub height as the characteristics to calculate Reynolds number, ranging from $Re$ = 1.66x10$^4$ to 1.73x10$^5$. Results suggested that the main flow statistics described above become independent of the Reynolds number starting from Re ≈ 9.4x10$^4$ (Figure 2.10). It was also shown that in general there is a stronger dependence in the near wake region compared to the far wake region because of the effect wind turbine blades have on the flow. The authors conclude that the results will allow these numbers to be extrapolated to full-scale

conditions, where by the far wake region will still show weak Reynolds number dependence. Being independent of Reynolds number allows for scaled simulations, both experimentally and numerically, to be carried out with confidence and yield results that are accurate.

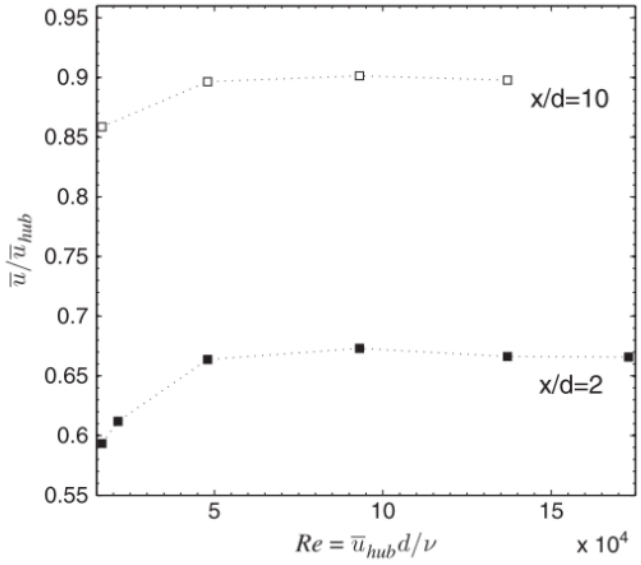


**Figure 2.10 Normalised velocity at two and ten rotor diameters downstream of the wind turbine for different Reynolds numbers, from** [35]

A numerical study carried out by Porté-Agel et al. [36] investigated the effects of changing wind direction on wind turbines wakes and related power production for Horns Rev wind farm located off the coast of Denmark (Figure 2.11).

**Figure 2.11 An image of the Horns Rev wind farm array, from** [37].

Using a CFD model where the wind turbines were represented using the actuator disc method, a total of 67 simulations were carried out and it was shown that the wind direction has a strong impact on spatial distribution of wake characteristics. Another way of looking at it is that the wind farm layout itself is changing relative to the incoming wind, which effectively alters the distances between individual wind turbines and thus wake recovery time. It was discovered that even a slight change in wind direction of 10° could increase the total power output by 43%. An important finding because often wind farms are designed to account for prevailing wind directions, but an understanding of all wind directions and the effect it has on the layout is crucial of maximising energy yield. Stevens et al. [38] simulated wind farms consisting of regular arrays with different span-wise offsets and over a range of prevailing wind directions. The streamwise spacing was kept the same throughout and by changing the prevailing wind direction the wind farm's effective layout changed and thus the turbine-turbine interactions varied with it. It was determined that the highest average power output is not necessarily achieved by staggering the wind farm equally throughout, but requires that the first several rows have minimal wake interactions from upstream wind turbines (Figure 2.12). Again, this led to the conclusion that wind farm design must account for all wind directions and how they affect wind turbine alignment in order to truly optimise its layout. Son et al. [39] were able to show that the spacing between the first and second wind turbines is important for the farm's efficiency as well as determining a base for an optimally laid out wind farm. By increasing the distance between the first and second wind turbines, the overall ability for the wind farm to perform increases, even if the third turbine is placed at a reduced distance from the second.

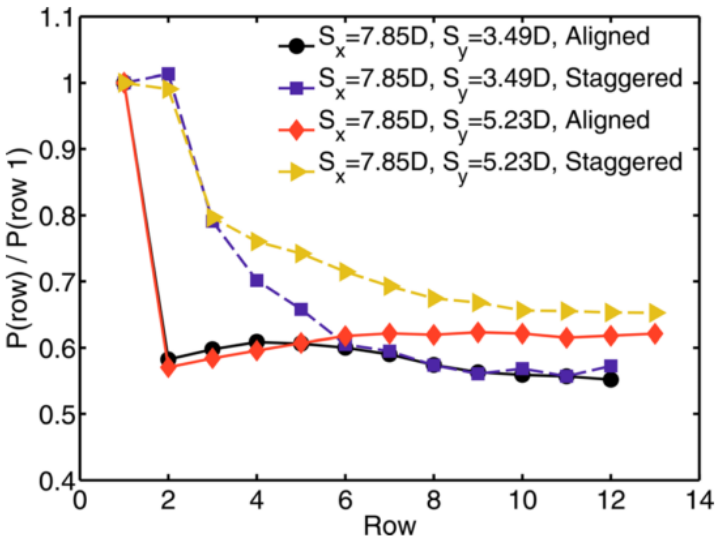


**Figure 2.12 Normalised power output for aligned and staggered wind farm layouts, from** [38].

McTavish et al. [40] researched the performance benefits of closely spaced wind turbines in the lateral direction within a wind farm layout. Using wind tunnel experiments it was observed that a maximum total increase in power from a three turbine setup occurs when the lateral tip separation is 0.5D or 0.25D compared to the same number of rotors in isolation. It was suggested that this is the result of a local in-field blockage effect that is caused by the reduced lateral spacing of wind turbines, which increases the local wind speed at the rotor plane.

Simulating the far wake experimentally and numerically is a key aspect of this thesis, as such the literature review on the subject continues throughout the remainder of this chapter while the focus also broadens to include associated characteristics. The far wake of a wind turbine interacts with the atmospheric boundary layer (ABL) by exchange of momentum [26], these interactions and the effects are discussed in the next section.

### 2.4.2 Atmospheric Boundary Layer (ABL)

With rotor diameters exceeding 150 m, wind turbines are by far the largest rotating structures on the planet. Nonetheless, wind turbines sit in the lowest part of the ABL where high intensities of turbulence are experienced [25]. As Wharton and Lundquist [41] discuss, it is important to have an accurate estimation of wind power availability, which is inherently dependent on understanding the ABL conditions, including stability. The ABL is by no means stable, for example, a wind farms power output will vary considerably and is determined by regional climatology [41]. Therefore, understanding how to accurately replicate the ABL in numerical and experimental simulations is imperative. The ABL can be approximated by using wind speed measurements at given heights with the following relationship, known as the wind profile power law:

$$\frac{U}{U_r} = \left(\frac{Z}{Z_r}\right)^a \tag{2.8}$$

Where U is the wind seed, Z is height, and r is the corresponding value at a reference height. $a$ is an empirically derived coefficient that varies depending on the stability of the atmosphere. For neutral stability atmospheric conditions, $a$, is approximately 0.143.

A phenomenon associated with large rotor wind turbines and the ABL is the effect of wind shear on the wake structure and performance. Wind shear is caused by the varying wind speeds as the height of the ABL increases, uniform flow is the same as no wind shear. In reality a steady vertical wind shear is dictated by the wind profile power law described above, however, transient extreme wind shear can also occur. Sezer-Uzol and Uzol [42] compared the three cases to understand how the wake structure and power levels varied. It was found that the asymmetrical inflow conditions resulted in

non-uniform downstream wakes and that the surface pressure variations causes high level fluctuations in power. The problem that comes of this is that it can set up severe vibrations that may impact on the structural integrity of the blades and reduce wind turbine lifetime.

Wind turbine wakes in the ABL is largely determined by the thermal stability, the effects of which were investigated by Zhang et al. [43]. By cooling the airflow down and heating up the test section floor of a wind tunnel resulted in a smaller velocity deficit when compared to a neutrally stable boundary layer, as depicted in Figure 2.13. This is due to an enhanced radial momentum transport leading a faster recovery of the wake.

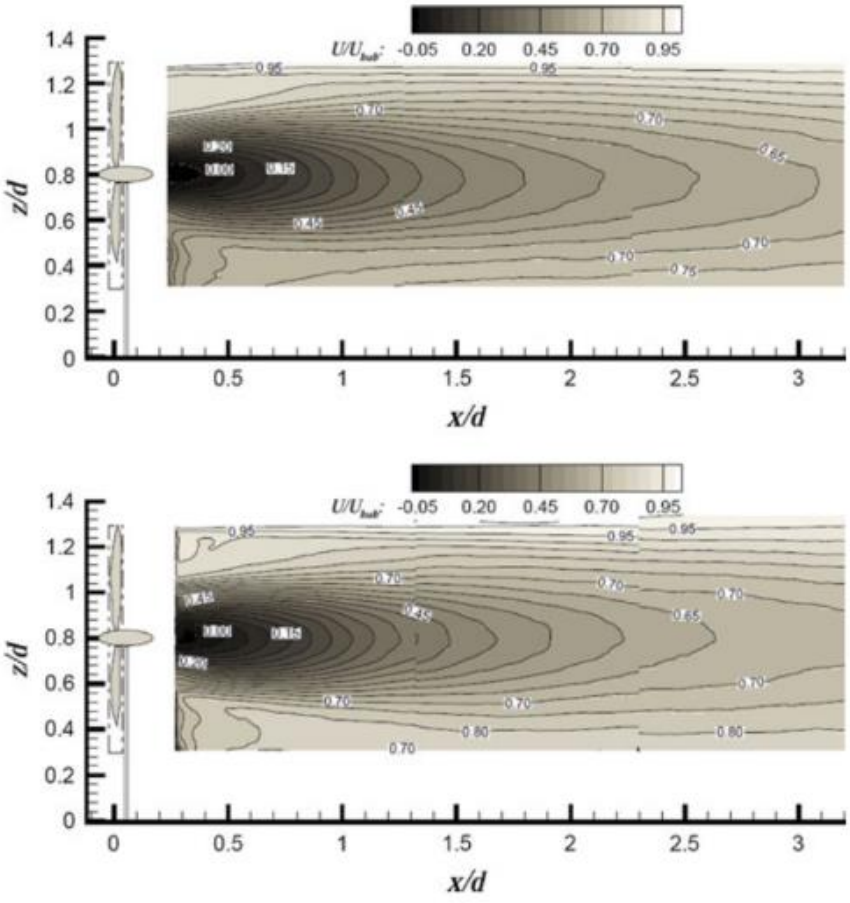


**Figure 2.13 Comparing the streamwise velocity behind the wind turbine model while in a neutral boundary layer (top) and convective boundary layer (bottom), from** [43].

Large wind farms now exceed 20 km in horizontal length; this is important because the ABL has an approximate characteristic height of 1 km and, therefore, may approach the asymptotic limit of an 'infinite' wind farm. This limit is relevant for wind farms on a flat terrain where the length exceeds the height of the ABL by at least one order of magnitude. As discussed by Meyers and Meneveau [44], the 'infinite' wind farm leads to a boundary layer which reaches a new fully developed scenario, this is dependent on the additional surface drag induced by the farm. It was found that an increased distance between wind turbines leads to a higher optimisation in terms of energy yield for wind farm layouts. However, this model only takes into account flat terrain topography and as it is shown in the next section, terrain plays a vital role in wind farm placement.

### 2.4.3 Terrain

An important aspect of wind turbine siting is the placement within the terrain itself. Complex terrain can have either have a positive or detrimental effect on wind turbine performance. Areas at the height of most hills and mountains tend to increase the mean velocity, which in turn means there is a greater potential for energy production. However, high wind shear and increased turbulence intensities can increase loads on wind turbines, greatly reducing their life span while simultaneously increasing the need for maintenance.

Flow over hills is an area of research that has spanned for decades; however, the focus has been predominately on simple geometric shapes with moderate slopes. Carpenter and Locke [45] investigated the flow over two-dimensional scaled hills in a wind tunnel. It was concluded that wind speed were highest over a single shallow hill when compared with a single steep hill and configurations of multiple hills. Røkenes et

al. [46] used a wind tunnel to determine the effects of terrain on wind farm siting. Their novel approach of simulating the flow over different types of mountainous terrain (sharp and rounded crests, with different inclination angles followed by a plateau as shown in Figure 2.14) could be combined in various ways. The results showed that flow above rounded hills were most favoured for wind turbines due to a combination of increased mean velocities and reduced turbulence intensities.

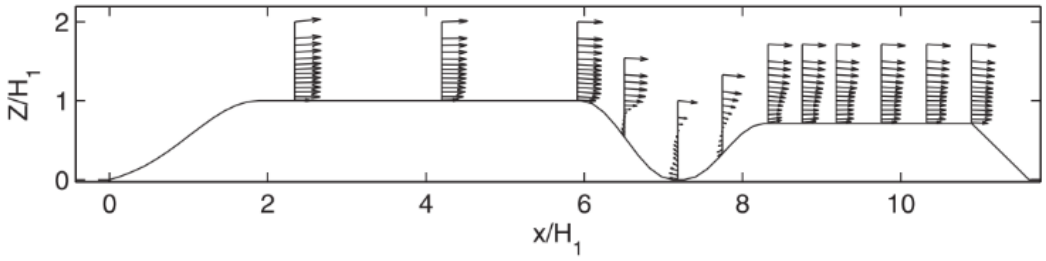


**Figure 2.14 Mean velocity vectors and terrain over changing terrain, from** [46].

Yang et al. [47] analysed the effects of three dimensional hills on the wake of a wind turbine using wind tunnel experiments and large eddy simulations (LES). In this study the hill was placed upstream of a model wind turbine with various distances between; when the hill is equal or 0.5D taller than the hub height the wake behind the rotor is able to recover faster when compared to a turbine located on flat terrain. The authors suggest that a result of this observation is that for wind farms placed on complex terrain, wind turbines can be sited closer together in order to produce a higher power density.

Lubitz and White [48] replicated the ABL in a wind tunnel and modelled complex terrain for locations in the Altamont Pass, California, USA. It was determined that calculating predictions is difficult due to the variability found in nature, hence, the simplicity of the simulations performed up to this point. Since then, modifications to standard turbulence closure models in CFD have been applied that take into account

such variables; notably by Kasmi and Masson [49] who found that while the modifications decreased the predicted velocity due to the terrain modelled, there was an increase in turbulent kinetic energy. An important aspect of simulating terrain is to include the wind turbines themselves within the model, however, as will be discussed in Section 2.5.3 modelling wind turbines is a computationally demanding process. Makridis and Chick [50] used the actuator disc technique to simulate turbine rotors and placed them on increasingly complex terrain for validation purposes. The increased complexity resulted in a methodology that gave good agreement to measured data, as shown in Figure 2.15.

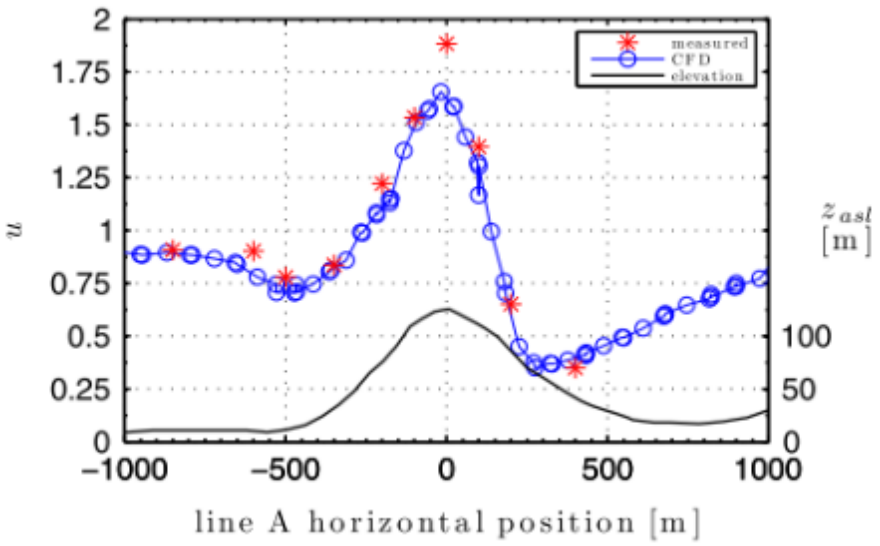


**Figure 2.15 Normalised velocity comparison of measured versus CFD on change in terrain, from** [50].

### 2.4.4 Geographic Information Systems

Geographic information systems (GIS) is a system that is used to store and manipulate all types of spatial data, including terrain and wind speed. A particular use of GIS for wind farm design is the ability to carry out spatial multi-criteria decision analysis; for example van Haaren and Fthenakis [51] used this methodology to evaluate potential wind farm sites in New York state based on spatial cost-revenue optimisation.

The paper laid out three stages of selection, which first excluded sites that are infeasible because of geographical and land-use constraints, the second identified the best sites, taking into account electricity generation potential, and cost of access to roads and the grid. The third considered the effects on bird habitats, and with all stages combined and compared with the existing wind farms. The developed tool was successful as it identified all 15 existing wind farms as feasible, as well as providing further suggestions. A similar analysis was carried out by Janke [52] for the US state of Colorado and provided potential locations for both wind and solar forms of renewable energy. Grassi et al. [53] used GIS to predict the annual energy production of four onshore wind farms as a form of validation to determine the effects of layout. The model included the wind direction and roughness of surrounding terrain; the annual energy production is calculated using technical information of the wind turbines combined with the wake effects and wind resource available. The research found that when a wind farm is designed for optimal layout for only the prevailing wind direction it can lead to significant overall energy losses. For example, if the wind direction is perpendicular to the prevailing wind, up to 60% of the available energy may be wasted. Therefore, it was concluded that wind farm layout requires optimisation for more than just one wind direction.

However, an inherent issue with GIS are the assumptions used for decision-making, which are based on both direct readings and past data. These are extremely useful for projects that are generally accepted by the public, but do not offer recommendations for how to overcome contentious issues, such as visual impacts which is discussed in Chapter 3, but rather yield to them. This could limit the possibilities for optimally laying out wind farms and compromises will be made. An

example of the problem described is shown by Baban and Parry [54] where GIS was used to locate wind farms in Lancashire. By using questionnaires to determine the attitudes of the local communities, a weighting for each layer from 0 to 10 based on the data collected was applied. Suitable sites that were likely to gain planning approval were found, but when compared to each layer being given the same weighting, it showed that the latter found more overall areas suitable for wind development (Figure 2.16).

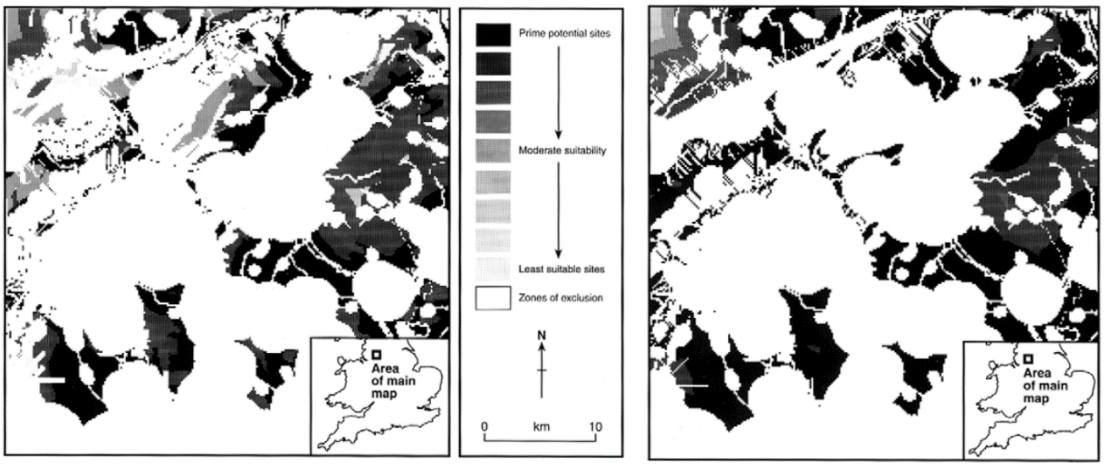


**Figure 2.16 Wind farm site suitability when each layer was given a weighting determined by the attitudes of local communities (left) and equal weighting (right), from** [54].

GIS can also account for the visual and noise impacts of a wind development and as discussed in the introduction the ability for a developer to gain planning permission is heavily dependent on these factors; the issues of which are discussed further in Chapter 3.

### 2.4.5 Summary of Wind Farm Aerodynamics

The section above provides a brief analysis of the key fundamentals of the aerodynamics for HAWT wind farms. While the intrinsic details for such farms are almost endless, much of them can be neglected when attempting to produce an overall understanding. Therefore, the main focus of this thesis is the far wake and how the

interactions of it and other wind turbines affect performance. There is also some consideration of the ABL and terrain effects.

The research reviewed has shown there has been much work done on individual aspects of wind turbine wake and the effects of the ABL and terrain, but there are few attempts at overlapping these processes in research with the exception of GIS. However, GIS is a Jack of all trades, master of none approach, and with it finer details are lost. The reasons for this are due to the difficulty of carrying out such experiments and simulations, but it is the author's opinion that a better general overview of the key aspects in wind farms should be considered. This is where the process of modelling and the ability to simulate these areas becomes a priority.

## 2.5 Methods

There exist many different methods for predicting wind turbine performance. Previously, the most popular technique was the classical blade element momentum (BEM) theory presented by Glauert [55]. The BEM theory is widely used in industry due to its versatility and low computational cost. Malki et al. [56] used a coupled BEM-CFD technique for modelling tidal turbines and while it is computationally efficient for simulating arrays, it is also extremely limited in terms of the performance data that can be extracted. Therefore, the requirement for more comprehensive and accurate data has led to experimental work in wind tunnels and detailed numerical simulations using CFD by research institutions.

### 2.5.1 Actuator Disc Theory

Prior to its application in wind turbines, the actuator disc (AD) concept was initially developed for mathematically modelling a propeller or helicopter rotor. The technique is now also used for simulating the wakes of wind turbines in wind farm

scenarios, because of the model's ability to reliably replicate the far wake region and interactions with other rotors [57]. The concept can be applied to both experimental and numerical modelling techniques. The flow field behind the wind turbine rotor is simulated using a simplified technique that lets the user mimic the energy extraction from a wind turbine without having to model specific rotor geometry [58]. The advantage of this simplification is a lesser requirement of computational power and time. A permeable disc with the same area as a full rotor distributes the forces found along the blade onto a circular disc. Due to conservation of mass and momentum, these forces alter the airflow through the disc, as well as the flow field surrounding it. Figure 2.17 shows the flow field around an actuator disc with expanding streamlines. Rankine-Froude theory describes the Thrust (T) and Power (P) for a non-rotating and uniformly loaded AD as:

$$T = \dot{m}(V_o - u_1)$$
$$P = \frac{1}{2}\dot{m}(V_o^2 - u_1^2) \tag{2.9}$$

where $V_o$ is the free stream velocity and $u_1$ is the far wake velocity. The mass flow through the disc is $\dot{m} = \rho u_1 A_1$, where $A_1$ is the far wake area and $\rho$ is the density. Assuming mass conservation through the disc, where $uA = u_1 A_1$, combining the equations found in (2.9) yields:

$$P = \frac{1}{2}(V_o + u_1)T = uT \quad where \quad u = \frac{1}{2}(V_o + u_1) \tag{2.10}$$

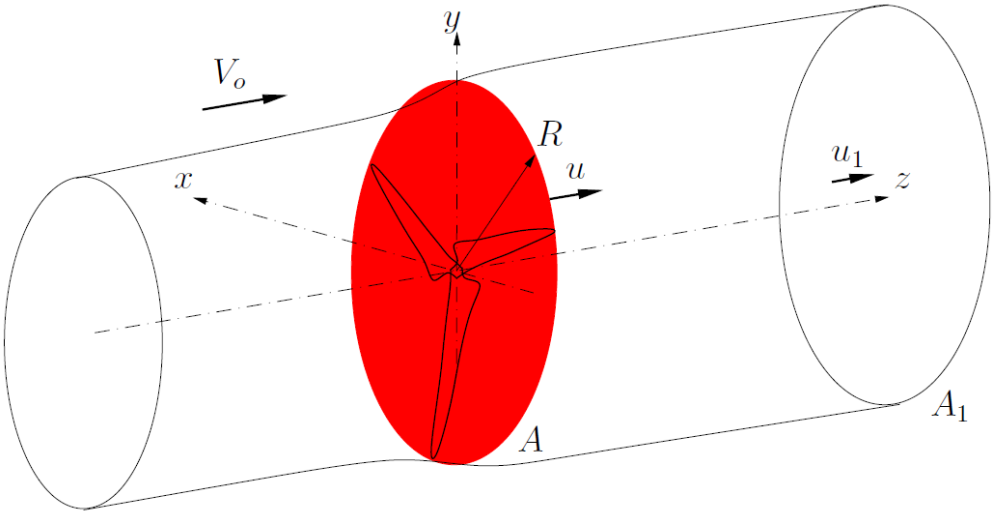


**Figure 2.17 Flow field around an actuator disc, from** [59]

This shows that the velocity at the disc (u) is the mean of the freestream velocity and the far wake velocity. With the introduction of the axial induction factor, this is defined as the fractional decrease in wind velocity between the free stream and the actuator disc:

$$a = 1 - \frac{u}{V_o} \tag{2.11}$$

Equation (2.9) can be presented in the non-dimensional form of thrust coefficient ($CT_h$) and power coefficient (CP):

$$CT_h = \frac{\rho u A(V_o - u_1)}{\frac{1}{2}\rho V_o^2 A} = 4a(1-a) \tag{2.12}$$

$$CP = \frac{\frac{1}{2}\rho u A(V_o^2 - u_1^2)}{\frac{1}{2}\rho V_o^3 A} = 4a(1-a)^2 \tag{2.13}$$

Where $u_1 = (1-2a)V_o$.

For experiments, wire meshes can be used with different porosities to create different wake characteristics. The porosity is the percentage of void space (open area)

of the total surface area over a porous disc; altering this allows the user to determine, by choice of induction factor, what the wake of the modelled wind turbine will behave like. The use of both numerical and experimental approaches for ADs is discussed in the next sections.

### 2.5.2 Experimental: Wind Tunnel

Due to the transient nature of the wind and atmospheric conditions the ability for consistent data to be extracted from real world wind turbines is extremely difficult, therefore, researchers use wind tunnels to provide an environment for measuring the effects that scaled models have on the flow. A full size wind turbine can be as tall as 150 m, which are orders of magnitude larger than any wind tunnel test section. Therefore, inherent issues come with using geometric scale models such as scaling characteristics of velocity and Reynolds number. This was shown by Chamorro et al. [34], where the Reynolds number was two orders magnitude lower than what is found for full size wind turbines. Hence, when interpreting results, details such as dynamic similarity must be taken into account and the focus must be put on the large-scale properties.

The models used for array testing in wind tunnels come in two forms: the first consists of a complete geometric scale model with turbine blades that form a rotor, and, the second is a mesh disc of the same diameter as the scaled wind turbine rotor area (actuator disc concept).

Cal et al. [60] used complete geometric scale models to simulate a 3 x 3 array to better understand the vertical transport of momentum and kinetic energy across a boundary layer flow. The wind turbine models were scaled at 1:830, replicating a rotor with a diameter of 100 m and a hub height of the same distance. With the use of particle

image velocimetry (PIV) measurements, it was discovered that the fluxes of kinetic energy associated with the Reynolds shear stresses are of the same magnitude as the power extracted. It is suggested that in theory in a "fully developed" or infinite array of wind turbines, this may become the dominant mechanism in providing kinetic energy to the rotor.

Aubrun et al. [61] used mesh discs at a geometric scale of 1:400 to simulate a 3 x 3 wind farm. A parametric study around the porosity level of the mesh discs was carried out as a form of validation and it was determined that the results were in good agreement with the literature, such that the velocity measurements downstream of the discs allowed for comparable thrust and power coefficients to be calculated (Figure 2.18). The simplification of using a mesh disc instead of a complete scaled model is important, because it allows for the use of carrying out detailed experiments that involve complex terrain or multiple layouts for wind farms, but still have the ability to replicate wind turbine wakes effectively.

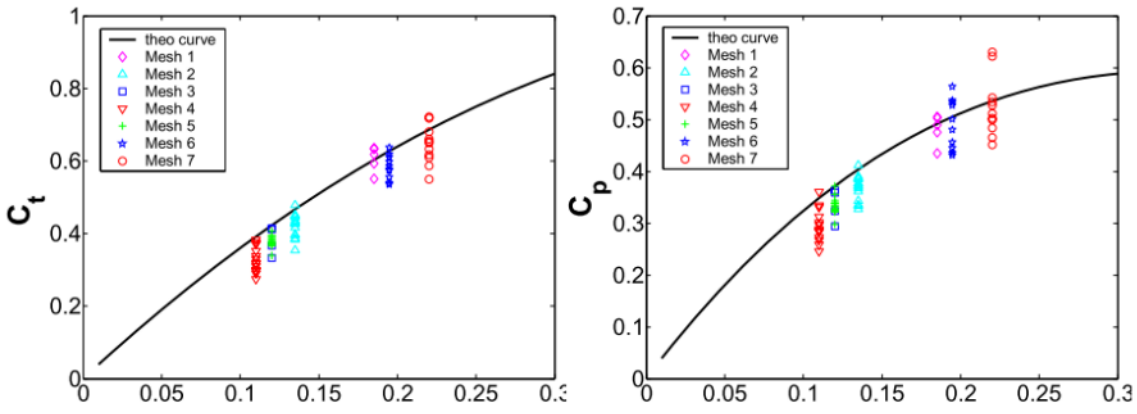


**Figure 2.18 The thrust coefficient (left) and power coefficient (right) both versus axial induction factor for discs made of different meshes, from** [61]

Wind tunnels also have the capability to replicate the ABL; España et al. [58] used actuator discs and physical modelling of the ABL to study the meandering of a wake. It was concluded that it is important to include the meandering process when estimating

loading on wind turbines, but as the instantaneous wake width remained nearly constant downstream, it is less important for overall power output. Zhang et al. [43] investigated how thermal stability changes the properties of the ABL, which affects wind turbine wakes. Wind tunnel experiments showed the velocity deficit at the wake centre decays the same regardless of the thermal stability, but the peak turbulence does change by as much as 20%.

### 2.5.3 Numerical: Computational Fluid Dynamics

The disadvantages of modelling experimentally in a wind tunnel can, in part, be overcome by using a computational model. However, the use of CFD to simulate anything from the flow around a section of an individual rotor blade to a whole HAWT farm requires substantial computational power. The last 15 years have seen advancements in computational resources that allow such simulations to take place in the offices of small companies and academic institutions. Along with this, the continual development of commercial CFD software packages has permitted engineers to model their desired environment with growing ease. As previously discussed the far wake is the main area of interest in this thesis and thus, the CFD review will concentrate accordingly.

Sanderse et al. [62] published a review of computational fluid dynamics for wind turbine wake aerodynamics. In the review a classification of computational methods used for wind turbine wakes can be found (Table 2.1), it covers a range that allows various levels of detail to be extracted depending on what is required.

Table 2.1 Classification of models, from [62].

| Method | Blade model | Wake model |
|---|---|---|
| Kinematic | Thrust coefficient | Self-similar solutions |
| BEM | Actuator disk + blade element | Quasi one-dimensional momentum theory |
| Vortex lattice, vortex particle | Lifting line/surface + blade element | Free/fixed vorticity sheet, particles |
| Panels | Surface mesh | Free/fixed vorticity sheet |
| Generalised Actuator | Actuator disc/line/surface | Volume mesh, Euler/RANS/LES |
| Direct | Volume mesh | Volume mesh, Euler/RANS/LES |

The generalised actuator disk method and the direct method are also called CFD methods, and it is these methods that are of importance.

### Generalised Actuator Disc

It is possible to represent the rotor of a wind turbine with a disc, or by replacing the individual blades with lines or surfaces [62]. This allows the user to avoid having to apply a fine mesh along the boundary layers, thus reducing the computational cost. Figure 2.19 illustrates these three approaches. All three methods work by exerting a force on the flow that acts as a momentum sink.

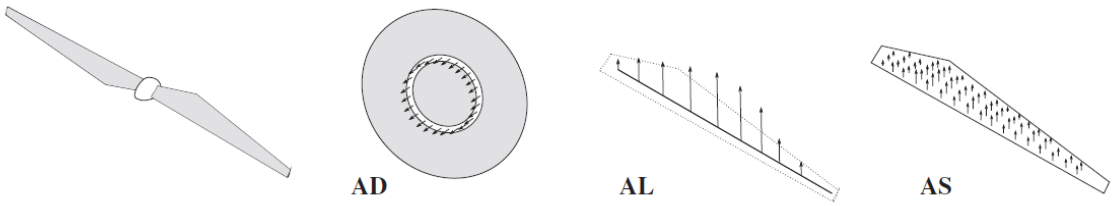


Figure 2.19 Rotor representation by actuator disc (AD), actuator line (AL) and actuator surface (AS), from [62].

The actuator disc (AD) is defined as a permeable surface normal to the freestream velocity on which an evenly distribution of blade forces acts upon the flow [63]. The model disregards fundamental characteristics of wind turbine aerodynamics; this is due

to the streamlines passing through the disc, which produce a velocity deficit so that the wind speed on the rotor is lower than the freestream velocity. As a result, this technique is unable to give any useable results in the near-wake region, but is the most reliable way to estimate power losses and representation of the flow in the far wake [64]. Réthoré et al. [57] verified and validated the use of an actuator disc model in an attempt to prove that the results in the regions beyond the near wake are acceptable for simulating large wind farms. The authors were able to show that by using a relatively coarse mesh, in the region of 10 cells/diameter in the near wake region of an actuator disc, the results matched well with a full rotor computation at a fraction of the computational cost. Although the vortex structures found in the near wake region were not modelled correctly, beyond this in the mixed out far wake region a close match is found. The authors concluded that simulating a wind farm of 100 wind turbines, equally spaced in a 10 x 10 grid, an adequate resolution could be achieved with approximately 128 million cells in total, which, given the size of the wind farm, is extremely useful in terms of computational time and cost. Crasto et al. [65] applied the AD method to simulate the Horns Rev wind farm found off the coast of Denmark and by calculating the power drop between the first two rows at 6 $ms^{-1}$ and 10 $ms^{-1}$ found that the results produced a good approximation to the power produced from the site, as shown in Figure 2.20 . Crasto et al. [65] also discussed that the AD provides better predictions at higher wind speeds and wider directional sectors.

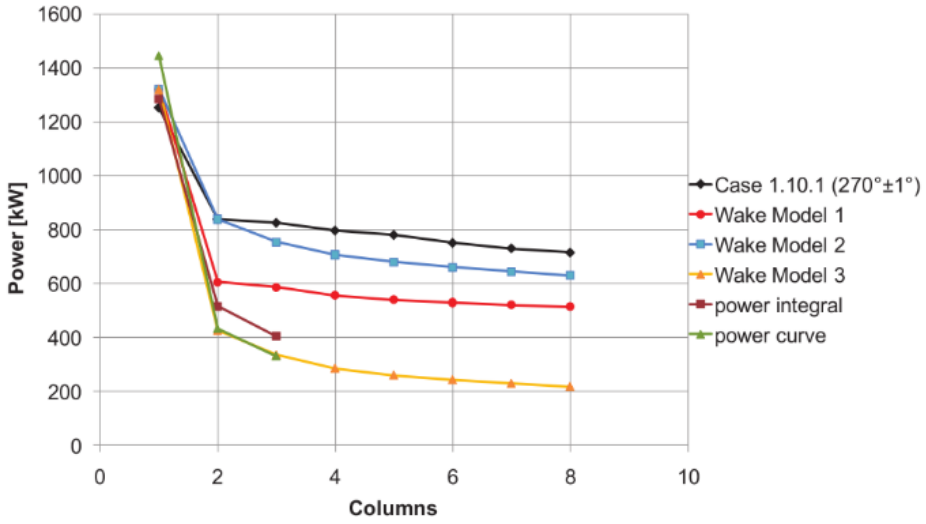


**Figure 2.20 Power prediction for Horns Rev wind farm using the actuator disc method, from** [65].

The actuator line (AL) allows for the influence of the blades to be captured without the requirement of a detailed three-dimensional geometry [66]. The method calculates forces by using the evolving flow field and tabulated aerofoil data [67] and unlike the AD method, the line technique is able to resolve trailed vorticity in the near wake as shown in Figure 2.21. Sørensen and Shen [68] demonstrated that the AL was in good agreement when compared with experimental results, in particular the postion of the tip vortices in the near wake region behind the rotor. However, the mesh density requirements also increase.

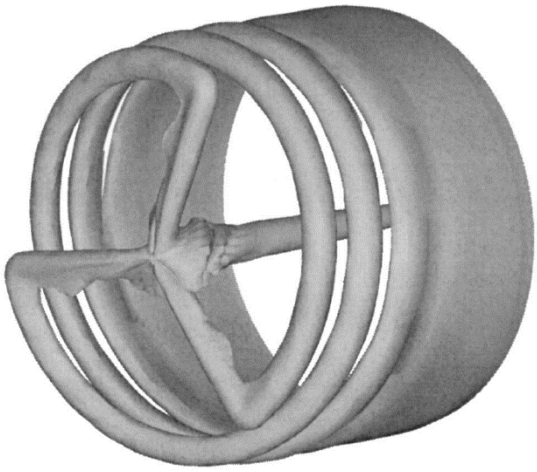

**Figure 2.21 Formation of the wake structure when using the actuator line method, from** [68].

The actuator surface (AS) model is a recent development by Shen et al. [69] in which tabulated aerofoil data is used to apply a pressure distribution by representation of body forces along the chord of a blade. However, the technique currently fails to accurately predict fundamental characteristc for moving flow using static aerofoil data and, therefore, cannot be presently used for simulating wind turbine for aerodynamic analysis.

More recently, Storey et al. [70] developed the actuator sector method, where by the forces are applied in a similar way as used in the AD technique but allow for increased time-step intervals when compared to the AL method (Figure 2.22). The model was shown to overcome the time-step restriction found in AL simulations while providing an increase in flow detail when compared to an AD model; all the above was achieved with no additional computational cost.

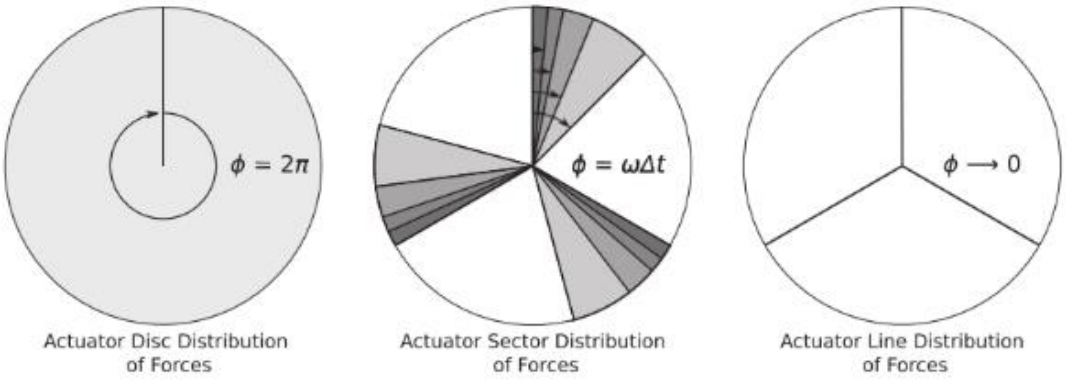


**Figure 2.22 The distribution of aerodynamic forces at the turbine rotor plane for the actuator disc model (left), the actuator sector method (centre) and actuator line model (right), from** [70].

### Direct Method

An extremely accurate approach to modelling wind turbines is with the use of the direct method; where by the complete geometry of a wind turbine is replicated exactly using a fine boundary layer mesh around the blade, instead of an approximation as done when using the actuator disc/line techniques. It allows for the accurate simulation of the boundary layer over the blade, including possible transition, separation, and stall. Bechmann et al. [71] modelled the turbine used in the Model Experiments in Controlled Conditions (MEXICO) wind tunnel experiment as a form of validation. The mesh consisted of $16x10^6$ nodes and represented a single blade with a 120-degree periodicity of the rotor, as illustrated in Figure 2.23. The disadvantage here is the computational cost and time is extremely high (a number of weeks even with a super computer) and for modelling far wake characteristics it is highly inefficient.

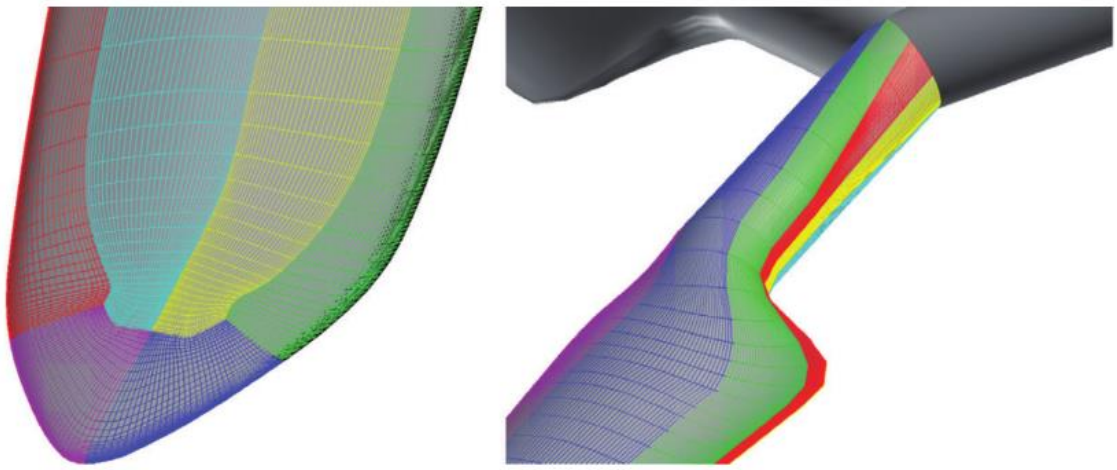

**Figure 2.23 Top surface mesh/blocking consisting of $16x10^6$ nodes, from [71].**

It is also possible to model two wind turbines interacting with one another using the direct method as shown by Weihing et al. [72]. The authors modelled two 5 MW wind turbines, including the tower and hub, that are located behind each other and are offset laterally by half a diameter (Figure 2.24). The total domain consisted of $110x10^6$ cells and was run using a hybrid of RANS and LES techniques for increased accuracy, while being able to, in part, minimise computational power required. The results showed that the asymmetric wake reduced the second wind turbine's power by 15% and affected the load experienced along the length of the blade, which in terms of fatigue is important to understand. The paper does not mention the time the simulation takes to reach convergence, and with the meshing requirements being specific to the case studied there is no flexibility in modelling multiple layouts. Therefore, such a method is pushing the limits of available computing power and is an example of an engineering exercise rather than a practical technique. Unfortunately, the paper offers no comparison to other simulation techniques to determine whether there is an appreciable increase in accuracy or not.

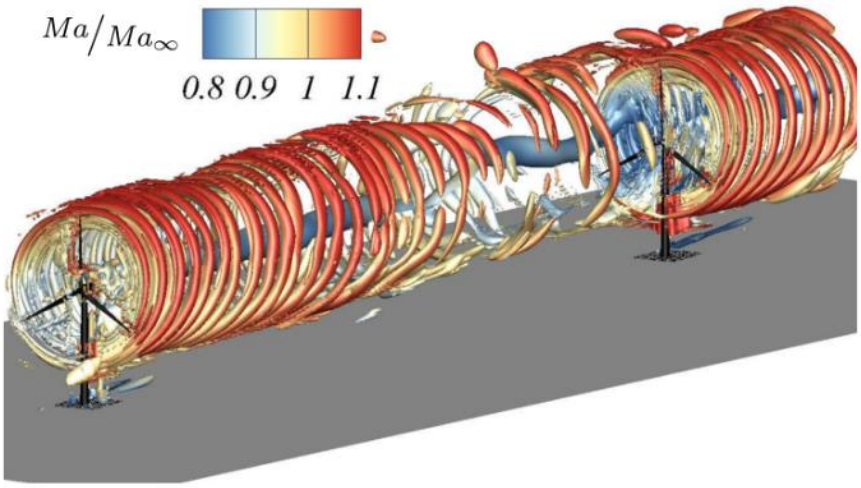


**Figure 2.24 Vortex visualisation of a turbine-turbine interaction using the direct method, from** [72].

The methods reviewed above for modelling and simulating wind turbine wakes have their advantages and disadvantages summarised by Castellani and Vignorali [64] in Table 2.2. This, in itself, provides a good summary of this section.

**Table 2.2 Wind turbine wake models, from** [64].

| Name | Advantages | Disadvantages |
|---|---|---|
| **Analytical Actuator Disc** | Fast and simple calculations | Wake losses calculated downstream of the wind field |
| | Average calculation effort | Effects of rotation cannot be simulated |
| | Contextual wind field and wake simulations | Extremely simplified geometry |
| | Coarse mesh | |
| **Actuator Line/Surface** | Effects of rotation are considered (able to model wakes vortices) | Finer mesh with high calculations effort |
| | Contextual wind field and wake simulations | Much more parameters for the turbine are necessary |
| **Full Rotor Simulation (Direct Method)** | Real geometry is modelled | Very high calculation effort |
| | | Knowledge of the geometry and many parameters for the turbine |

**Turbulence Modelling**

The flow field in the wake of a wind turbine is considered to be incompressible as the velocities experienced in normal atmospheric conditions sit in the range of 3-30 $ms^{-1}$, increasing up to 100 $ms^{-1}$ for blade tip velocities. This leads to the use of the incompressible Navier-Stokes equations to define the aerodynamics behind a wind turbine. While the Navier-Stokes equations are able to completely describe turbulent flows, they are inherently non-linear, which introduces unknown stresses throughout the flow. Known as Reynolds-averaged stresses, they result in additional unknown quantities and without the addition of any equations are impossible to solve. In order to attempt to solve the Navier-Stokes equations requires the use of closure equations, also known as turbulence models. The turbulence models are used to give an approximate time-averaged solution to the Navier-Stokes equations and are subsequently known as Reynolds-averaged Navier-Stokes (RANS) equations. Thus the RANS equations provide an approximation of what is actually happening.

It is important that an appropriate choice of a turbulence model is made when simulating wind farms in CFD. A key indicator as to whether a turbulence model is suitable is how the results from numerical simulations compare with experimental data and therein lies the issue with length scales associated with wind turbines and farms. These can range from 1 km in the ABL to sub 1 mm for the blade boundary layers. Therefore, in the case of wake calculations a simplification of the wind turbine is required. The advantages of simplifying the wind turbines is made obvious by Montavon et al. [33] and their application of the AD method to accurately model a 54 turbine wind farm in a circle of complex terrain with a radius of 15 km. Had the direct method, as previously discussed been applied, the ability to model the same farm would

have taken years of computational time. The following review of turbulence models are for when they are applied to the AD method and wake calculations.

Réthore et al. [73] studied the atmospheric wake turbulence using the standard *k*-*ε* closure model and found that the wake recovers faster than expected. Therefore, a canopy model (originally developed for forest and urban areas, where modifications are made to how the turbulence kinetic energy and dissipation is simulated) was adapted to take into account the faster recovery time, with results showing promise for future wind farm analysis.

Bechmann and Sørensen [74] demonstrated the use of a hybrid RANS/LES technique, which allowed the user to also run the model as pure RANS. The two-equation *k*-*ε* turbulence model with modified constants suitable for ABL flows was applied. A complex terrain located near Wellington, New Zealand was used for the simulations and it was shown that the RANS approach was able to capture the overall flow field for velocity and turbulent kinetic energy. Cabezón et al. [75] also used the modified *k*-*ε* turbulence model as the default constants led to an underestimation of the wind speed deficit. With the new constants, the results yielded were well matched in the far wake region due to the ability counteract the excess of turbulent diffusion in the near wake.

Castellani and Vignorali [64] used the RNG *k*-*ε* closure model and used a data set taken from a wind farm in Finland. The model was not proposed for detailed wake simulation, but to estimate the power loss of a wind farm by reliably predicting the characteristics of the far wake. Politis et al. [76] applied the AD approach to predict power production from an entire wind farm in complex terrain and compared the *k*-ε and *k*-ω turbulence closure models. It was found that the complex topography added

extra sources of uncertainty and thus the requirement for not only calibrating the models for ABL but for the terrain too is essential.

An important aspect of simulating wind farms is to be able to correctly replicate the flow over a complex terrain; Montavon et al. [77] used field data from the Danish coast and in central Wales to draw comparisons with results using two different turbulence models. The closure models used were the $k$-ε and shear stress transport (SST); both used adjusted constants to compensate for the ABL and ground roughness. From the simulations it was found that both models gave comparable results, with SST tending to show regions of separation. However, the authors noted that the field data was not comprehensive enough to verify which of the models provides better predictions.

In addition to the commonly used RANS turbulence models, there are also other ways of simulating turbulence; large eddy simulations (LES), detached eddy simulations (DES) and direct numerical simulations (DNS). These methods are able to provide a far more comprehensive method for modelling and simulating wind farms, however, all are more demanding in terms of computational resources. The most detailed of the above techniques is DNS, but currently it is unworkable for studying wind farm aerodynamics because it does not use a turbulence model to solve the Navier-Stokes equations [78]. In doing so all scales of the flow must be resolved, therefore, making it computationally expensive. LES is beginning to become an acceptable trade-off between cost and detail, especially for simulating wind farms and the interaction with the ABL [44], as it eliminates the small scales within the solution and only resolves the large scales of the flow field. DES is a hybrid methodology that combines RANS and LES; RANS is used near solid boundaries where the turbulent length scales are smaller, it switches to LES when

the scales increase in the outer flow region [72], the result of which it is less demanding than pure LES.

### 2.5.4 Summary of Methods

The methods and ability to model wind farms have become extensive in recent years. The techniques include the application of actuator discs both experimentally and numerically, modelling fully scaled wind turbine, and simulating complex terrain in ABL conditions. Much of the work has been looking at how to improve these modelling techniques with the resources (wind tunnel and computational power) that are currently available; this includes approaches of modelling a wind turbine and the in the case of CFD, the most accurate turbulence models. It has now reached the point where the users have the ability to replicate situations for wind farm layouts that currently exist and produce results that give accurate predictions. However, little work has been done using this to show optimal layouts and performance for current and future wind farms; this thesis aims to increase the link between modelling techniques and application for industry use. In Chapter 4 a hybrid method that combines two of the numerical modelling techniques described is developed and validated.

An important aspect of wind farm design is the social impact it has on local communities, as the general public is particularly influential in the decision making process. This is where it crucial to understand the process by which wind developments go through town and regional planning and how this works with the engineering design to yield maximum success. The next chapter discusses the practical and policy application of wind farm design and the effects it has on optimising land-use and energy yield.

# 3 THE PRACTICAL AND POLICY APPLICATION OF WIND FARM DESIGN

## 3.1 Introduction

Planning consent for onshore wind farms has become a contentious issue in the UK as the push for renewable sources of energy sometimes comes up against intense community resistance on grounds of visual impact and potential impacts of noise, and on health and safety. At the very least this can lead to considerable delays and often rejection of applications for wind farm developments. Of the total number of applications for onshore wind farms per year in the UK, on average up to 50% of those do not pass the planning application stage, as shown in Table 3.1. UK governments have used a range of mechanisms to help stimulate wind farm development as part of a broader strategy of market-based energy decentralisation. Initiatives include: a generous Feed in Tariff (FiT) introduced in April 2010 (but reduced after August 2011 because of concerns the coalition government had with the disproportionate amount of

funds that developments in England would receive in comparison with the rest of Europe [79]); and greater support for renewable energy development in national planning policy, including regional targets for renewable energy generation and targets for on-site renewables in major new developments.

**Table 3.1 Total number of wind farm applications accepted and rejected per year in the UK from 2006 – 2011, from** [11]

| Year | Number approved | MW approved | Number rejected | MW rejected |
|---|---|---|---|---|
| 2011 | 84 | 1109 | 84 | 860 |
| 2010 | 82 | 1357 | 83 | 1238 |
| 2009 | 97 | 1324 | 67 | 760 |
| 2008 | 72 | 1780 | 51 | 1563 |
| 2007 | 63 | 1145 | 48 | 869 |
| 2006 | 38 | 877 | 31 | 669 |

Given the emphasis on visual amenity, noise, and wildlife as the main source of public opposition and application refusal, wind turbine impact has tended to be seen primarily as the domain of landscape assessment and local environmental impact [80]. This is perhaps understandable given that those impacts tend to determine whether wind turbine planning applications are refused or accepted, but as will be discussed, that also reflects the fact that questions about viability or efficiency of the development is left as a matter for the developer. This has been reinforced by difficulties in bringing climate change mitigation impacts into established Environmental Impact Assessment (EIA), either because calculating the greenhouse gas reduction is fraught with difficulties or there is resistance to including detail on climate change mitigation [81]. Even where $CO_2$ emissions could be calculated, there would still be difficulties in weighing this environmental benefit against other environmental or ecological impacts. This issue is compounded by the fact that in countries like the UK, engineering aspects,

and specifically the energy yield, is neither a matter for public debate nor consideration in the process of planning consent. This is curious as it might be expected that from the perspective of efficient decentralised energy investment, the energy output of the wind farm should have some bearing in determining whether or not a proposal is appropriate. This is especially the case where a trade-off is being made between visual amenity and renewable energy generation (siting arrangements and energy yield), particularly in a country with a high population density such as the UK.

Questions of energy yield are notably absent from growing literature on planning for wind turbines. The aim of this chapter is to consider whether and how questions of energy yield and especially the optimisation of favourable sites should be brought into the consent regime for wind turbine development. This analysis covers Environmental Impact Analysis and broader land-use regulations and reflects a concern that public policy should aim to maximise the return from wind turbine developments both in terms of the sunk costs invested in the turbines and the limited resource of land. The focus for this investigation is the UK planning system. As planning theorists are quick to point out, national planning systems are all distinctive, if not idiosyncratic, in their regulatory emphasis and legal basis. The context for decentralised energy provision also varies widely between countries in terms of incentive structures and ownership rules, though the remit of state regulation of wind turbines is broadly similar. While the focus is on the UK planning system, the issues described may be of relevance to other national contexts.

This chapter begins by first looking at the UK planning consent regime from the 'engineering perspective' of energy yield. Energy yield is a developer's responsibility and the effect this can have on siting decisions is then analysed. From this, arguments

for changing the consent regime are made by drawing on examples from Denmark and Scotland. The analysis draws on a policy analysis and interviews with local planning officers in England and Scotland.

## 3.2 Placing Energy Yield within the UK Wind Turbine Consent Regime

In countries such as the UK, wind turbine development has been highly controversial. This controversy reflects concerns about potential visual, noise and health impacts in a context of significant level of societal and political opposition, especially to the visual appearance of wind turbines. In this context of broad opposition, the process and methodology of impact assessment has become crucial for those seeking to develop or prevent wind farms. As Selman [82] argues, the UK may be entering an era in which citizens are "learning to love" the low-carbon landscape, but this is a slow process.

The UK planning system is a discretionary system in which individual applications are assessed by weighing up impacts and other material considerations. This is currently a plan-led system strongly influenced by national guidance within the National Planning Policy Framework (NPPF) [83], which replaced the previous system of national planning policy guidance in 2012. Elected members acting on officer recommendations take decisions locally, but applicants can appeal to national government. In general, the UK government policy has become more supportive of wind farm development, and this is reflected in the 2012 NPPF. The environmental role discusses the responsibility of mitigating and adapting to climate change including moving to a low carbon economy [83]. The previous coalition government (2010-2015) has also been seen to be strengthening its current policy views by the removal of John

Hayes from the Department for Energy and Climate Change (DECC) due to his very vocal opposition of onshore wind turbines [84].

In adherence with EU regulations, wind turbines will be expected to go through an Environmental Impact Analysis (EIA). The EIA is now a well-established method used around the world and is a tool that takes into account the likely significant effects of a development and are objectively analysed, playing an important part in determining the final decision.

For a wind farm the EIA is likely to cover [85]:

- Construction and infrastructure impacts;
- Landscape and visual impacts;
- Noise impacts;
- Ecological impacts;
- Hydrological impacts;
- Archaeological impacts;
- Electromagnetic interference;
- Public health and safety;
- Socio-economic effects both positive and negative;
- Wider global environmental benefits.

The concern of this research is with the assessment of energy yield from a wind turbine or wind farm. In assessing applications, planning authorities weigh up the costs and benefits; however, the 'benefits' is in the general contribution of decentralised energy. Whilst, in theory the specific energy contribution in terms of energy yield might be cited as a material consideration in favour of the development, it can also be placed under the EIA criteria of 'socio-economic affects both positive and negative' and 'wider global environmental benefits.' Therefore, the issues with the energy yield element of the

equation raises concerns to what extent is it seen to be mitigating some of the other impacts, such as visual intrusion. There is suggestion that the EIA should not consider climate change as the environmental impact is negligible [81]. The issue of mitigation extends to how a single wind development can have an effect on the overall reduction of global greenhouse gas emission, when on this scale any net reduction is deemed insignificant. This approach is somewhat constrictive, as only focusing on a single development is compounded by the fact that impact assessments are reviewed on a local case-by-case basis rather than within a cumulative regional or national framework. Therefore, while the topics covered by the EIA are crucial for the wind farm planning process, the EIA framing of wind turbine development impacts is likely to mitigate against climate change goals.

The EIA process raises questions about the weight given to energy yield in conflicts over wind turbine development. However, in most marginal cases where considerations of maximising energy yield might make a difference, it is prevailing planning policy guidance that determines the weight that can be given to various arguments for and against wind turbine development. It might be expected that where governments are seeking to facilitate renewable energy development but face intense opposition, policy-making ought to include some consideration of energy yield from wind turbines. This might indicate whether a sensitive site is being used effectively or indeed, whether a developer should be given state subsidy in the form of a feed in tariff (FiT) or such like. This is where the issues of energy yield and ultimately, engineering play a key role, because from an overall perspective it fundamentally determines the viability of a development, not only financially, but environmentally too.

An impact that is not quantifiable through the planning process is how renewable energy is beneficial in order to reduce carbon emissions and provide future energy security in the UK. It could be argued that by including values regarding energy yield and the overall effect it has in the context of energy security may sway public opinion and decision making for wind developments. This is especially relevant in the context of visual amenity that is highly sought after by the public.

However, in countries like the UK, questions of energy yield from wind farm developments are in effect a matter of development viability that is left to the developer. Moreover, if the UK is moving to a system in which energy yield was a material consideration in EIA or development control, it raises questions about how this should be achieved and also the capacity of the regulators to assess the potential energy yield. This issue is explored in more detail in the following sections, which looks at current developer's responsibilities and how siting decisions are made.

### 3.2.1 Energy Yield as a Developer Responsibility

The UK planning system has tended to become reactive and market-driven [86]. For wind turbines, developers apply for planning permission by providing the fixed locations for wind turbine placement and infrastructure. This siting is primarily based on developer understanding of prevailing wind direction, turbine performance, and the ability to be connected to the grid. It is also essential that a siting layout must be optimised, as it will minimise the need for repowering (the process of replacing multiple turbines with a single more efficient one), which would prove expensive. However, within the UK system, the precise location of wind turbines has to be fixed and agreed upon prior to development. Altering the siting of wind turbines to improve efficiency and output in response to site conditions would require a new planning

application. This approach sits uneasily with the difficult task of predicting the aerodynamics of the terrain and atmospheric conditions of the region.

There has been considerable research into optimising the power output of a wind farm via the placement of the wind turbines themselves [44], [46], [76], [87]–[90] and most notably the work carried out from Risø National Laboratories in Denmark on the European Wind Atlas, providing comprehensive wind statistics [91]. The issue of wind turbine siting is important for overall energy yield and relies heavily on how each turbine is placed with respect to its surroundings and more importantly, other turbines. The importance of using the designed siting configuration is of paramount importance, as it will determine the total power output, which ultimately affects the ability for the wind farm to succeed. To emphasise the sensitivity of wind turbine siting, this area of research has been reviewed. An example is the work carried out by Husien et al. [89] which found that a wind farm consisting of 16 wind turbines aligned in a single row, with all facing the optimal wind direction is 20% more efficient than if the same 16 turbines were placed in a 4x4 square arrangement. Another example looks at how the terrain plays an important role for efficiency; Røkenes & Krogstad [46] shows that placing a wind turbine on top of a hill can yield an increase in wind speed of up to 15%, which is advantageous for maximum power output (for example a doubling in wind speed gives a factor of eight increase in wind power). In this case a 15% increase in wind speed yields a 50% increase in power in the wind due to the cubic relationship between wind speed and power in the wind (Equation (4.9)). Meyers & Meneveau [44] looked into the optimal spacing between wind turbines and found that for realistic cost ratios (land surface and turbine costs), the ideal average spacing is 15D apart, which is considerably higher than the current 7D often used in wind farms. This distance allows

for the wake caused by the rotating blades to dissipate (recover) enough so that it has a minimal effect on downstream turbines. Therefore, an ideal layout would be a single line of wind turbines facing the oncoming wind placed on top of a hill; however, this is the configuration most likely to meet opposition for reasons of visual intrusion if nothing else.

### 3.2.2 The Limits to Wind Turbine Assessment

In order to illustrate the impact that the lack of an energy consideration has on scheme approval, the following section examines three cases of planning for wind turbines in the North of England. The three examples are taken from a single local authority area and reflects different constraints on effective planning for energy yield. The local authority is generally supportive of wind turbine developments and has a wind energy target of 34 MW by 2021 [92]. However, there has been intense opposition to development in sensitive rural areas that offer the most potential for wind energy.

**Case Study 1: 12.5 MW Five-Turbine Wind Farm (2009)**

In 2008 a developer applied for permission for a five-turbine wind farm with a height of 125 m to blade tip and combined power output of 12.5 MW, which divided opinion within the local community due to its sensitive location within view of (but not within) the Peak District National Park [93]. The scheme would deliver over a third of the local authority's target of generating 34 MW from wind by 2021. Unusually, the project had approximately the same number of letters of objection as letters of support at 1075 and 1037, respectively. Objections covered a range of issues including noise impacts, highway hazards such as potential distractions to drivers and damage to the roads, ecology impacts that were not specific to the site (impact on bird and bat populations), no benefit to the local communities, and almost all objectors referred to

the landscape and visual impacts. Those in support, including a letter received from New Zealand, were so because wind farms are a carbon free method of producing electricity, tackling climate change, and improving the UK's energy security. It is also worth noting that two neighbouring local authorities objected to the scheme due to the potential impact on visual amenity. The application was ultimately refused because of significant harm to the character and appearance of the nearby National Park.

On one hand, this scheme is an example of the difficulties faced by developers and local authorities in securing consent for wind farms. However, it also points to a missing strategic dimension to policy capable of weighing up the different environmental benefits and costs of the scheme. As decisions are taken on a case-by-case basis there is little or no consideration of the benefits of maximising local or regional energy generation potential as part of a broader renewables/low-carbon strategy.

**Case Study 2: Single Wind Turbine (2012)**

In 2012, Empirica Investments submitted an application for a single wind turbine with a height of 67 m to blade tip, to be located on a farm in a rural area of the district [94]. Footpaths cross the surrounding fields and a byway runs adjacent to the site. The application was then amended, with the assumption being that a smaller wind turbine had a greater chance of gaining approval due to the proposed location within the Green Belt. As a result the height of the turbine was reduced to 55m to blade tip and the output reduced from 0.9 MW to 0.3 MW. Despite this, the conclusion was that $CO_2$ emissions reduction was outweighed by local significant landscape and visual impacts. Ultimately, the wind turbine application was refused, even with compromises made by the developer.

**Case Study 3: 6 MW Three-Turbine Wind Farm (2009)**

E.ON Energy Company applied for planning permission for a three-turbine wind farm with a height of 100 m to blade tip in 2008 to be located on Blackstone Edge; it was granted planning permission in 2009 subject to 27 planning conditions [93]. The developers applied for an amendment to one of the conditions regarding operating noise levels. The original condition limited the maximum noise level to 43 dB during the day and 35 dB at night as observed from two locations. However, the applicant advised that this condition would have significant restrictions on energy output. Therefore, the application sought to vary the condition to permit the noise level limit to be increased as recommended in the Planning Policy Statement (PPS) 22 Companion Guide [95]. It was decided that the original condition was restrictive, therefore, significantly reducing the energy output and a reasonable justification for the amendment.

In this case diminished energy yield meant that the enforced conditions for the development were altered. However, the amendment was only accepted because the noise level limit was more restrictive than the government's suggestion and not solely due to the reduced energy output.

The Blackstone Edge case study is taken further in Chapter 6 from an engineering standpoint, where the visual amenity is placed behind energy yield. Rearranging priorities provides a pragmatic approach to maximising the land-use. In Chapter 7 the discussion analyses how the changes from the case study may affect planning implications and what this says about renewable energy policy.

### 3.2.3 The Capacity to Manage Siting Decisions

So far the argument has been that the UK consent regime is inflexible when it comes to the detail of site location, but the detail of site location can have a significant

impact on the energy yield of wind farms. In the UK the tension between these issues has tended to be played out around the dispute of minimum distances between dwellings and wind turbines on grounds of visual and noise impacts. Local authorities seeking to constrain wind farm development have sought to impose minimum distance requirements and wind farm developers have challenged this. Milton Keynes Council is an example of this; they tried to set a minimum distance of 1000 m for wind turbines over a height of 100 m [96]. However, RWE NPower challenged this motion as they were looking to build two wind farms in the area, arguing that the local authorities had no power to do so.

It is argued that wind turbine siting might need to be more flexible if energy yield is to be maximised. However, this poses challenges of technical capacity within the regulatory regime. All the planning officers interviewed during this study agreed that the level of knowledge provided by the government is sufficient, despite stating that the guidance is a bit "woolly." Notwithstanding the recent introduction of the new NPPF [83] that supersedes existing planning guidance, planning officers rely heavily on the PPS22 Companion Guide [95], which is still the best guidance available. This further inhibits energy yield considerations, as the document is out-dated for both technical information and renewable energy objectives. However, there is a desire for better clarity on siting issues such as a minimum distance between wind turbines and dwellings, as in the UK none exist at present. In most UK local authorities there are technical trained staff within local councils who can assess noise impact, landscape impact and environmental health, but often there is no in-house professional engineer to consult on wind turbine placement and maximising energy yield. Some local authorities do offer relevant courses for their staff to gain knowledge in this area, but it

is not a necessity and one planning officer was even said to use "Google" as a final resort in solving engineering related issues. Introducing a stronger regulatory emphasis on energy yield either through planning consent or EIA would require access to technical knowledge and expertise that is currently beyond local authorities, especially if developers were to be held to account on promised generation capacity.

### 3.2.4 Developer Interaction

Throughout this thesis there have been various interactions with a small renewable energy developer, Infinis. As a developer they have high levels of success with onshore wind developments and minimising the planning process times. There are many considerations that have to be taken into account through the early stage of development and putting together the planning application, these include:

- Choosing a site;
- Maximising land-use within the land ownership boundary – initially this is done by maximising potential energy yield;
- A minimum wind turbine separations – 5D (prevailing wind direction) and 3D (perpendicular to prevailing wind direction);
- Ecology – minimum of one-year bird monitoring;
- Wind mapping – measurement masts placed every one square km apart;
- Noise – this helps determine the choice of wind turbine model;
- Radar limitations;
- Visual – this helps determine the maximum tip height of the wind turbine;
- GIS mapping constraints – dwellings, paths, streams, boundaries, a maximum gradient of 14% for delivery of wind turbines blades and, a maximum gradient of 20% for wind turbine placement.

Once consent is given then the developer determines what model of wind turbines should be used on the site. This process is largely influenced by wind turbine manufactures and their wind server management system, with the ideal case of maximising energy yield given the constraints of planning policy.

However, the industry is entering a new period in terms of onshore wind energy. The majority of sites with ideal wind conditions and probable chances of gaining planning permission already have wind farms in place. This leaves developers fewer options without policy change occurring, as there are sites in the UK that have been phased out through policy constraints because of visual impacts, such as national parks. As a matter of practice developers are beginning to overcome this hurdle by involving the surrounding communities in the development process. The general public can be influential in the decision making process, which has bearing on the design of a wind farm. This becomes especially important when choosing a site because one of the most difficult aspects of development is gaining permission from land owners.

### 3.2.5 Argument for Changing the Consent Regime

Planning policy could become more interventionist in identifying optimal wind turbine developments and ensuring that prime sites are maximised in terms of energy yield and the overall use of land. To some extent this is already achieved through the market-based system given the incentives on developers to maximise the returns on their investment (if a wind turbine farm is inefficient it will generate less revenue under a FiT scheme and so be less of a financial burden on government revenues). Yet to the extent that wind turbine development often depends on some sort of state subsidy, then governments might have an interest in ensuring that wind farm efficiency is optimised. It might be a case that the yield from wind turbines is something that should be weighed

up against other impacts in planning decisions (such is described in the EIA section above). Finally, the lack of flexibility present also means that developers cannot put multiple potential layouts forward, so should one arrangement be refused, the planning officers cannot currently move on to a provided 'Plan B'. A backup option would allow developers to devise alternate plans that engineers have established as a reasonable compromise in the event there is local opposition. A process of zoning areas where onshore wind farms can be placed in parts of the UK is an aspect of policy that would need to be introduced if renewable energy in the UK is to continue to grow. This would provide developers with national guidance and a greater possibility to maximise chosen sites. The discussion of what occurs to optimal sites that are coming to the end of their 25 year life span is also beginning to appear as some of the first wind farms are now reaching this point. Arguably, these are the sites that should continue to be used for onshore wind purposes and an option for this is through repowering. Both these points are discussed further in the next section by the way of a comparison with countries already doing it.

### 3.2.6 International Comparison

As seen previously, the UK consent regime has a particular approach to wind turbine regulation. This section looks at the approach used in Scotland and Denmark; Scotland because land-use regulation has a common basis with England, but a different system of land-use planning regulation; and Denmark because it is often seen as an exemplar in onshore wind turbine development [86].

The System for EIA in Scotland and Denmark is similar to that of England. In those countries, energy yield (i.e. climate change offsetting) is generally not a detailed consideration for EIA. What is however noticeable is that onshore wind turbine

development is more supported within national planning policy. Of particular interest is how Denmark and Scotland use land zoning to steer siting decisions. The issue of zoning is relevant because it involves a strategic decision about where the presumption should be in favour of wind turbine development and areas that should be avoided. This sort of approach had started to be introduced in English regional planning during the early 2000s with regional planning authorities required to identify sites for a certain level of renewable energy generation [95]. The shift away from regional planning has removed requirements for regional planning and regional renewable energy targets, but the zoning approach is hinted at in the NPPF under section 10, "consider identifying suitable areas for renewable and low carbon energy sources" [83].

Scotland has perhaps been more proactive than England on wind turbine development, reflecting a strong emphasis on national energy security via renewable resources and the country's potential for wind power [97]. Scotland, like England, has sensitive landscapes. One way of reconciling increased renewable energy generation and landscape protection has been for Scottish Natural Heritage to set out a system of zoning for wind turbine developments with a three-zone sensitivity approach [97]. Zone 1 represents the lowest natural heritage sensitivity; these areas are least sensitive to wind farms with the greatest opportunity for development (70% approval rate) and covers 15% of Scotland's land area. Zones 2 and 3 represent medium and high sensitivities, respectively, with applications unlikely to be accepted (a maximum of 30% successful applications in Zone 3). Zone 2 comprises of 55% of Scotland's land area with Zone 3 the final 30%. However, these zones do not take any consideration of energy yield, wind speed and direction, and siting optimisation; instead, visual amenity and landscape heritage are the primary concern.

The Danish government identified renewable energy sources as an important policy and used incentives and subsidies to encourage development [86]. Denmark began with clear objectives in terms of renewable energy in the 1990s, which allowed for potential development zones to be established [98]. This reflects a clear understanding between the general public and the drive for sustainable energy sources, especially as an Energy Agreement in Denmark means developers must offer at least 20% of the ownership to people living within 4.5km of the site [99]. This cooperative ownership contributes significantly to the success in securing public support and acceptance.

Denmark also reviews and updates its wind turbine development plan (to achieve set renewable energy targets) every four years, as it is recognised that the correct regional locations must be identified because wind strength has direct economic implications for energy yield and minimising the number of turbines required in a development area [86]. This process of 'zoning' means that different areas are designated as appropriate for the following types of development: individual wind turbines, local wind farms and clusters, and large-scale region wind farms as well as zones where development is strictly prohibited. The zones are clearly laid out and remove certain subjective arguments from the planning process. The public are also encouraged to directly enter debates on all aspects of wind development planning issues, with the relevant authorities holding seminars and meetings and even allowing those who are interested in helping select potential development sites [86].

However, one particular area that relates directly to the energy yield and efficiency of wind farms is the repowering scheme that Denmark has introduced. This scheme was implemented to reduce the total number of wind turbines by replacing an

array of small turbines with a single larger and more efficient one. As a result of the repowering subsidy in addition to the FiT, a total of 1208 wind turbines were removed between the years 2000 and 2003, but with an overall increase of 202 MW in capacity [99]. This clear appreciation of technical knowledge from the national and local governments means that wind developments are kept as viable as possible, along with providing the public with benefits and assurance for their support.

## 3.3 Summary

This chapter has highlighted the 'engineering dimension' of wind turbine assessment, emphasising potential shortcomings in current approaches in countries like the UK. The particular concern has been about optimisation of the potential for energy generation and energy yield issues in the planning consent for wind farms. The argument is that this dimension is somewhat marginalised in EIA and land-use planning consent regimes. The energy yield gap runs counter to the ideal of maximising investment in energy decarbonisation, as local authorities have less concern with optimising wind farm layouts, despite having to meet local renewable energy targets. The research has suggested that there are various reasons why regulators might seek to integrate planning with energy yield more centrally into the consent regime. The advantages would include being able to weigh up energy yield against oppositional factors, and also using energy yield considerations to inform a more flexible approach to siting. If access to technical knowledge for planning officers could be increased, this will allow the engineering aspect of an optimal energy yield to determine whether a development is viable and, therefore, beneficial to the nation; as well as removing some of the more subjective reasons for rejection, such as visual and noise impacts. However, some of the challenges this could meet have been pointed out.

It is concluded that the current approach of the EIA and land-use planning is restricted in terms of energy yield, as the focus is on the impact of a single wind development detached from broader local or regional renewables strategy. One solution would be to situate wind turbine development within a process of energy zoning in which priority locations are identified on the basis of their potential energy yield, including or excluding areas that pose difficulties in terms of landscape/visual amenity or wildlife protection. Those sites would have a degree of flexibility for detailed wind turbine design and location within an overall brief that would set the parameters for development.

However, what is abundantly clear is that there is a need to produce engineering solutions that allow developers and planners to determine the performance of wind farms for given locations and layouts. The methods described in the next chapter aim to show the development process of how this can be achieved.

# 4 METHODS: EXPERIMENTAL AND NUMERICAL

## 4.1 Introduction

The aim of this chapter is to describe the experimental techniques employed and the development of the various models used for all the CFD simulations carried out in this thesis. The techniques were designed with the intention of being able to determine the performance of a wind turbine within a wind farm layout. In order to achieve this, models and simulations of increasing complexity have been established, with each level applying the proven techniques of previous runs. An explanation of experimental work carried out is first described, here the wind tunnel facility, experiment design, and measurement techniques are discussed. The numerical domain of the wind tunnel is presented in which the boundary conditions, mesh independence study, and chosen turbulence model are laid out. Then the process by which the wind tunnel experimental data is used to validate the CFD application of actuator disc theory is explained. Next there is a description of a full rotor model and how it is used in combination with the

validated actuator disc methodology. This novel hybrid technique is then tested to determine time step size and time required to reach convergence. Finally, brief explanations of numerically modelling terrain, ABL, and scaling of the full rotor model are discussed.

Used throughout this thesis is the widely available CFD package Ansys Fluent 14.0 along with the meshing software Ansys ICEM.

## 4.2 Validation and Verification: Actuator Disc Method

The actuator disc (AD) technique, as described in Section 2.5.1, is used to replicate the rotor of a wind turbine as it is able to reproduce the flow characteristics of the far wake region to a high level of reliability [57]. However, the application of the method used in this research must first be validated before use in performance analysis of wind farms. This is carried out in a two-stage process. First, with a wind tunnel experiment, by measuring the velocities of the wake and increasing the distance behind a metal mesh disc. The second replicates the wind tunnel test section numerically, and involves close attention to mesh independence, turbulence modelling, and boundary conditions.

### 4.2.1 Experimental Methods

The Department of Mechanical Engineering at The University of Sheffield has a low-speed wind tunnel (Figure 4.1), which has been used for all the experimental work carried out in this thesis. The wind tunnel is an open circuit suction tunnel, driven by an eight-blade axial fan positioned at the outlet. The flow enters the inlet, going through a honeycomb mesh (with cells 0.01 m wide and 0.1 m long) that straightens the flow and breaks any large-scale flow structures. The flow then streams through a fine 1 mm cell mesh to further break down flow structures as well as evening out the flow with the generation of small scale turbulence and a pressure drop. The flow settles before being

accelerated by a 6:1 contraction section leading to a turbulence grid at the entrance of the 1.2 m high x 1.2 m wide x 3 m long test section. The 0.025 m x 0.025 m turbulence grid generates a turbulence intensity ($T_u$) of approximately 1% at the midpoint of the test section. The fan itself is controlled using a variable frequency drive that allows for precise fan speed settings with a 1 rpm resolution, with a potential maximum speed of 900 rpm, which produces a wind speed of up 25 $ms^{-1}$. However, due to safety restrictions a maximum velocity limit of 10 $ms^{-1}$ was enforced throughout.

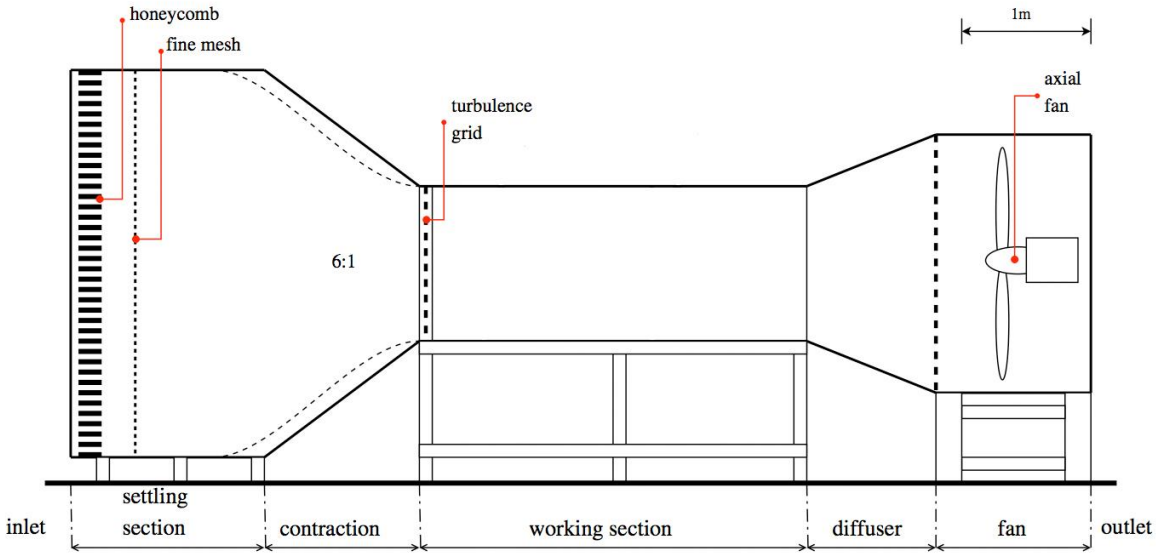


Figure 4.1 Wind tunnel schematic (not to scale).

#### 4.2.1.1 Experiment Design

A 100 mm in diameter metal mesh disc was used to replicate the rotor of a wind turbine; the disc has an open area of 45%, with a wire diameter of 280 μm and a nominal gap aperture of 0.57 mm. By application of actuator disc theory, the resulting measured induction factor is 0.34 (see Section 2.5.1) was inferred by the effect the mesh disc had on velocity directly downstream. A typical wind turbine has an induction factor of approximately 0.11. The disc is attached to a 400 mm high rod that can be attached to

a removable floor in the wind tunnel that allows the disc to be placed in various positions of 200 mm apart, or 2D. Figure 4.2 details the final experimental design, it allowed for wake measurements downstream at 2D, 4D, 6D, 8D and 10D, which were taken at velocities 10 $ms^{-1}$, 7.5 $ms^{-1}$ and 5 $ms^{-1}$.

Using a reference length of 0.1 m (the diameter of the actuator disc), the Reynolds number of the mesh disc at 10 $ms^{-1}$ is $6.18x10^4$, which is two orders of magnitude lower than that experienced by full size wind turbines. However, the Reynolds number becomes less important when modelling the far wake [35], [100], but this will still affect the overall correctness of the results. Whale et al. [101] also showed that the characteristics of the wake are mostly independent of the blade Reynolds number. Therefore, validating the AD method in a wind tunnel using a scaled model will not affect the overall correctness of the results.

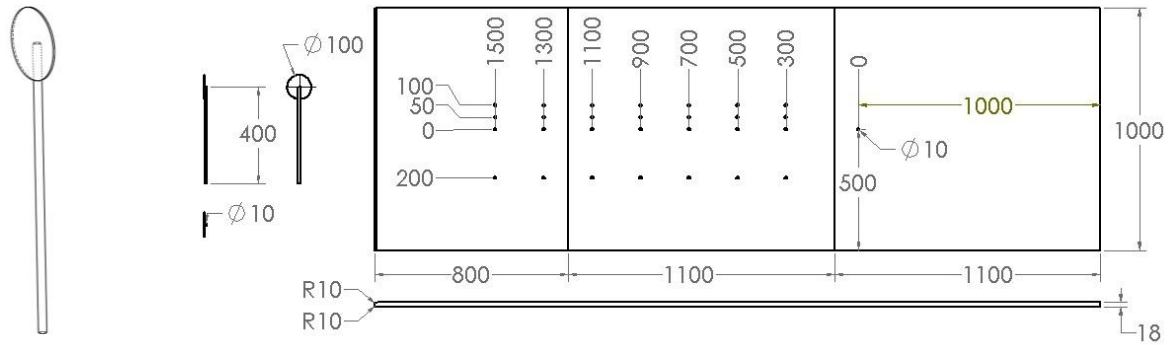


**Figure 4.2 Drawings of the actuator disc (left) and the experiment dimensions (right).**

### 4.2.1.2 Measurement Techniques

In order to determine the uniformity of the flow within the wind tunnel test section, the velocity profile was measured across the width in the plane that the actuator disc sits. A Pitot-static tube was traversed across the working section horizontally at 0.05 m intervals and the fan was kept constant at 250 rpm throughout.

The wind velocity was calculated using Equation (4.3), which relates Bernoulli's equation (Equation (4.1)) and the measured pressure difference (Δp) to velocity (V) using the ideal gas law (Equation (4.2)). This required the temperature ($T_{ab}$) inside the test section and the atmospheric pressure ($p_{atm}$) to be taken at the start of each test in order to determine the density of the air ($\rho$).

$$\Delta p = \frac{1}{2}\rho V^2 \tag{4.1}$$

$$\rho = \frac{P_{atm}}{RT_{ab}} \tag{4.2}$$

$$V = \sqrt{\frac{2(\Delta p)}{\rho}} \tag{4.3}$$

The velocity profile within the area that the experiments took place can be seen as uniform across the test section (Figure 4.3).

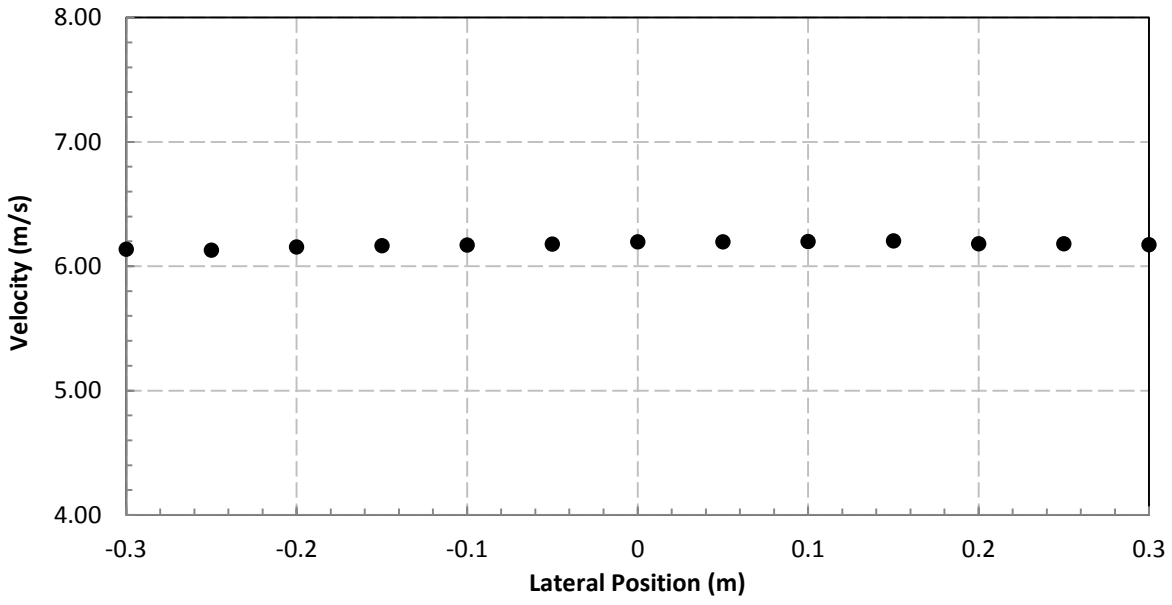


**Figure 4.3 Velocity profile across the wind tunnel test section.**

A study to determine the level of turbulence was conducted by Danao [102] in order to match turbulence intensity ($T_u$) decay in the wind tunnel to the later CFD

simulations. Measurements were taken using a constant temperature hot-wire anemometer in increments of 0.2 m. Danao [102] used a logging frequency of 100 Hz. The hot-wire data was taken over an average of 30 seconds, along with the last 25 seconds from the manometer, were used to compute the coefficients of a simplified form of King's Law Equation (4.4) for hotwire anemometry using a simple least-squares curve fitting method.

$$V^2 = A + B \cdot U^n \tag{4.4}$$

Where V is hotwire voltage, U is wind speed, and A, B, n are constant coefficients (n~0.5). It was observed (Figure 4.4) that at $x$ = 0.4 m from the test section inlet, $T_u$ = 3.43%, before rapidly decaying to 1.80% at $x$ = 0.8m. When it reached $x$ = 1.4 m, the turbulence intensity had fallen to 1.04%.

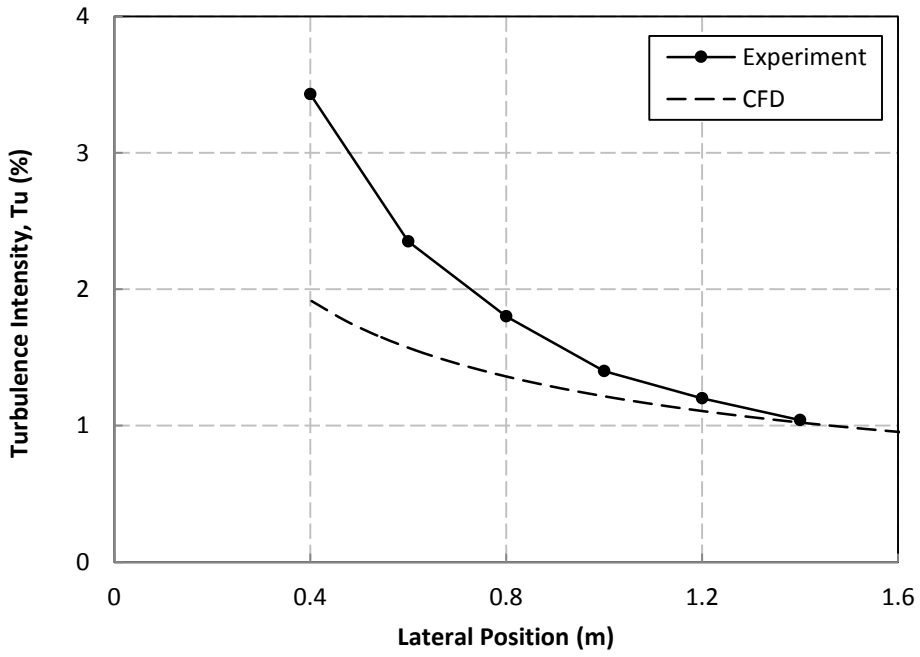


**Figure 4.4 Comparison of turbulent intensity between CFD and wind tunnel experiment (x=0: test section inlet), experimental data from** [102].

The experiment velocity measurements were taken using a pitot-static probe, where the pressure difference was measured using a Furness Controls Micromanometer (model FC0510), providing a velocity accuracy of +/-0.5%. The probe was attached to a manually controlled traverse system (Figure 4.5) and readings were taken horizontally along the centre line at 10 mm intervals behind the disc and at 20 mm apart either side. Due to the nature of the techniques employed for recording measurements, each experiment was repeated five times to yield a confidence interval of 99%.

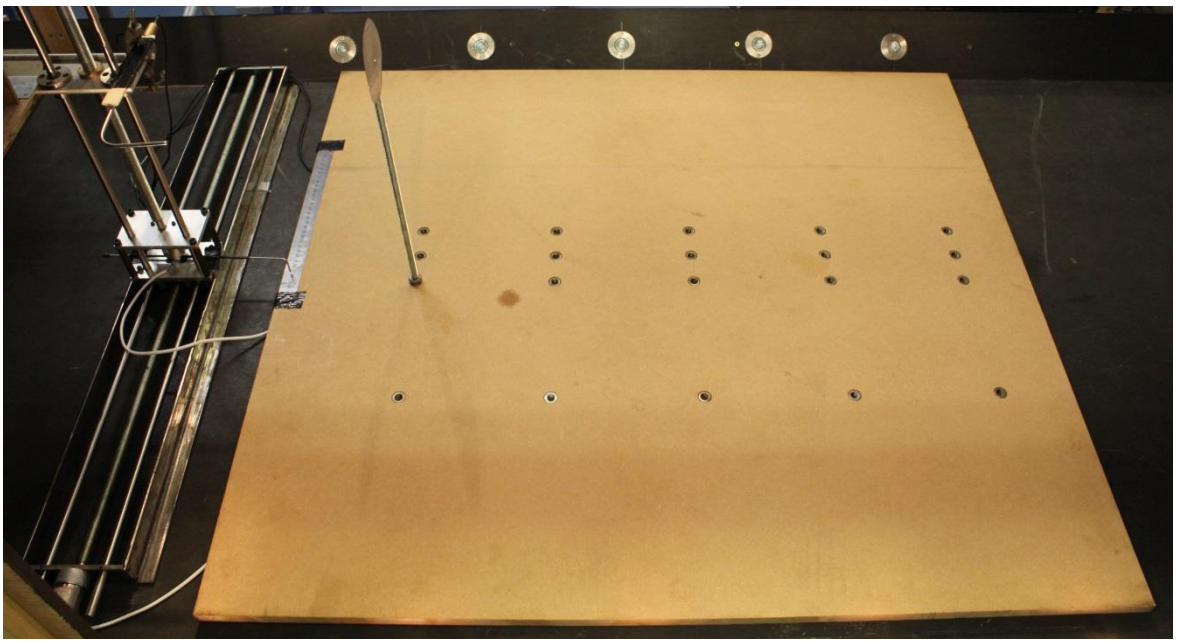

**Figure 4.5 Traverse system, Pitot-static tube and actuator disc set up in the wind tunnel.**

### 4.2.2 Numerical Methods

The wind tunnel experiment carried out is for the purpose of validating the CFD application of the actuator disc theory. By confirming the uniformity of the wind tunnel, and matching the conditions for later CFD simulations, it can be said that the experimental results are adequate for their required purpose. The results in themselves are only of interest when compared to their numerical counterpart.

#### 4.2.2.1 Boundary Conditions

A pressure-based solver was selected because of the use of incompressible flow, along with the coupled algorithm to increase efficiency. Initially, all discretisation terms were set to 1st order for the starting 200 iterations to encourage convergence, before being switched to 2nd order for increased accuracy. The boundary conditions (Table 4.1) have been applied so that it replicates the flow field characteristics of the wind tunnel. It was found that an initial $T_u$ of 8% and turbulent viscosity ratio of 14 yielded a matching $T_u$ at the point the actuator disc is placed within the wind tunnel test section (Figure 4.4).

In order to define the actuator disc, Ansys Fluent recommends boundary conditions based on experimental data [103]. Experimental data from the wind tunnel in the form of pressure drop against velocity through a porous disc (actuator disc) was extrapolated to determine the coefficients of the medium. In order to replicate the mesh disc qualities used in the wind tunnel for CFD purposes, the following process was applied. An *xy* curve is plotted to create a trendline through these points yielding the following:

$$\Delta p = aV^2 - bV \tag{4.5}$$

where a and b are constants, Δp is the pressure drop, and V is the velocity. Using a simplified version of the momentum equation, relating the pressure drop to the source term can be expressed as:

$$\nabla \mathrm{p} = S_i \tag{4.6}$$

or

$$\Delta p = -S_i \Delta n \tag{4.7}$$

Hence, comparing Equation (4.5) to Equation (4.7) yields the following curve coefficients:

$$a = C_2 \frac{1}{2} \rho \Delta n \tag{4.8}$$

Where $\rho$ is the density of air, $\Delta n$ is the porous medium thickness, and $C_2$ is the inertial resistance factor, which in Fluent is called the Pressure Jump Coefficient. The Face Permeability, α, which is calculated using the viscous inertial resistance factor, $\frac{1}{\alpha}$:

$$b = \frac{\mu}{\alpha} \Delta n \tag{4.9}$$

**Table 4.1 Boundary conditions used for CFD simulations of the wind tunnel.**

| **Boundary Type** | **Specific Condition** | |
|---|---|---|
| **Velocity Inlet** | Velocity Magnitude | 10 $ms^{-1}$ |
| | Turbulent Intensity | 8% |
| | Turbulent Viscosity Ratio | 14 |
| **Pressure Outlet** | | |
| **Floor (Wall)** | Roughness Height | 0.0015 m |
| **Top, Sides (Wall)** | | |
| **AD (Porous Jump)** | Face Permeability | 2.57 x $10^{-8}$ $m^2$ |
| (Represents an induction factor of 0.34) | Porous Medium Thickness | 0.0025 m |
| | Pressure-Jump Coefficient (C2) | 807.03 |

#### 4.2.2.2 Mesh Independence

A three-dimensional CFD model of the wind tunnel section was built in Ansys ICEM. The number of elements used in a mesh of this kind of domain must be optimised before applying a full simulation; this reduces the computational cost and time required to reach convergence. For the wind tunnel domain, three independent studies were carried out that looked at the optimal number of cells in the axial direction (x-direction), lateral direction (z-direction), and across the AD (y and z-directions). The number of cells in the y-direction above and below the disc has been prescribed based on

recommendation for surface boundary layer modelling [104], which yielded 19 cells below and 30 cells above the actuator disc.

In the x-direction the actuator disc itself is thin at only 2.5 mm (2.5% of a turbine diameter), therefore, the thickness in terms of mesh remains constant at two cells for all cases in the study. The actual required thickness of the AD is applied within the boundary conditions of Fluent. Table 4.2 shows the test matrix of all the simulations carried out in the mesh independence studies.

**Table 4.2 The test matrix for the mesh independence simulations carried out for the wind tunnel domain.**

| Test Number | Number of Cells | | | | | | |
|---|---|---|---|---|---|---|---|
| | x-direction | | | y-direction | z-direction | | |
| | Upstream | Disc | Downstream | Disc | Left | Disc | Right |
| **Axial Direction** | | | | | | | |
| **1** | 30 | 1 | 30 | 7 | 18 | 7 | 18 |
| **2** | 45 | 1 | 45 | 7 | 18 | 7 | 18 |
| **3** | 60 | 1 | 60 | 7 | 18 | 7 | 18 |
| **Lateral Direction** | | | | | | | |
| **1** | 45 | 1 | 45 | 7 | 12 | 7 | 12 |
| **2** | 45 | 1 | 45 | 7 | 18 | 7 | 18 |
| **3** | 45 | 1 | 45 | 7 | 24 | 7 | 24 |
| **4** | 45 | 1 | 45 | 7 | 30 | 7 | 30 |
| **Across Disc** | | | | | | | |
| **1** | 45 | 1 | 45 | 5 | 18 | 5 | 18 |
| **2** | 45 | 1 | 45 | 10 | 18 | 10 | 18 |
| **3** | 45 | 1 | 45 | 12 | 18 | 12 | 18 |
| **4** | 45 | 1 | 45 | 12 | 18 | 14 | 18 |

## Axial Direction

The first study looked at the axial direction, where the free stream flow is introduced at the inlet of the domain. Figure 4.6 shows between tests 2 and 3 the relative change in centre line velocity is negligible, therefore, taking this into account, the numbers of cells in test 2 was used in the final simulations. For some of the simulations there will be two ADs present, thus the number of cells that will be applied

equates to 23 cells/m upstream of the first AD and 45 cells/m downstream each AD thereafter. This is equivalent to approximately 2 cells/diameter upstream and 5 cells/diameter downstream of the AD.

**Lateral Direction**

The second study looked at the lateral direction and the number of cells either side of the AD. For this study the number of cells across the AD itself was kept constant for all cases at 10. Figure 4.7 shows the relative change in velocity across all simulations varied by approximately 0.5%, with the gap between tests 2, 3 and 4 being the smallest. Therefore, test 2 was shown to provide the optimum number, corresponding to 18 cells either side of the AD.

**Across the Actuator Disc**

The final study looked at the number of cells across the AD itself, this is particularly crucial as this greatly affects the velocity deficit of the wake produced, as shown in Figure 4.8. The largest difference in the velocity not only at the disc but either side of it was shown between tests 1 and 2; after this the flow is shown to change very little. Therefore, the optimal number of cells across the AD is 10.

The mesh independence study resulted in a computational domain that consists of approximately 237,000 Hexa elements (when only containing a single AD, as shown in Figure 4.9).

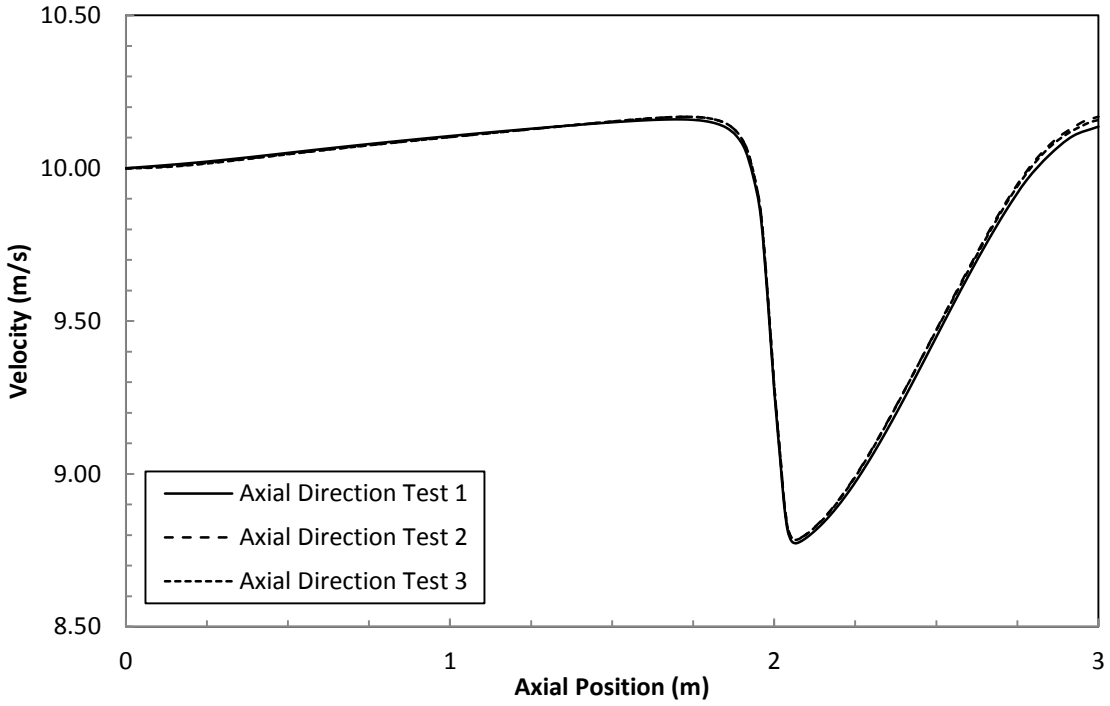


**Figure 4.6 Mesh independence study for the wind tunnel domain in the axial direction. The actuator disc is located at an axial position of 2 m.**

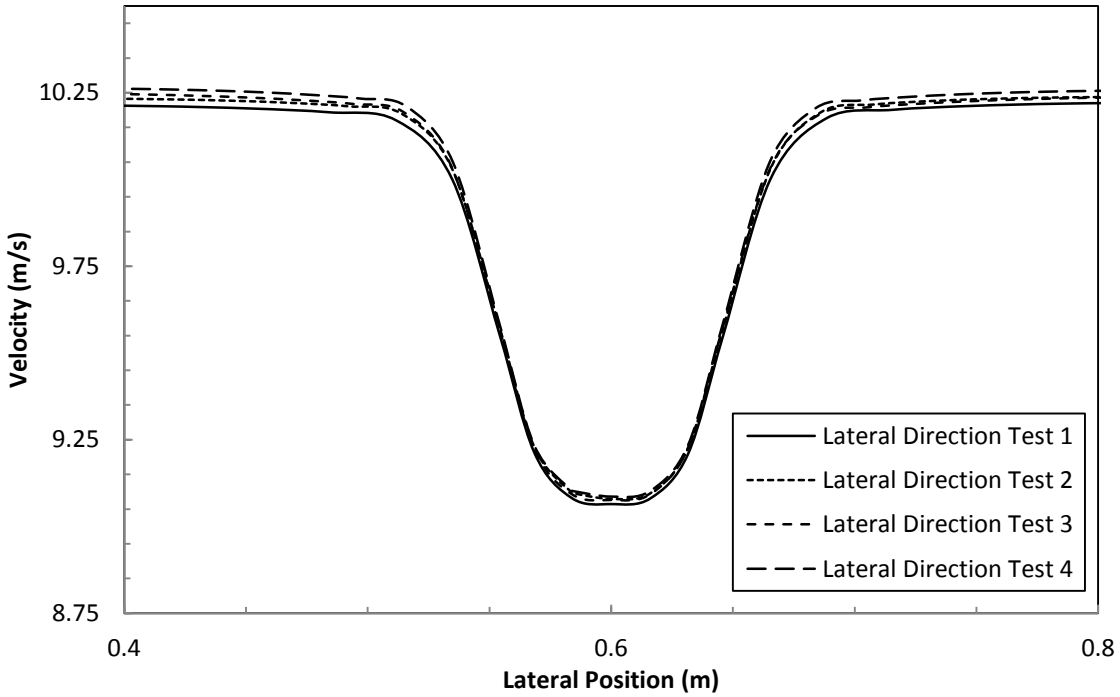


**Figure 4.7 Mesh independence study for the wind tunnel domain in the lateral direction.**

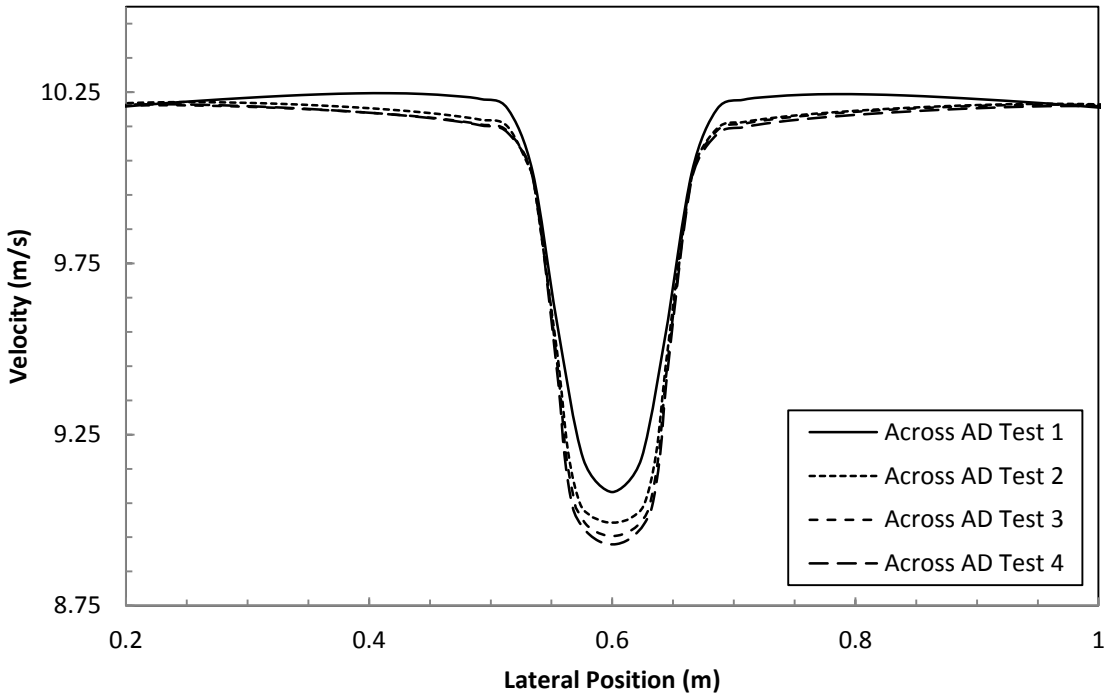


**Figure 4.8 Mesh independence study of the number of cells across the AD.**

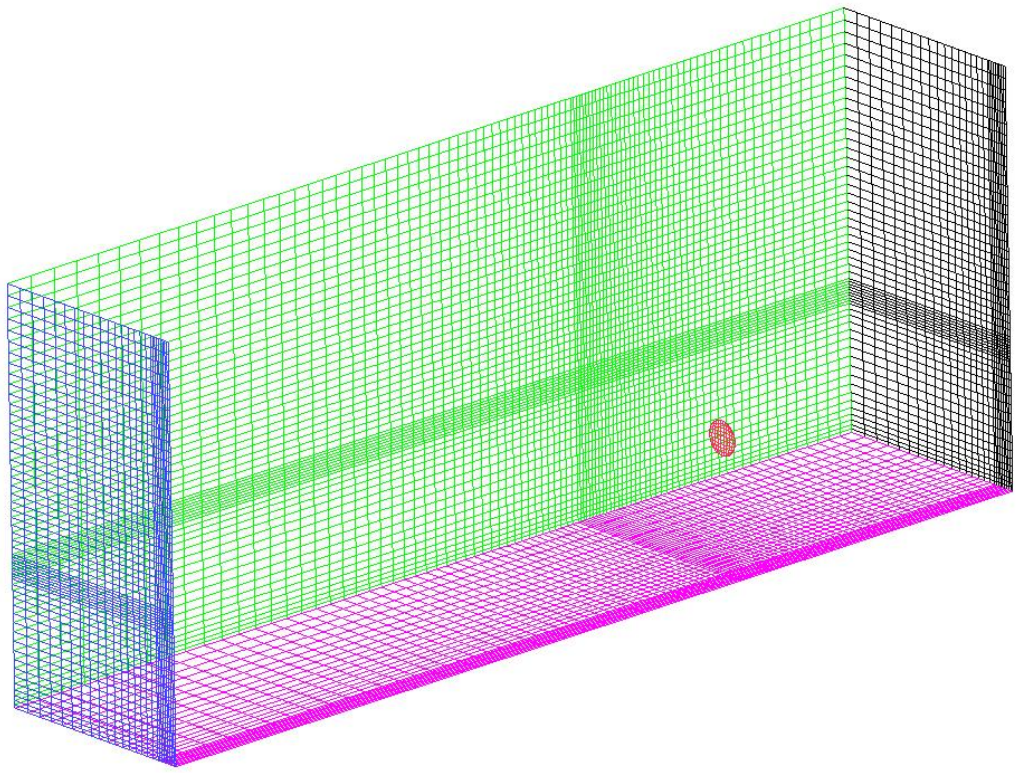

**Figure 4.9 Computational mesh visualising half the mesh topology (but the full actuator disc) for the wind tunnel domain.**

#### 4.2.2.3 Turbulence Modelling

The velocity in the wind tunnel experiments was set no higher than $10ms^{-1}$, this leads to the use of the incompressible Navier-Stokes equations for the CFD simulations. The inlet conditions (Table 4.1) were pre-determined to produce a matching turbulence intensity at the location of the AD observed in the experiment, as shown in Figure 4.4. The decay of the turbulence upstream is not very well matched but at streamwise positions around 1 m downstream of the inlet the turbulence matches very well and from a distance of 1.2 m is, for the purposes in this thesis, the same between the experiment and the CFD.

To appropriately select a turbulence model to replicate the wake from a porous disc, a study was conducted for initial validation. Two-equation turbulence models such as $k$-$\varepsilon$ and $k$-$\omega$ are widely used for actuator disc CFD simulations due to their ease on computational power and relatively stability in reaching convergence [62]. Both have their advantages, for example the $k$-$\omega$ is more accurate in formulating near-wall regions, whereas $k$-$\varepsilon$ has free-stream independence in the fair field [105]. In Figure 4.10 the experimental measurements taken from the wind tunnel are compared to the results at the same points from the CFD simulations using three different turbulence models. It is evident at 6D $k$-$\omega$ more accurately replicates the wake at this distance, however, further downstream at 10D $k$-$\varepsilon$ proves superior. The *SST* $k$-$\omega$ turbulence model applies the $k$-$\omega$ solutions to the inner part of the boundary layer, so it can be used for low Reynolds number applications. It then switches to a $k$-$\varepsilon$ model in the free stream, where the $k$-$\omega$ has difficulties replicating the flow correctly with inlet turbulence properties [105]. As will be described further on, a full rotor model is used in conjunction with the actuator disc technique and for consistency it was decided that overall the *SST* $k$-$\omega$ turbulence

model is most appropriate. This is due to the low $Y^+$ achieved in the full rotor model in order to better predict flow along the blades.

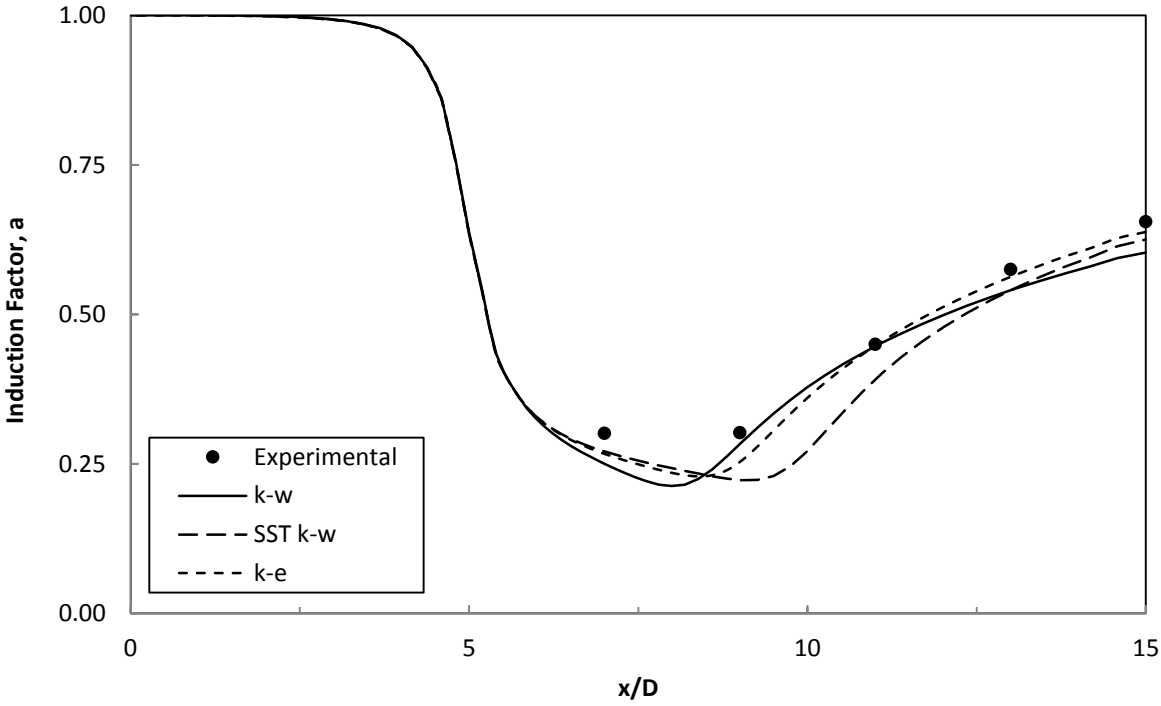


**Figure 4.10 Wake recovery predicted by three turbulence models and compared with the wind tunnel experiment results, with an inlet speed of 10 $ms^{-1}$.**

### 4.2.3 Numerical vs. Experimental Results

As described in Section 4.2.1, the experiments carried out in the wind tunnel are used to validate the CFD technique, which has been done by comparing both sets of data (Figure 4.11). Experimental results yield a pattern of velocity recovery similar to that found by Aubrun et al. [61], where a study of varying porosities and sizes of discs were measured in a wind tunnel to determine the effectiveness of using a porous disc for replication of the far wake region. Numerical work carried out by Cabezon et al. [75] compared different turbulence models against experimental data to show the ability for the actuator disc to replicate the far wake of a wind turbine. It was shown that while the ability for the wake to recover, overall shape of the wake, and maximum velocity deficit was simulated correctly; the wake width did not match up. This is also the case for the

research carried out in this thesis. There is also a marginal difference in centreline velocities, however, in the far wake this becomes minimal and this is the area of interest when applying the actuator disc method. Overall this shows that the actuator disc technique and current turbulence modelling is not a perfect way to represent the far wake by any means, but it is more than acceptable for the purposes of this thesis.

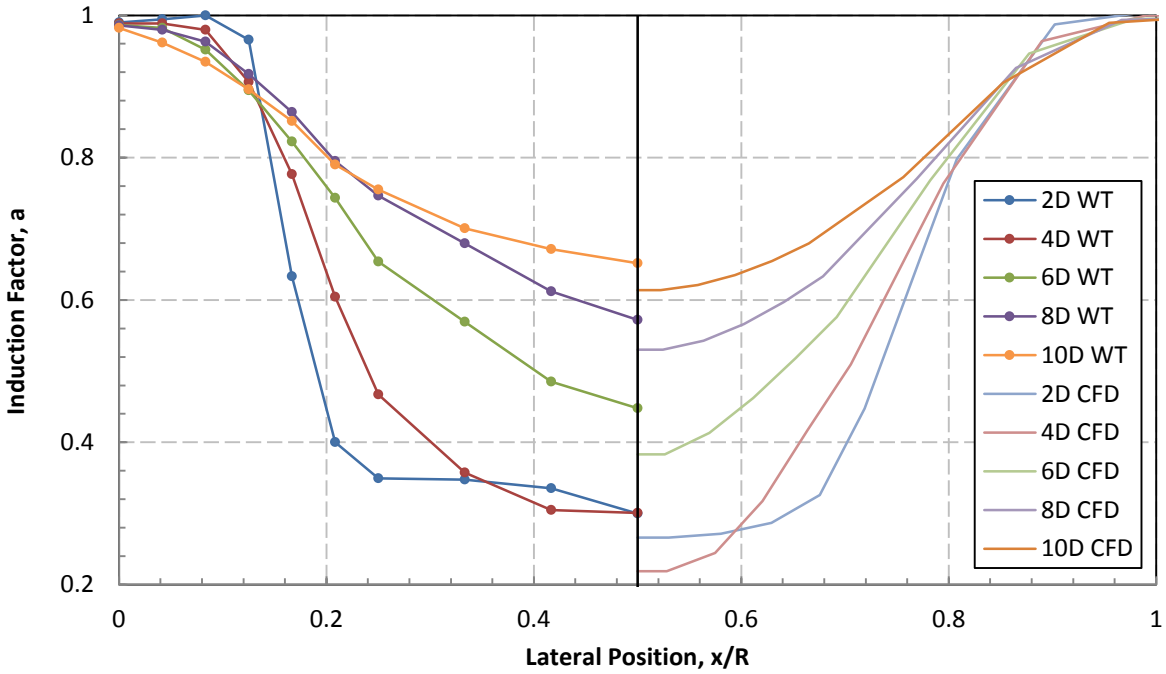


Figure 4.11 Comparing numerical and experimental results with an inlet speed of 10ms$^{-1}$.

This technique has been adequately validated by wind tunnel experiments and is suitable for predicting the physics of wake development required for this thesis. Using this information it is now possible to tailor and replicate the far wake of a wind turbine with confidence by adjusting the induction factor of a porous disc.

## 4.3 Hybrid Actuator Disc – Full Rotor Method

The development of this technique combines the validated actuator disc method within CFD and a full high fidelity CFD wind turbine rotor model. This high fidelity model and user defined function (UDF) was generated and validated by a member of the

same research group as the author, Sobotta [106]. While Sobotta's model and UDF is used in this thesis, the author developed the novel hybrid technique, ran all subsequent simulations, and is entirely responsible for all the analysis of the results.

The next sub-section aims to summarise the model designed by Sobotta [106]; it should be noted that some of the figures used to aid the discussion (Section 4.3.1) are not the authors.

### 4.3.1 Full Wind Turbine Rotor Model

A full rotor CFD model was built replicating the two bladed NREL Phase VI rotor [107] using the software Gridgen and TGrid. The full 360° rotor is modelled in a computational domain that extends 2, 3 and 2.5 diameters in the upstream, downstream and radial directions, respectively. The flow enters through a velocity inlet, over the turbine blades, which were modelled using a no-slip wall boundary condition and exits through a pressure outlet. The outer edge of the domain applies a symmetry boundary condition

Figure 4.12 shows the topology of a 180° section the full rotor mesh; the mesh of the second blade is identical to that shown. The reason for using a 2-bladed full 360° mesh is to allow for non-symmetrical layouts to be simulated. The topology is divided into four blocks; the far-field block (Block 4) consists of a fully structured mesh, while the inner domain, which consists of Blocks 1, 2 and 3, is made of a hybrid mesh. Both blades are surrounded by a structured boundary layer (Block 1). This is enclosed by an unstructured block (Block 2) to allow for heavy clustering of the cells around the blades in order to better resolve the complex flow. Block 3 is made of a structured mesh to ease the transition between unstructured and structured blocks as well as between the stationary (Block 4) and rotating (Blocks 1, 2 and 3) blocks.

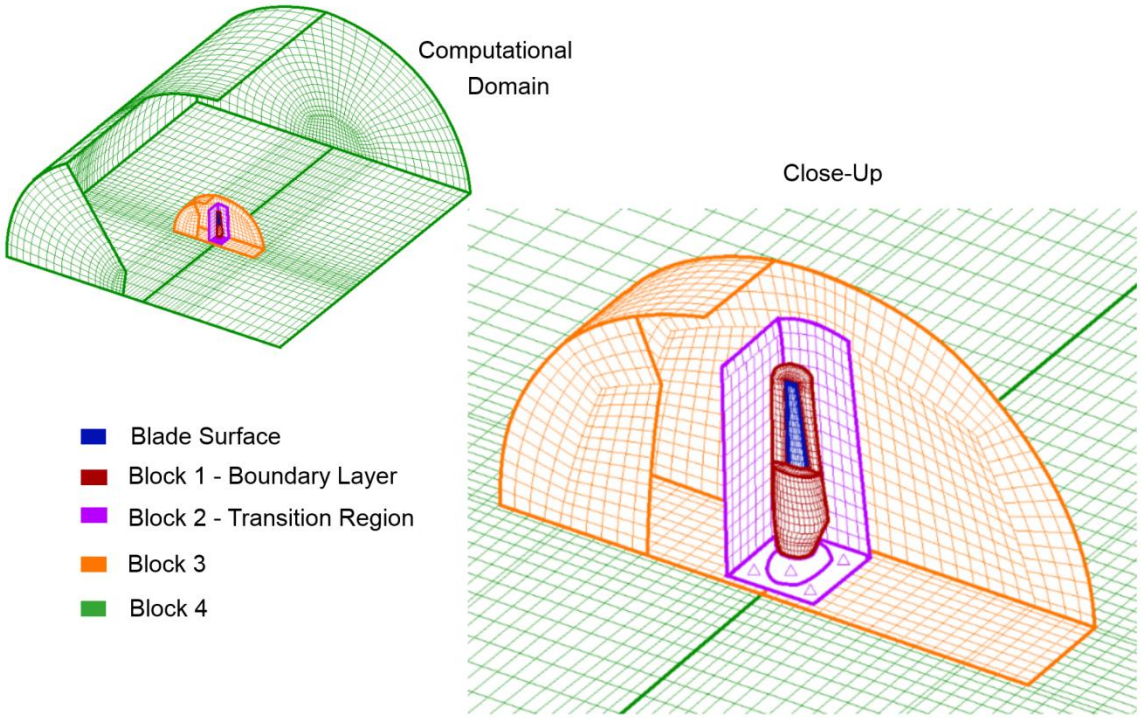


**Figure 4.12 Half of the computational mesh topology for the full rotor, reproduced from** [106].

An extensive mesh independence study was conducted by Sobotta [106] using the described mesh topology and validated against experimental data from the project carried out in the NASA Ames wind tunnel [108]. The total grid sizes of the meshes analysed ranged from $8.4 \times 10^6$ to $25.2 \times 10^6$ cells as described in Table 4.3, which also contains detailed information about the corresponding number of nodes in the boundary layer of each grid. For all the mesh densities the far field (Block 4) remained constant at 6 million cells.

**Table 4.3 Cell count of meshes of varying density and detailed boundary layer grid description, from** [106]

| Mesh Density | Cells (x10$^6$) Total (Including Block 4) | Boundary Layer (Block 1) | Transition (Block 2 and 3) | Nodes Span Wise | Nodes Chord Wise | Growth Rate |
|---|---|---|---|---|---|---|
| **Very Coarse** | 8.4 | 1.2 | 1.2 | 84 | 116 | 1.1 increasing to 1.2 |
| **Coarse** | 10.4 | 2.6 | 1.8 | 115 | 176 | 1.1 increasing to 1.2 |
| **Medium** | 12.4 | 5.2 | 3.2 | 161 | 248 | 1.1 increasing to 1.2 |
| **Fine** | 25.2 | 13.8 | 5.4 | 227 | 360 | 1.1 |

Figure 4.13 shows the results of the mesh independence study. The NREL Phase VI turbine was simulated over a wind speed range of 7 ms$^{-1}$ to 25.1 ms$^{-1}$ at a constant rotational speed of 72 rpm. The power coefficient (CP) has been used a metric to gauge mesh suitability because ultimately the interests in thesis are of energy yield, where CP is the best indicator of success of the meshing involved. The CP is shown to match exceptionally well between the experimental and numerical simulations, particularly at lower values of tip-speed ratio (λ). However, as λ increases to 5.4 differences between the results become more evident, and interestingly at this condition, the pressure coefficient ($C_p$) distributions around the blade are in the closest agreement for all λ conditions tested. Overall, the results from all meshes are in close agreement and for this reason the mesh labelled 'Coarse Mesh' was chosen by Sobotta [106] for all work carried out in their thesis and has been chosen for use in the rest of this thesis. Around the turbine blades a $Y^+$ of approximately 0.8 was achieved for all conditions tested and is, therefore, suitable for the use with the *SST k-ω* turbulence model.

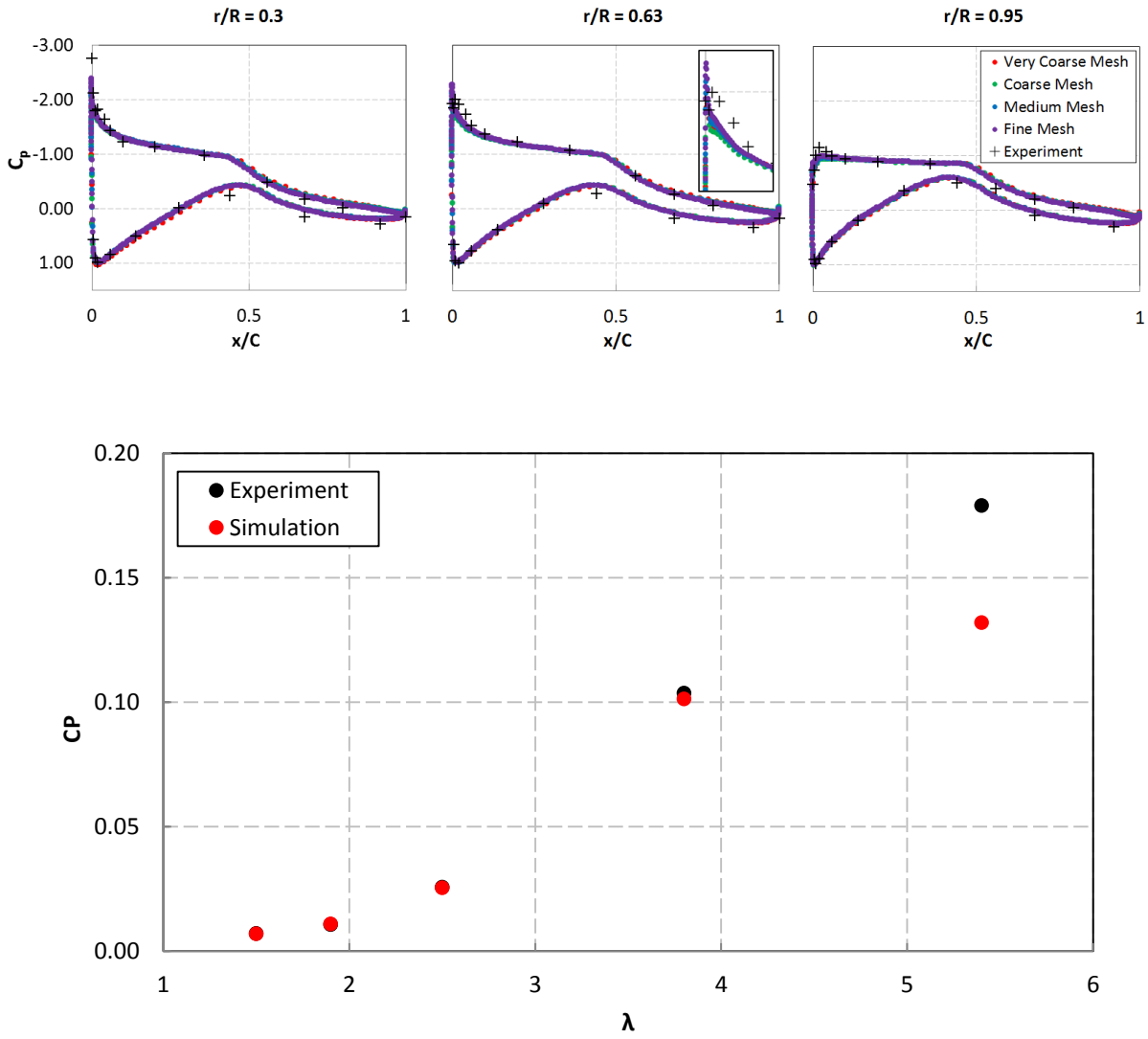


**Figure 4.13 Mesh independence/validation: Pressure Coefficient ($C_P$) at TSR=5.4 (top) and Power Coefficient (CP) results ranging from TSR 1.5 to 5.4 (bottom), data from** [106].

It is worth repeating at this point that any subsequent studies, simulations and analysis of results from here on in uses the full rotor mesh created by Sobotta [106], but are otherwise carried out by the author only.

### 4.3.2 Combing Actuator Disc and Full Rotor Models: The Hybrid Technique

Simulating wake interactions on multiple full rotors in a single computational domain is possible, as shown by Weihing et al. [72]. However, due to limitations of available computational power means it is currently unrealistic to perform such simulations within the development cycle of a wind farm and when modelling multiple

layouts. This is because of the increased mesh density required downstream of the rotor to accurately capture the flow physics of the far wake. Therefore, a new technique of extracting the data collected from the actuator disc method and applying it upstream of a high fidelity wind turbine CFD model has been developed [109]. The advantage of the new method is that the computational cost and time is kept low, while still having the ability to analyse detailed full rotor performance in various array layouts. Blade Element Momentum Theory (BEMT) is arguably a quicker and simpler method in yielding similar results. However, research carried out by Malki et al. [56] shows that the limitations of blade element momentum produces far less detailed results than the CFD equivalent.

Combing the two techniques allows for a novel way of analysing performance of a wind turbine in the wake of another. In order to achieve this, an actuator disc simulation of the same diameter as the NREL rotor was constructed. Once this simulation fully converges, the velocity field (an example is presented in Figure 4.14) from 7D downstream can be extracted and then applied as the inlet boundary condition velocity field for the full rotor simulation. The flow chart found in Figure 4.15 describes how the two techniques have been combined.

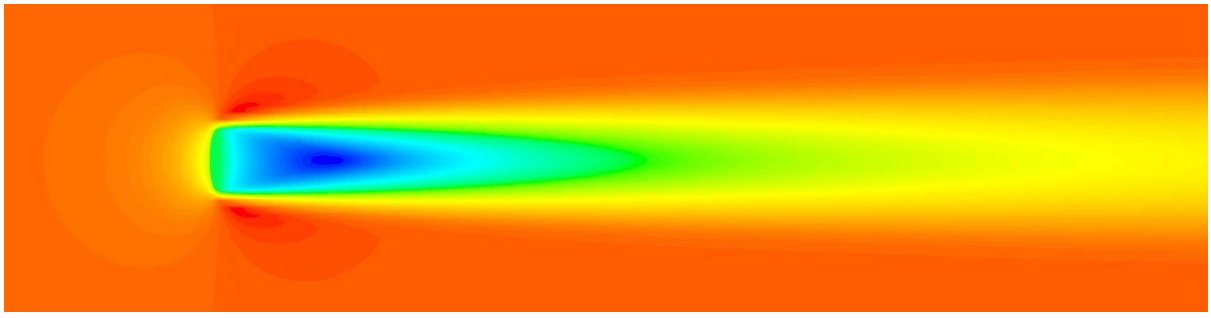

**Figure 4.14 Velocity magnitude contour plot of a wind turbine wake using the actuator disc technique (Red = 10 $ms^{-1}$ and Blue = 5 $ms^{-1}$).**

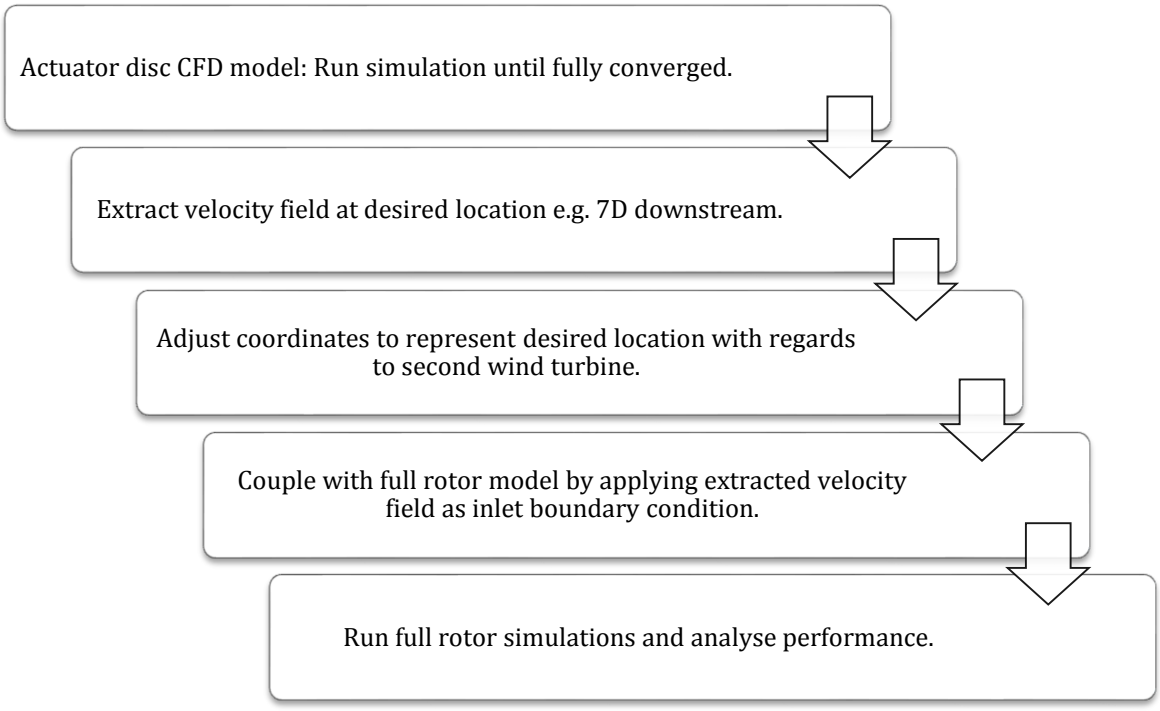


**Figure 4.15 Flow chart of the methodology for the hybrid CFD simulations.**

When extracting the downstream velocity field from the actuator disc model, it is possible to use the same data for different positions by adjusting the coordinates. An example of the wake from the actuator disc being used as the velocity inlet boundary condition for the full rotor model is illustrated in Figure 4.16.

An inherent issue with simulating an offset actuator disc upstream of the full rotor is that the blades will rotate in and out of the wake, which unlike a constant inlet leads to transient changes throughout a single rotation. Eight full rotations of the wind turbine had to be completed to allow for periodic torque convergence before data could be collected, as shown in Figure 4.17. This plot shows the torque produced by each turbine blade through the evolution of the solution. It can be seen that periodicity is not reached until the 5$^{th}$ second, which corresponds to the 8$^{th}$ revolution.

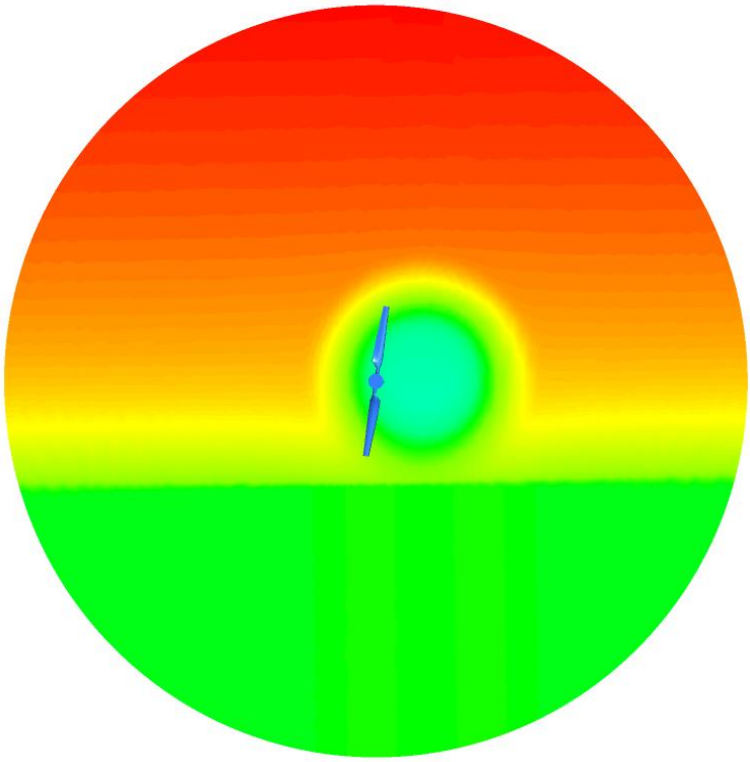

Figure 4.16 An example of how a 'slice' of the wake behind an actuator disc can be set as the velocity inlet boundary condition for the full rotor model. The vertical variation in velocity is as a result of simulating the atmospheric boundary layer, which is used for the case study (Red = 10 $ms^{-1}$ and Light Blue = 2.5 $ms^{-1}$).

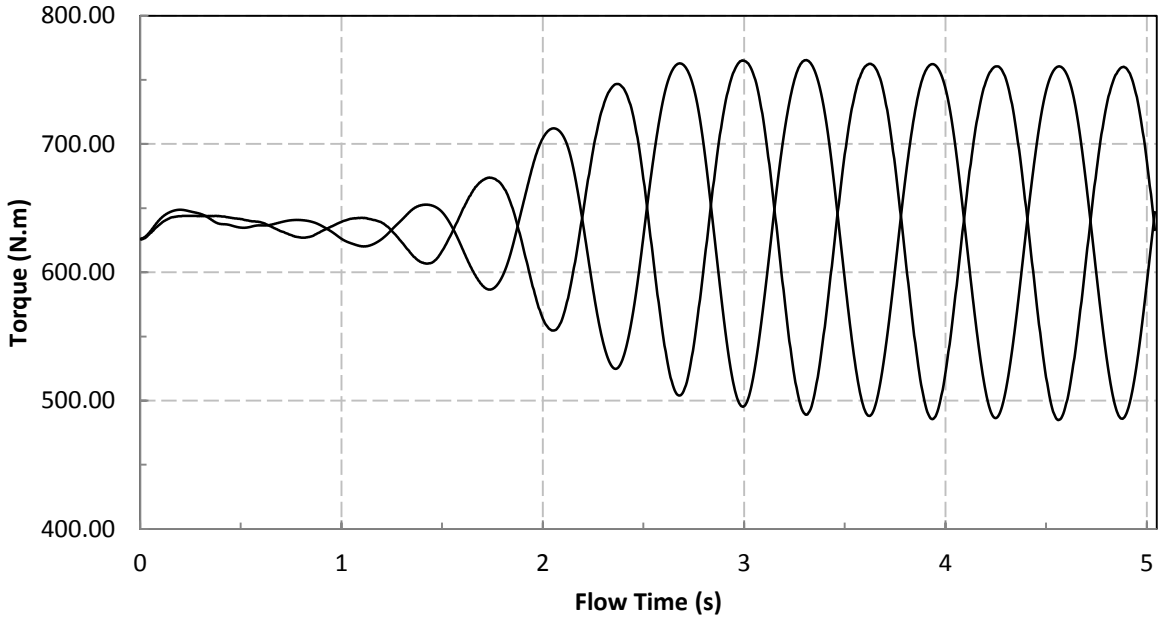


Figure 4.17 The full rotor simulation reaching torque convergence after eight rotations.

### Time Step Study

Using the mesh created by Sobotta [106] a new time-step study was carried out by the author because of the transient nature of the flow in this thesis. Due to the heavy computational cost of the high-density mesh, it was necessary to determine which time step size was most suitable. For this, three time steps were compared (Figure 4.18) 0.01 s, 0.005 s and 0.001 s. As discussed in Section 4.3.2, torque convergence was reached after eight rotations. After four (48 CPU) days of simulation run time the smallest time step of 0.001 s was only able to complete a third of this and was therefore ruled out. The difference in computational time between 0.01 s and 0.005 s was much less and with the increased accuracy in results from time step = 0.005 s this was chosen for all future simulations.

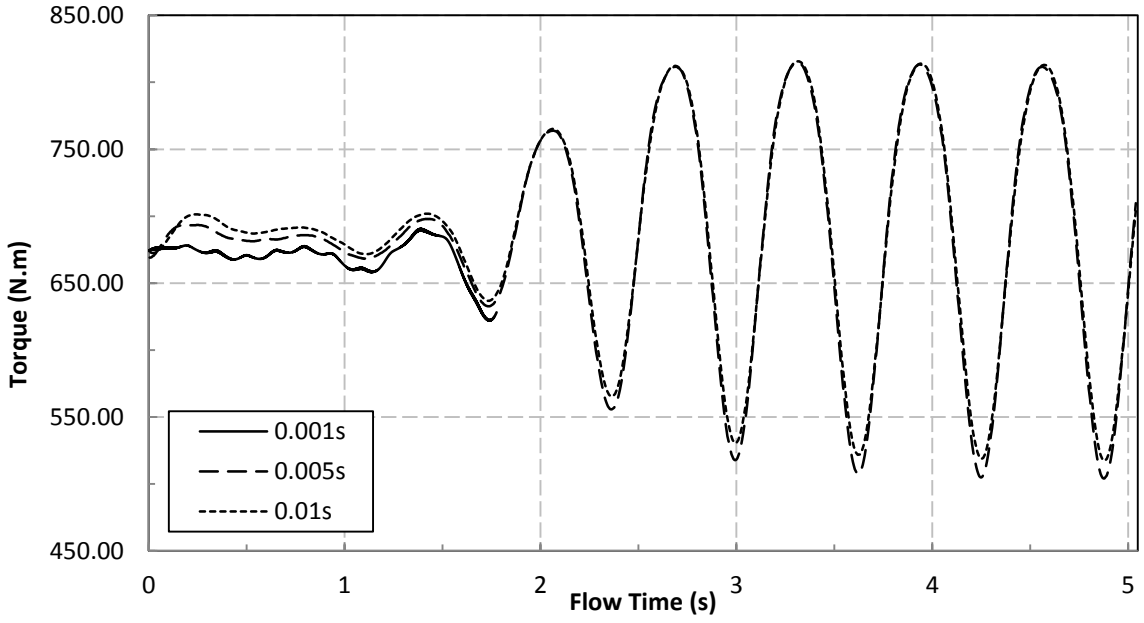


Figure 4.18 Torque convergence for time steps: 0.001 s, 0.005 s and 0.01 s.

## 4.4 Simulating Atmospheric Boundary Layer

A key element of wind farm aerodynamics is the fact that the structures of wind turbines sit within the atmospheric boundary layer (ABL). It is vital that this condition

is simulated as an increase in height results in higher wind speeds, which will play a crucial role when designing a wind farm. Modelling the ABL is a straightforward process that relies upon at least one wind speed measurement for a given height, which is then applied to the Equation (2.8). A curve is produced that spans from the height of 0 m up to a desired maximum, which is applied as an inlet boundary condition in Fluent. This technique is described further and then applied in the case study in Section 6.2.

## 4.5 Modelling Terrain

While terrain is not the main focus of this thesis, the effects it has on wind farm placement means it should not be ignored. There are various techniques that allow for the computational modelling of terrain; from simple two dimensional sinusoidal hills [45] to complex use of Geographical Information System (GIS). GIS provides a wealth of information including socio-economic, technical, physical and environmental factors [110]. However, for the purposes of this research the author has developed a technique that uses data from Google Maps, which can be exported as a Stereolithography (STL) file that can be converted into a mesh for CFD simulations (Figure 4.19).

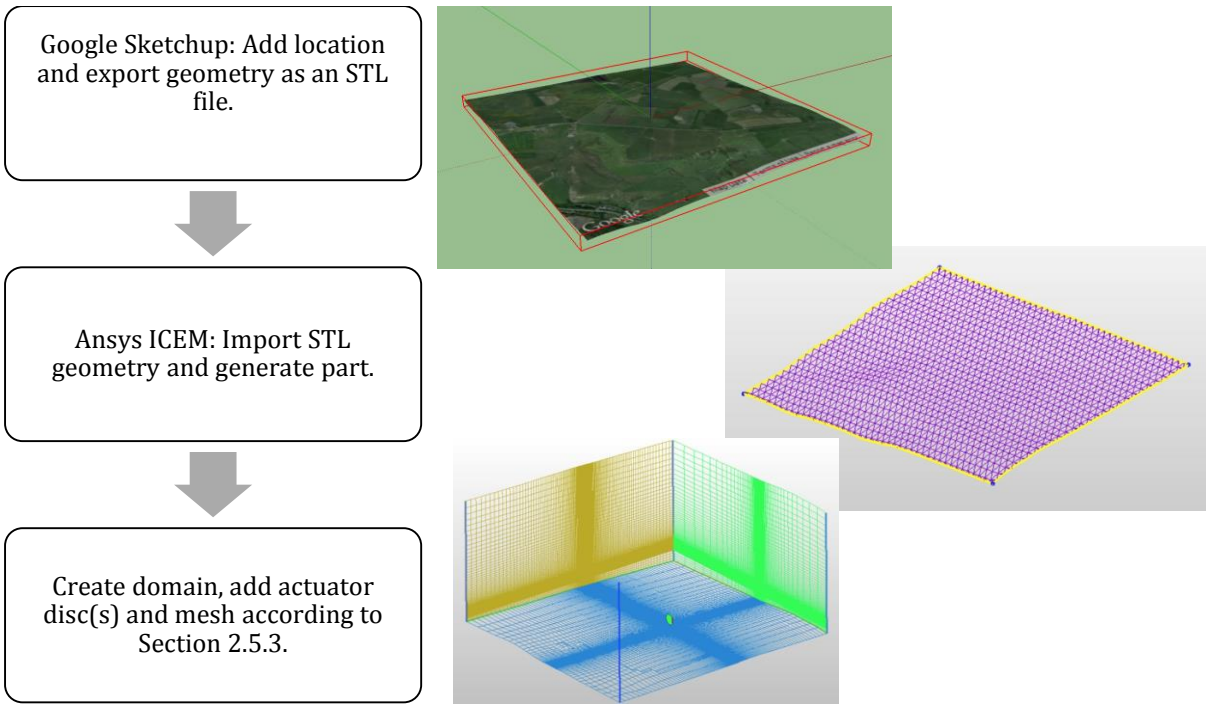


**Figure 4.19 Flow chart of the methodology for using Google SketchUp to produce terrain geometry for meshing in ICEM.**

## 4.6 Scaling Full Wind Turbine Rotor Model

The NREL rotor that has been used throughout this thesis has a diameter of 10 m. While this is adequate for simulating turbine-turbine interaction, the rotor size used in wind farms are in the region of ~100 m. An advantage of CFD is the ability to scale meshes to a desired size, and this process has been applied for the case study in Section 6. As described in Section 4.3.1 a $Y^+$ of below 1 was achieved as is required for the *SST k-w* turbulence model, however, the distance when scaled between mesh cells also increases. For example, scaling from a 10 m rotor to a 100 m scales the $Y^+$ by 10, which means that another appropriate turbulence model must be employed, in this case *k-e*. The use of a different turbulence model is also applied for modelling the actuator disc at larger diameters for consistency, as previously discussed all turbulence models agree relatively well to experimental data (Figure 4.10). An increased sized actuator disc CFD

domain was constructed and simulated to provide the velocity field on the inlet of the scaled high fidelity rotor.

## 4.7 Summary

The methods described throughout this chapter vary extensively, but all tie into the aim of detailed modelling and simulations of turbine-turbine interactions and wind farm conditions. The actuator disc theory was validated against wind tunnel data over a range of velocities, turbulence models, and distances. A NREL Phase VI rotor CFD mesh was briefly discussed, showing the mesh independence and validation process carried out by Sobotta [106]. An application of the two distinct modelling methods were put together that resulted in a novel hybrid technique that allows for a more efficient, but detailed way of analysing turbine-turbine interactions. Developing this technique further with the introduction of an ABL boundary condition, terrain, and scaling allows for a more realistic wind farm simulations. The next two chapters apply these numerical methods by first setting out a set of reference cases compared with an ideal case to provide a 'go-to' set of results of wind farm layouts. Secondly, a case study is carried out of which further simulations are used for suggesting improvements to an existing wind farm.

# 5 NUMERICAL RESULTS

## 5.1 Introduction

The numerical results analysed in this chapter apply the methodology developed throughout the first half of this thesis, with the aim that a better understanding of turbine-turbine interactions is formed.

To begin, an ideal reference case is studied at two different TSRs to describe aerodynamic characteristics when there is no wake interaction. This is followed by a further set of reference cases of various layouts between multiple wind turbines, which are analysed in order to provide a fundamental understanding of the aerodynamics, flow physics, and characteristics. The turbine separation distances chosen for this study represent the most likely choices made by developers of wind farms [44] with worst case scenario alignments.

## 5.2 Ideal Case

The aim of the ideal case analysis is to supply a base for which the reference cases can be compared to, Figure 5.1 illustrates the wake behind a wind turbine when there is no downstream interaction with another turbine. The flow enters from the left where there is a noticeable dip in velocity slightly upstream of the disc, this is a result of the blockage effect caused by the rotor in very sub-sonic (essentially incompressible) flow. After the wind turbine, the flow velocity drops considerably and continues to drop until approximately 2.5D downstream; the turbulence in the wake causes the low velocity fluid in the wake to mix with the high velocity fluid outside of it, this way momentum is transferred into the wake causing it to expand (increase in width) and the velocity deficit to recover. However, the centre of the wake remains at a lower velocity and takes longer to recover when compared to the outer edges. The wake is also seen to recover more quickly immediately after the near wake region and then the improvement declines further down in the wake.

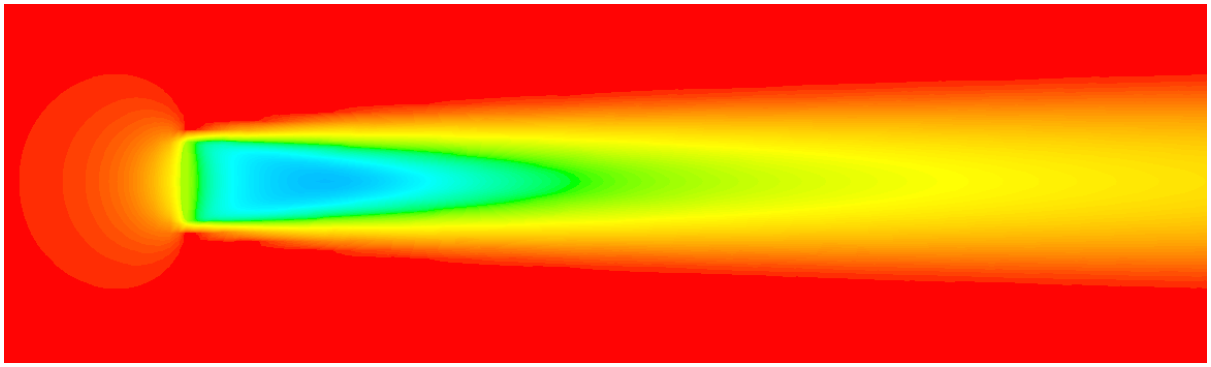

**Figure 5.1 Velocity magnitude contour plot of a wind turbine wake using the actuator disc technique (Red = 10 $ms^{-1}$ and Blue = 4 $ms^{-1}$).**

The ideal case assumes that there is no upstream wind turbine and, therefore, no wake interactions occurring. With a constant velocity inlet, the turbine blades are experiencing the same conditions at every point throughout a rotation. The optimal TSR

for the NREL Phase VI rotor is approximately 5 (Figure 4.13), in this section this is compared with a TSR of 2.5. For the purposes of this comparison an inlet velocity of 10 $ms^{-1}$ was applied for both cases and in order to alter the TSRs, the rotational speed was dropped from 10 $rads^{-1}$ for TSR 5 to 5 $rads^{-1}$ for TSR 2.5. A consequence of the drop in TSR is a fall in performance; Figure 5.2 compares the coefficient of pressure ($C_p$) at five radial positions along a single blade for both TSRs. Along the length of the blade for TSR 5 there is negative pressure present along two-thirds of the chord and a gradual pressure recovery toward the trailing edge. This demonstrates that the blade is able to use the available power in the wind and yield lift; the area between the curves is the total lift, therefore, the larger the area the more lift produced. Conversely, for the lower TSR there is mostly a small suction peak that rapidly drops close to zero across the chord of the blade. This is happening because the relative angle of attack that the blade is now seeing is less than optimal as the incidence has increased. However, at r/R=0.3 there is a large suction peak that is likely a result of the aerofoil profile which is better suited to the wind conditions simulated. The constant pressure coefficient, $C_p$, along the majority of the blade illustrates the less than optimum TSR for the given wind velocity. Another clear difference is how the pressure surface reacts along the chord length, initially for the TSR 5 case the stagnation point is sitting at approximately a $C_p$ value of 1, before turning into negative pressure at the mid-chord, this distribution of pressure is beneficial to the overall ability of the blade to perform. At TSR 2.5 the stagnation point is slightly lower, however, there is minimal change along the chord and negative pressure is never achieved. Overall, the enclosed area of the $C_p$ vs. surface plot (Figure 5.2) at TSR 5 is far greater than at TSR 2.5; this integrated pressure difference corresponds to less induced drag forming and an ability to produce more lift and, therefore, increased performance.

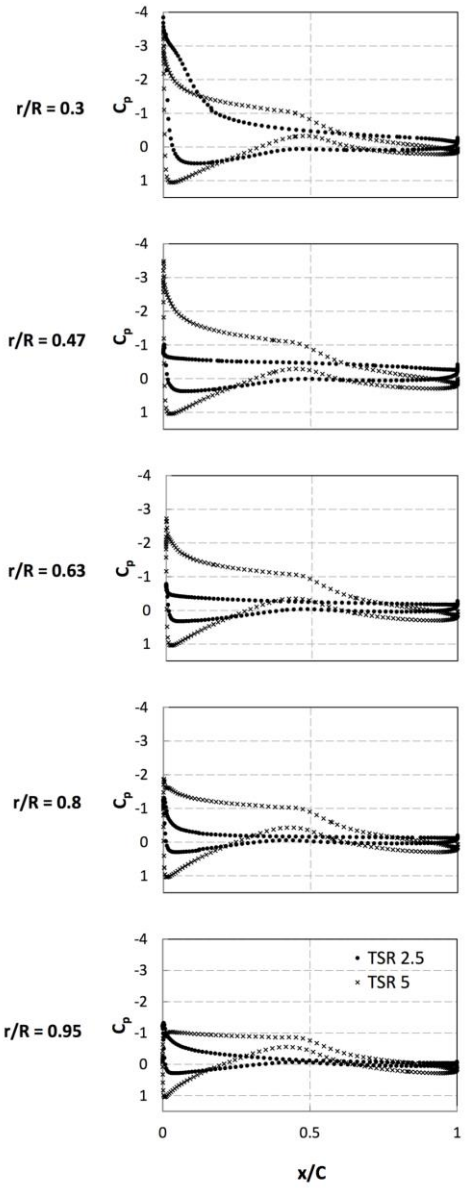


**Figure 5.2 $C_p$ plots along the blade at five radial distances for the ideal case at TSR 2.5 and TSR 5.**

The pressure contour plots illustrated in Figure 5.3 expands on the $C_p$ plots presented above. The gradual pressure recovery and smooth pressure distribution is clear for the TSR 5 case. At TSR 2.5 the change in pressure along the blade is sudden and varies depending upon location along the surface. There is also a clear wavy pattern caused by the disrupted flow where the pressure transitions about zero as a result of the effective AoA that the slower rotational speed has for the given velocity of the wind,

which will most likely cause adverse pressure gradients. The adverse pressure gradient, due to high momentum diffusion, can result in separation bubbles forming in which a region of reversed flow forms and this is particularly detrimental for the ability of the blade to produce lift. The effect of which is reflected in the coefficient of power (CP) and torque production in Figure 5.4, which is presented at one span wise position rather than the average torque along the whole blade. Overall, TSR 2.5 (CP = 0.14) has a CP half of that at TSR 5 (CP = 0.28) and produces a little over a fifth of the torque.

By comparing two TSRs, one of which is the optimal condition for this wind turbine, it is obvious that the blades are extremely sensitive to variations in wind speed, or in this case, rotational speed. As will be shown, a similar scenario occurs when the blade finds itself in the wake of an upstream wind turbine; the reduced relative wind speed has dramatic effects on performance and removes the turbine from its ideal operating conditions, because the downstream turbine sitting in a wake will see a lower velocity and so a higher TSR.

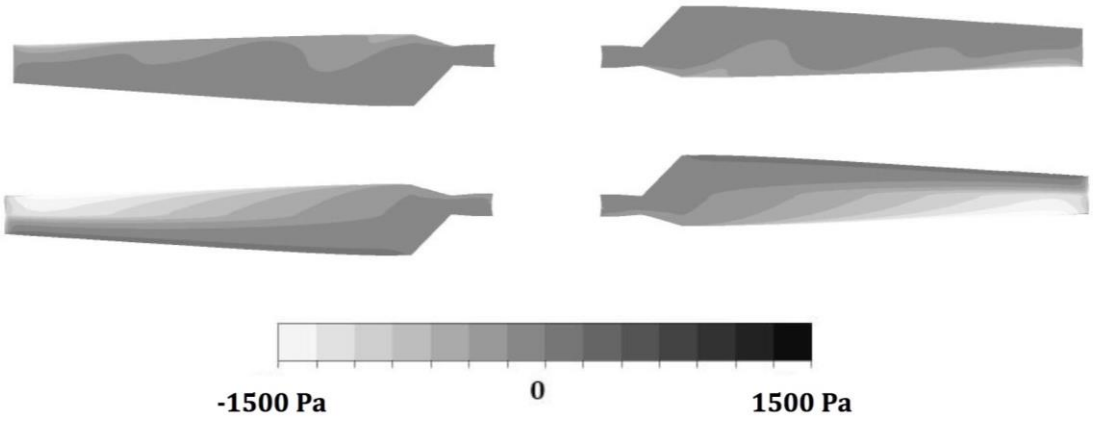


**Figure 5.3 Pressure contour plots on the suction surface of the blades for ideal case at TSR 2.5 (top) and TSR 5 (bottom).**

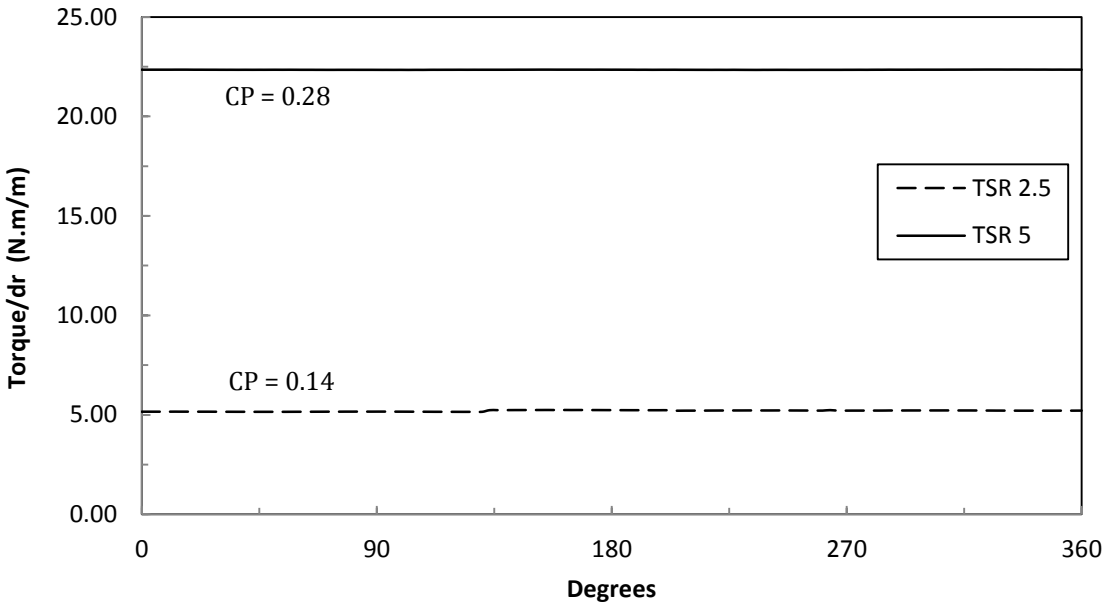


**Figure 5.4 Torque plot for position r/R=0.7 on a single blade throughout one rotation for ideal case at TSR 2.5 and TSR 5.**

The next section of this chapter analyses how turbine-turbine interactions affect the ability of a wind turbine to perform. However, as is shown in the ideal case analysis, performance can vastly reduce when the rotor is met with reduced wind speeds, affecting the angle of attack and TSR. It is acknowledged that in reality a wind turbine will employ a control system to adjust the TSR of the rotor when in the wake of another to try achiever a higher CP. However, for the purposes of the following references cases all conditions were kept equal as to draw direct comparisons between interations of the wake and downstream wind turbines.

## 5.3 Reference Cases

For the purposes of the reference cases, twelve layouts were investigated as illustrated in Figure 5.5. The bold lines represent each alignment case for visualisation purposes and it should be noted that the lines surrounding the cases in that figure do not represent the computational domain size used. As described in the flow chart found in Figure 4.15, the distance between the separately simulated actuator disc and full

rotor is controlled by a velocity field taken downstream (7D for example) of the actuator disc and applied as the inlet on separate the full rotor domain. In the case of a three wind turbine analysis, two actuator discs are simulated in a single domain and the velocity field is taken from behind the second disc. The ideal reference case (TSR 5 with no wake interaction) in the previous section is used as a basis for comparison. The top set looks at one actuator disc upstream of a full rotor, applying the method described in Section 4.3.2, at distances[1] of 5D, 7D, and 10D and for each case the two wind turbines are aligned at their centres, offset by 0.5D, and 1D. The bottom set models three turbines consisting of two actuator discs and a full rotor, each at 7D apart with the same three alignments used in the top set.

[1] One diameter (D) for this case is equal to 10 m.

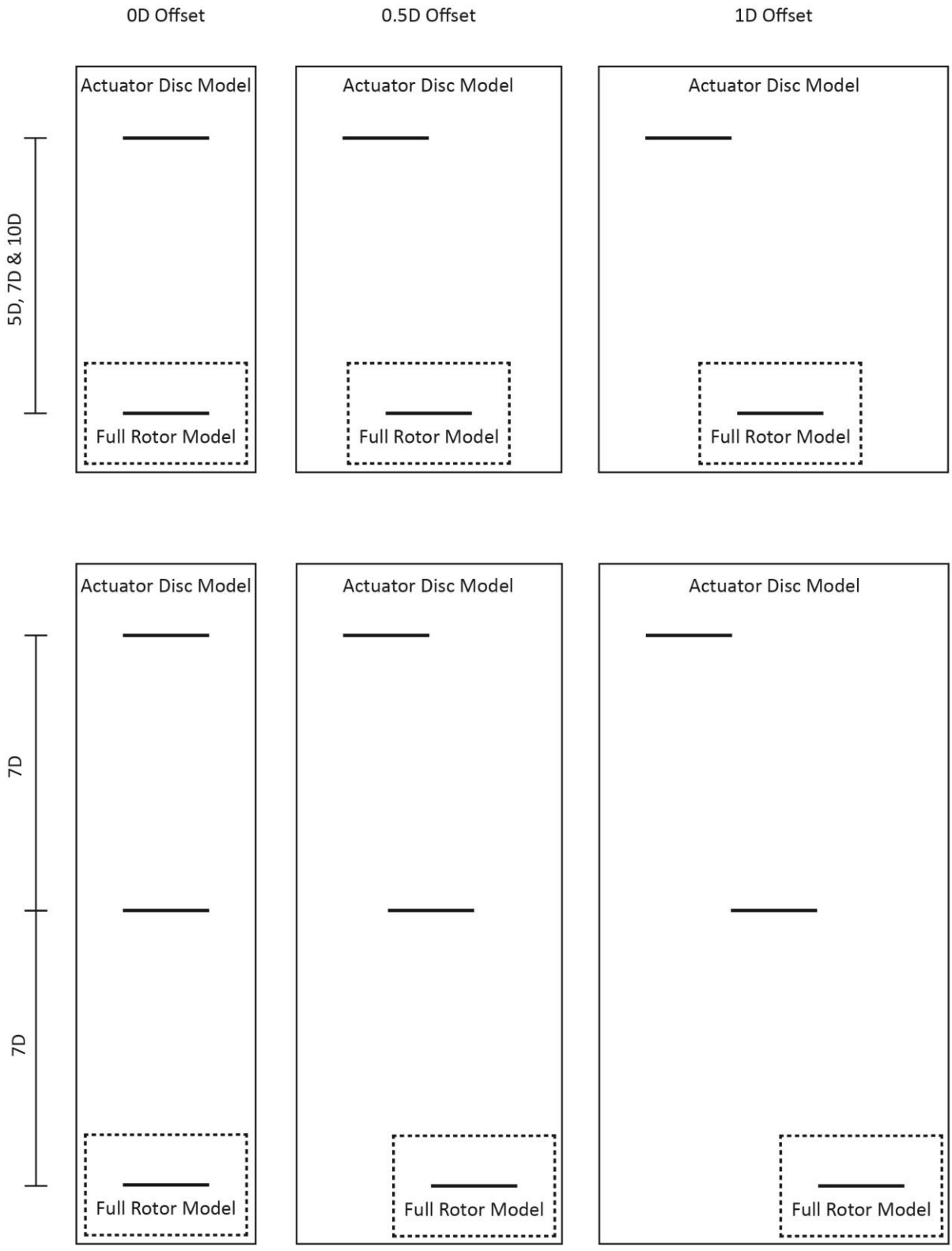


**Figure 5.5 The reference cases used to study the effects of wake on wind turbine performance. One actuator disc placed upstream of the full rotor model at distance of 5D, 7D and 10D and offset by 0D, 0.5D, and 1D (top). Two actuator discs upstream of the full rotor model at a distance of 7D between each and offset 0D, 0.5D, and 1D (bottom). Note: the lines surrounding the cases do not represent the computational domain.**

The CP provides the simplest, yet most valuable description of a wind turbine's performance; Figure 5.6 shows the CP for the twelve cases described above and the ideal case at TSR = 5. The CP calculated here uses the undisturbed wind speed (i.e. without any upstream turbine present) in the denominator of the definition of power coefficient. However, the power available in the wind to the downstream turbine is reduced due to the presence of the upstream turbine, so it could be argued that the actual power in the wind should be used in the calculation of CP. However, the interest lies in the reduction of power from the downstream turbine, therefore, it is appropriate to use the undisturbed wind speed to calculate the power coefficient.

The CP of each reference case were normalised against the ideal single turbine case, which had an undisturbed velocity inlet. It can be seen in Figure 5.6 that overall the effect of the upstream turbine results in an interaction that is detrimental to the performance of the downstream turbine. This is no surprise, of course, but the extent to which this power reduction occurs depends on layout and turbine separation distances. As expected, the most severe drop in power is experienced when the two wind turbines are completely aligned at their centres. An increase in separation distance between the turbines improves the CP of the downstream turbine significantly, with a 45% rise with a doubling of the distance from 5D to 10D; this has also been documented in previous literature [44], [89]. A similar trend is shown when the two turbines have an offset alignment of half a diameter, but with an overall improved CP. Counterintuitively, when the turbines are misaligned by one diameter and the distances between increases, the CP decreases. An explanation for this occurring is that the wake produced by the first wind turbine expands as it travels downstream and interacts less at a distance of 5D, but as the distance increases beyond 5D so does the wake width and, therefore, more of

the downstream turbine rotor further downstream locations eventually ends up in the wake and this outweighs the recovery in the flow velocity. Figure 5.7 shows the wake recovery behind the actuator disc as viewed from the centreline of the downstream wind turbine for the three layouts simulated. The explanation for an increased CP with a decreasing downstream distance for the 1D offset case is seen with a slight rise in wind speed at the point of the first turbine before a fall to a 'recovered' velocity.

In a three-turbine layout, the performance of the wind turbine of interest differs when compared with two turbines. As shown in research carried out by Stevens et al. [38] and Porté-Agel et al. [36], when the wind turbines are aligned the most affected turbine is found in the second row, after which there is a slight increase in performance of the following rows. This is the opposite case when wind turbines are offset by half a diameter, because of the diverging wake and the lack of power available from the incoming wind. When offset by one diameter, the diverging wake at this distance from the first turbine is likely to have little effect on third turbine in comparison to the second, explaining the increase in CP at this point.

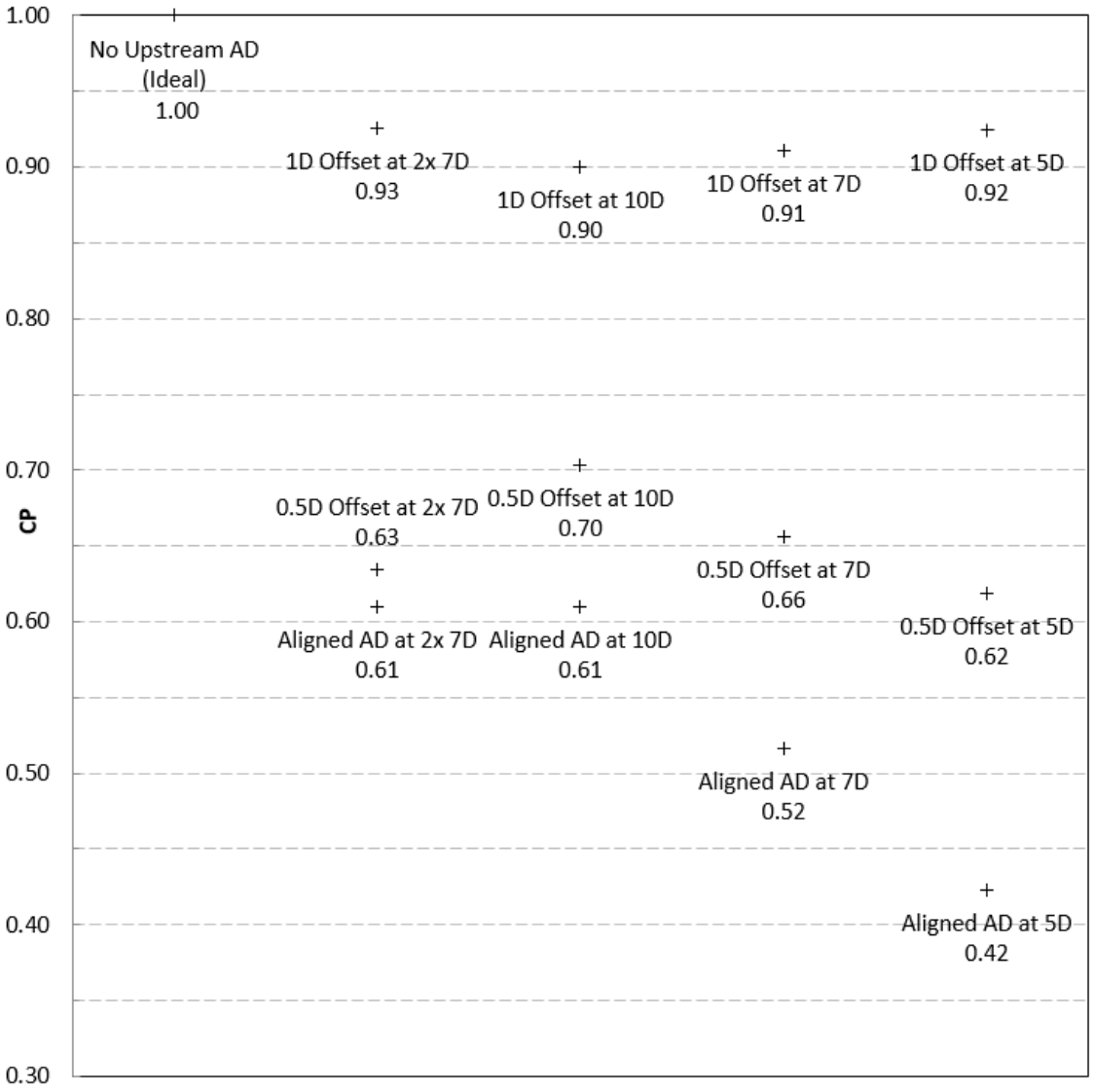


**Figure 5.6 Comparing the normalised Coefficient of Power (CP) from all cases.**

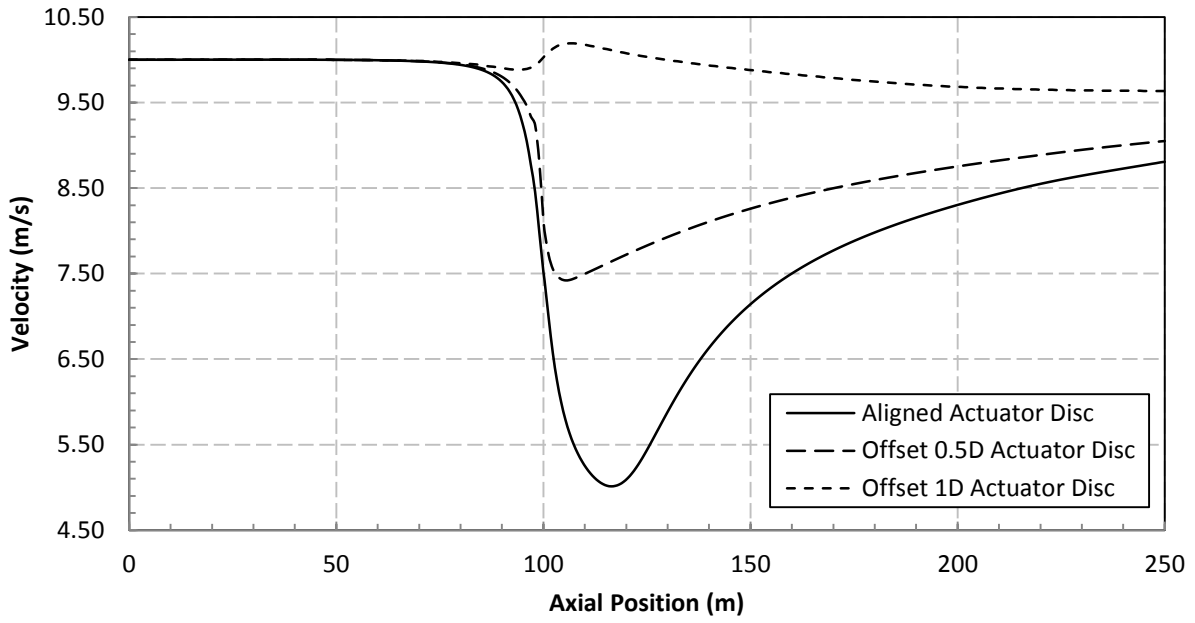


**Figure 5.7 The wake recovering behind a single actuator disc at the centre lines for the three alignment cases.**

The reason for using a full rotor simulation is that it allows for the calculation of the details of the aerodynamics of that turbine which would not normally be available. As such it is possible to determine the torque along the blade as it rotates in and out of the incoming wake. This is useful for the many purposes such as determining blade loading (for fully FSI type calculations) but here it is used to demonstrate the effect that wake interactions with wind turbines have on performance. Figure 5.8 illustrates the blade of interest as it completes a full rotation, the dotted line describes the approximate position of the incoming wake for the 0.5D offset case; the actual wake diameter will vary depending on the distance between turbines. For the remainder of this chapter, the relative position of the blade will remain the same for all reference cases, and the torque values presented will be taken at r/R=0.7 along a single blade for a full rotation. In the case of the $C_p$ curves, the blades are analysed in their horizontal position as to reflect a comparison between being in the worst part of the wake and outside of it.

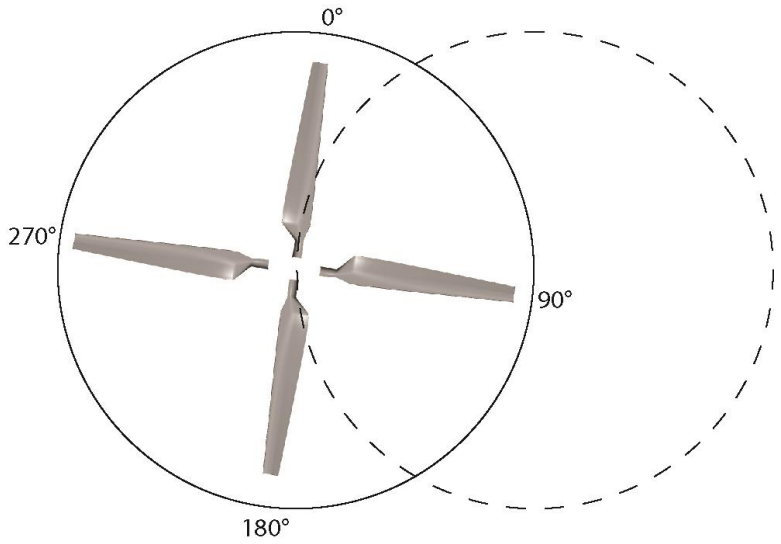


**Figure 5.8 Relative position of a single turbine blade relative to upstream wake for case 0.5D offset. The actual wake width varies depending on distance between wind turbines.**

### 5.3.1 Actuator Disc Aligned with Full Rotor

A worst case scenario in a wind farm would be to have multiple wind turbines aligned at their centres; the wake from the first rotor would encompass the second, which affects the energy in the wind available and compromises the aerodynamic characteristics that the blades have been designed to perform in. The negative consequence of having a wind turbine directly behind another is illustrated in Figure 5.9. It is immediately apparent that the second turbine is seeing a lower wind speed because of the wake from the first and the added issue is that the majority of the rotor is located in the centre of the wake where recovery takes far longer, and so increasing the separation distance required for the power in the air to recover. The result of this is that if two turbines are aligned at their centres, for the second to perform well the distance between them must be far greater than often available. The overall effect on performance of this particularly detrimental interaction is now further analysed by looking at the second turbine in detail.

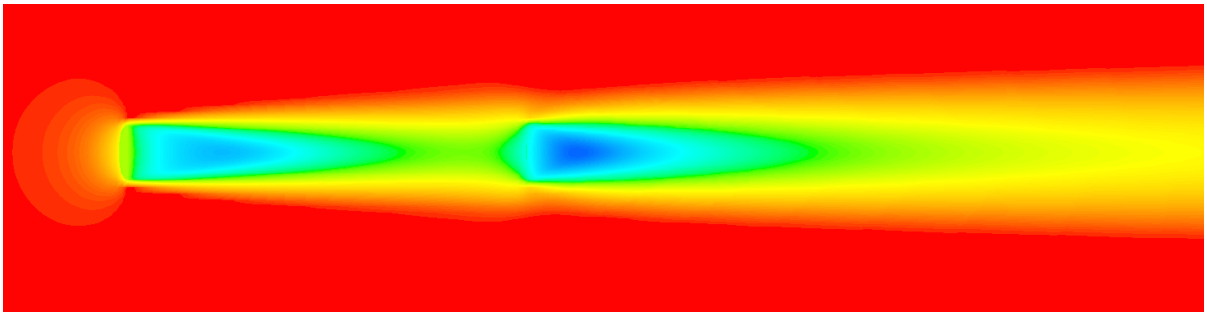

**Figure 5.9 Velocity magnitude contour plot of a wind turbine wake interaction between two aligned wind turbines 7D apart using the actuator disc technique (Red = 10 $ms^{-1}$ and Blue = 4 $ms^{-1}$).**

The three plots in Figure 5.10 compare the $C_p$ around one of the blades at five radial locations from root to tip, both behind the aligned wake and the ideal case. Reflecting the CP results, $C_p$ at 5D is particularly poor when compared to the ideal case for the bottom two-thirds of the blade. The difference between suctions peaks means that the integrated area between upper and lower surfaces is significantly reduced when there is a turbine-turbine wake interaction. For the upper third of the blade the changes between cases is less noticeable, and near the tip it becomes close to identical. The reason for the lower two-thirds being where a drop in performance occurs is illustrated in the velocity contour plot in the Numerical Methods chapter (Figure 4.14). When the two wind turbines are aligned at their centres, the areas of the blade towards the hub are experiencing the largest deficit in the wake. The 'u' shaped wake has comparably less wind disruption the further away from the centre and, therefore, the areas toward the tip are less affected.

By increasing the distance between turbines, the wake begins to recover and as a result there is more available kinetic energy in the wind. Assuming the wind turbine is spinning the optimal TSR, the increase in velocity begins to realign the relative wind to the ideal angle attack. When the distance has reached 10D, the differences in $C_p$ at the tip are almost indistinguishable and the leading edge suction peak begins to increase in

negative pressure. For all the cases the stagnation point moves along the surface of the blade when in the presence of a wake due to a reduced wind speed, which changes the relative AoA. However, despite the different rates of pressure recovery, it ultimately leads to the same trailing edge pressure for all cases.

The plots shown in Figure 5.11 compare how the pressure is distributed across the suction surface of the turbine blade. It is evident that there is a large reduction in negative pressure at the leading edge along the length of the blade when in the wake of another wind turbine. This is because of the angle of attack will have changed due to reduced wind speeds, the result is that the lift it is able to produce decreases. Negative pressure is also more distributed across more of the blade for the ideal case in comparison and the pressure is seen to switch to positive further back in the undisturbed case, resulting in a more efficient blade.

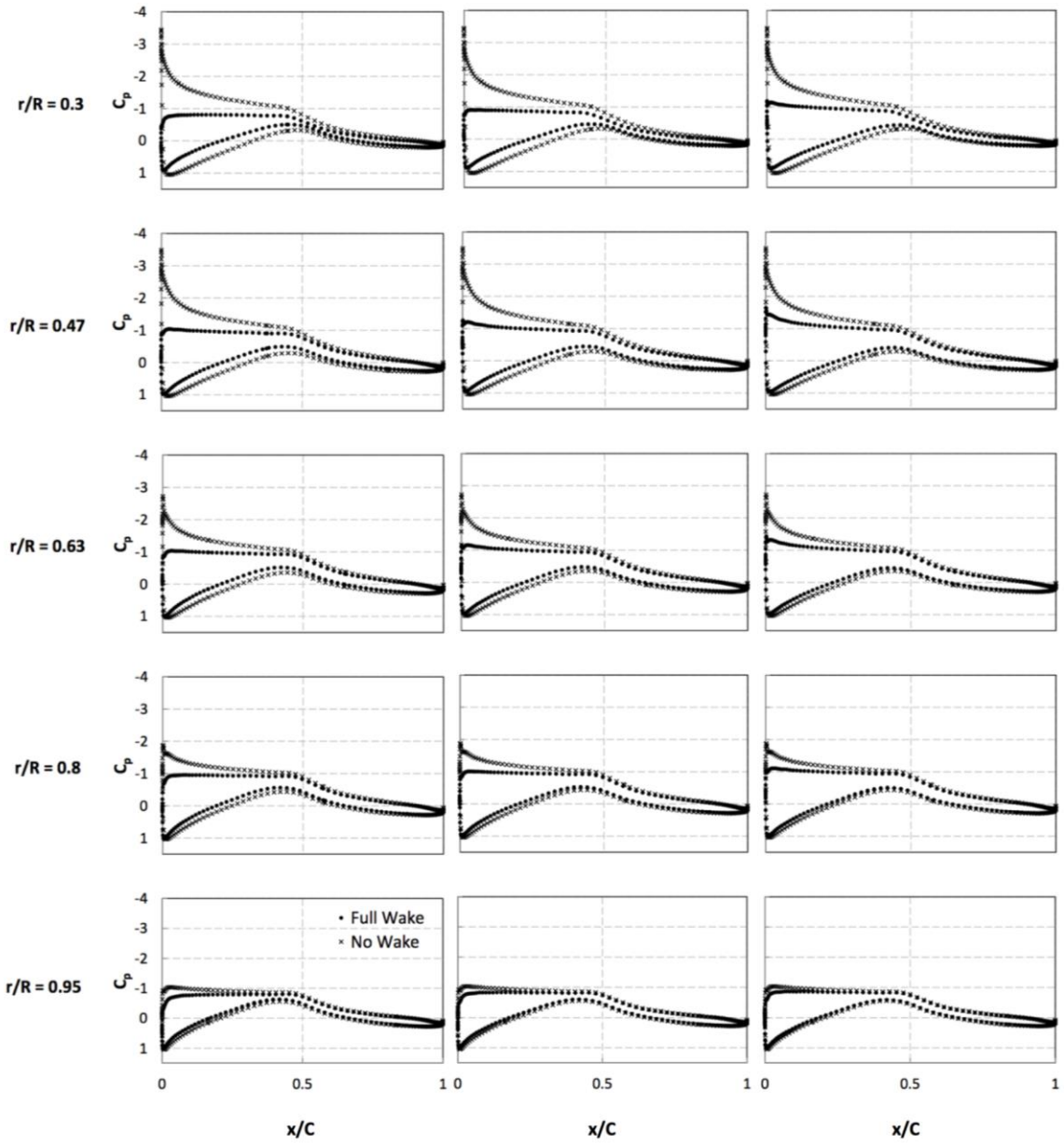


**Figure 5.10 $C_p$ plots along the blade at five radial distances for cases: Aligned AD at 5D upstream of rotor (left), Aligned AD at 7D upstream of rotor (middle), and Aligned AD at 10D upstream of rotor (right) – all versus no upstream AD or rotor.**

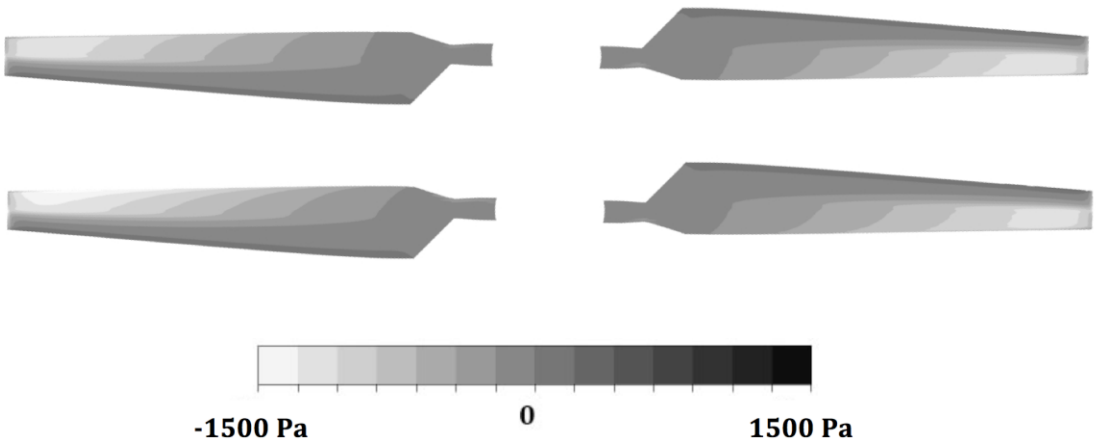


**Figure 5.11 Pressure contour plots on the suction surface of the blades for cases: No upstream AD (top). Rotor 7D downstream of aligned AD (bottom).**

Reduced wind speeds as a result of the wake from an upstream wind turbine means that the blades are producing less lift. The torque at r/R=0.7 along a single blade is plotted for a full rotation in Figure 5.12. As the two wind turbines are aligned at their centres, the torque at the same point on the blade will remain unchanged regardless of its position within the rotation. However, the recovery in toque production is small as the distances between wind turbines increase and even at 10D is not sufficient to yield desirable results. The torque emphasises how even minor changes in velocity can affect CP and power production, this is because of the cubic relationship between velocity and power.

Analysis of aligning two wind turbines at their centres has shown that it is a layout that should be avoided when designing a wind farm. While there is noticeable recovery in the wake for increasing distances, the overall performance gain is minimal and will reduce the viability of any wind development.

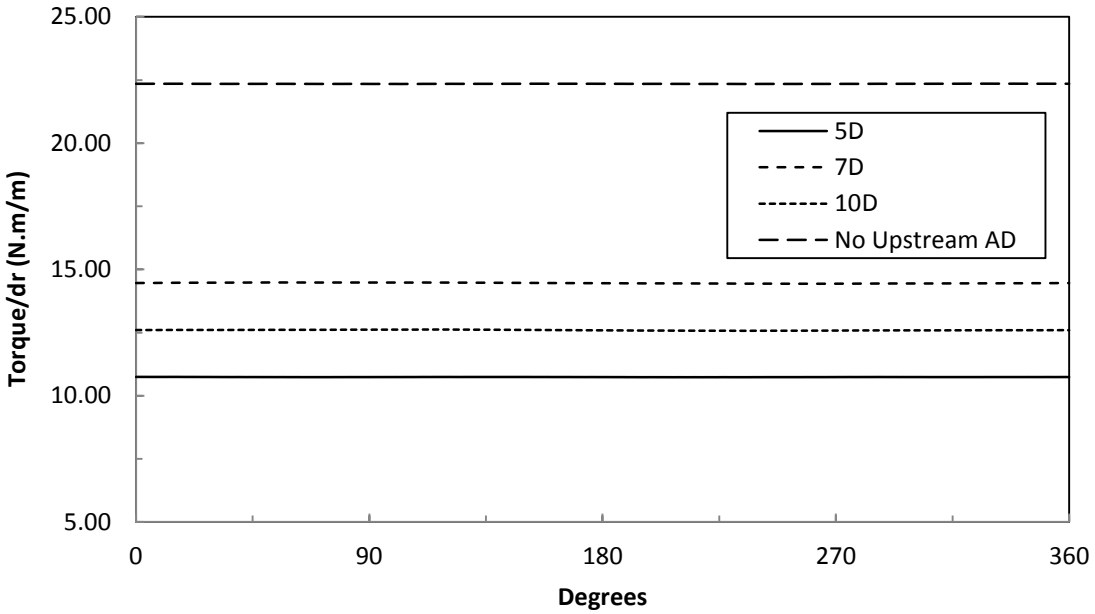


**Figure 5.12 Torque plot for position r/R=0.7 on a single blade throughout one rotation for aligned AD.**

### 5.3.2 Actuator Disc Offset Half a Diameter with Full Rotor

It is unlikely that multiple wind turbines will be aligned at their centres because of the hugely detrimental effect that it has on performance and the relative ease that it can be avoided when designing the layout of smaller wind farms. However, it is possible that two rotors will be offset by half a diameter relative to another for some prevailing wind directions. And this is especially the case for larger wind farms. With this offset there is an increased complexity between the interaction of wake and wind turbine, as depicted in Figure 5.13. The centre of the wake affects one side of the second turbine far more than the other and because of diverging, overall the rotor is always seeing a lower velocity when compared to the ideal case. The maximum wake deficit behind the second turbine appears skewed because of the misalignment and differences in velocities across the wake. This begins to even out further down the wake, but the wake width is noticeably wider and this is still detrimental to a third wind turbine; reflecting the drop in performance seen in the CP plot (Figure 5.6).

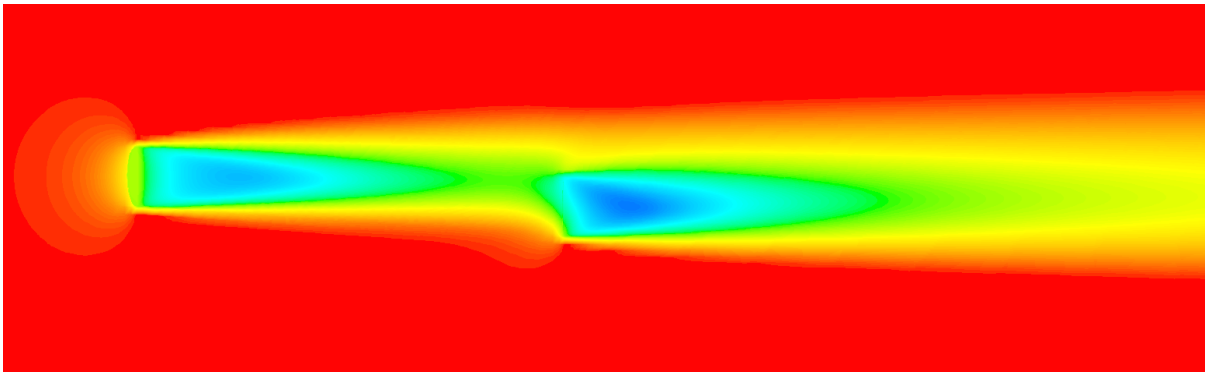

**Figure 5.13 Velocity magnitude contour plot of a wind turbine wake interaction between two wind turbines 7D and offset by half a diameter using the actuator disc technique (Red = 10 $ms^{-1}$ and Blue = 4 $ms^{-1}$).**

The $C_p$ plot found in Figure 5.14 compares the pressure changes along the same blade when fully behind the wake and outside of the wake. When the leading edge suction peak is compared to that of the ideal case (Figure 5.2), it is immediately apparent that it is reduced for all distances when the blade is out of the wake. It begins to improve with distance, but by 10D it has still not reached the ideal level of negative pressure; a result of the diverging wake mixing out with the surrounding airflow. For the blade directly in the wake itself the $C_p$ curve exhibits similar characteristics to that of the aligned case. However, at the leading edge there is little difference because the whole blade is now in the worst part of the wake rather than the lower two-thirds for the previous case. The wake has recovered and mixed out enough that by 10D the blades are experiencing only minor differences in $C_p$ along the chord of the blade both in and out of the wake. The $C_p$ plots describe the difficulty of optimising the TSR of a wind turbine when the blades are continuously rotating in and out of a wake, because the relative wind speed never remains the same through a 360˚ rotation, the AoA the blade is able to achieve also varies. The inherent issue with this is that compromises will be made by the wind management system that controls the pitch of the blades, which in turn effects the operating TSR.

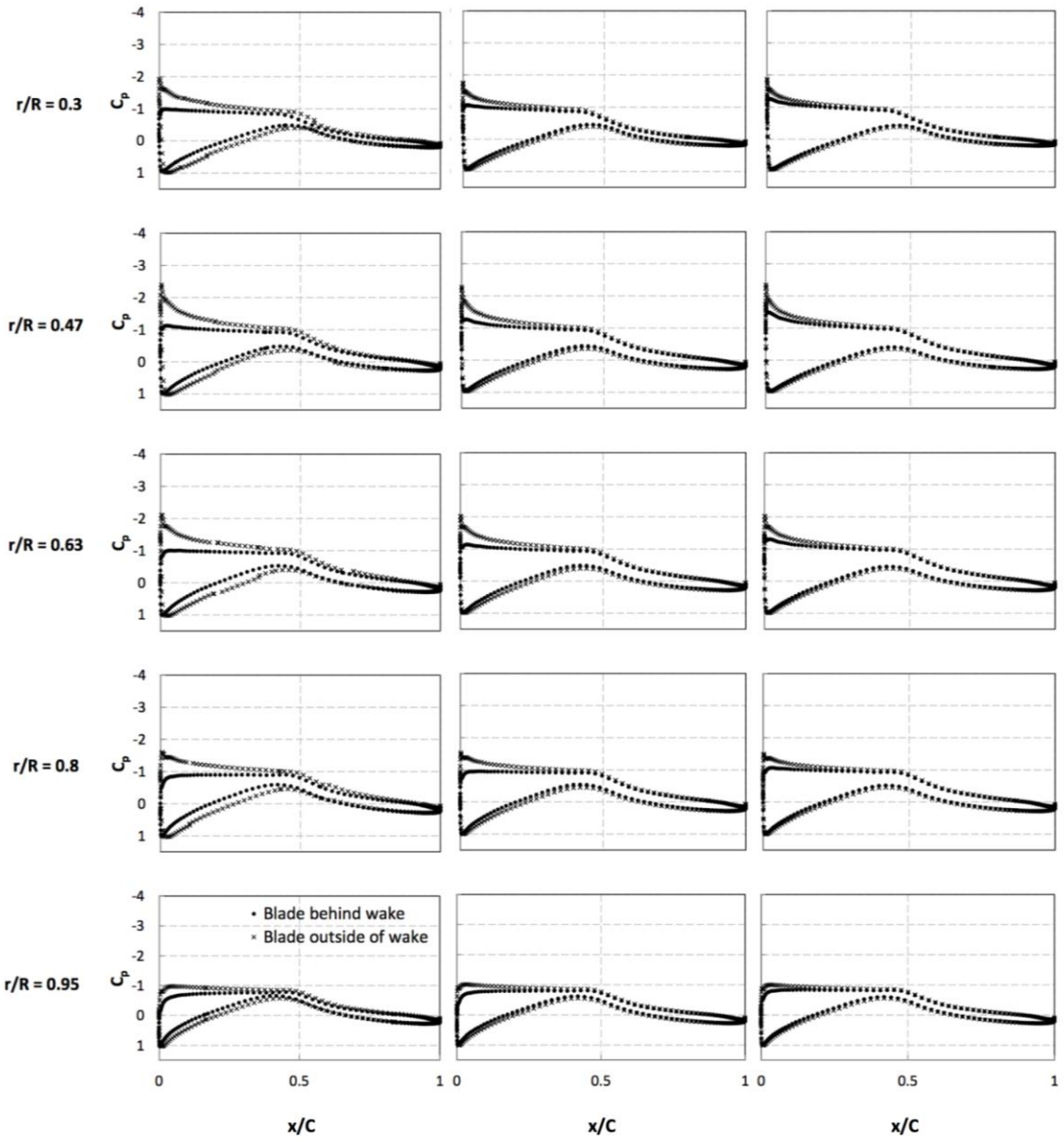


**Figure 5.14 $C_p$ plots along the blade at five radial distances for cases: 0.5D offset AD at 5D upstream of rotor (left), 0.5D offset AD at 7D upstream of rotor (middle), and 0.5D offset AD at 10D upstream of rotor (right) – all versus no upstream AD or rotor.**

The pressure contour plot (Figure 5.15) illustrates the difference between the pressure distributions along the surface of the blade as it rotates in and out of the wake. Out of the wake the blade sees an increased area of negative pressure that translate the length of the blade, but the differences overall are small. It is, however, enough to mean that the rotor half in the wake of another wind turbine is preferable to that of one deeper into the wake.

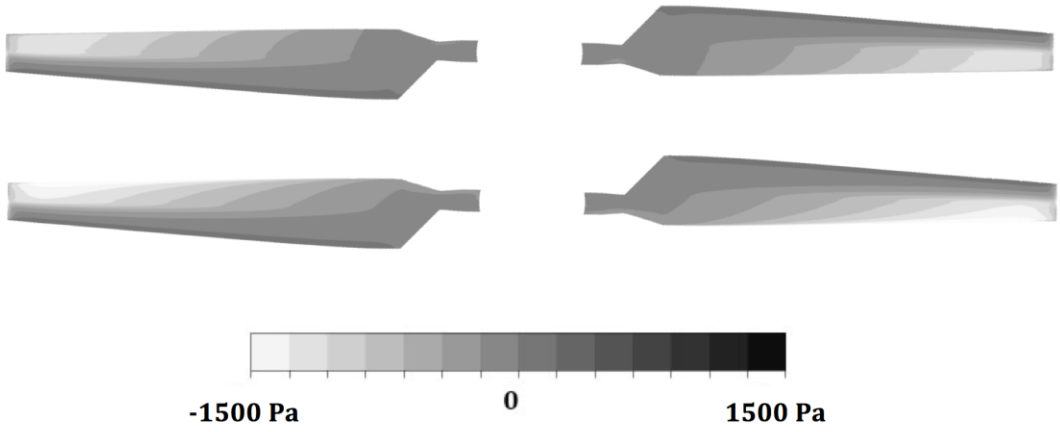


**Figure 5.15 Pressure contour plots on the suction surface of the blades for cases: No upstream AD (top). Rotor 7D downstream 0.5D offset AD (bottom) - out of wake (left) and behind the wake (right).**

As the second wind turbine becomes offset by half a diameter, the aerodynamic interactions between the two become more complex. At this point half the turbine is always in the wake of the upstream one, while the other half is outside. A result of this is when monitoring one blade through 360 degrees the torque values (Figure 5.16) are shown to be periodic. When the blade is fully in the wake of the upstream wind turbine at 90˚, the torque produced rapidly falls. It begins to gradually rise as it rotates through and out of the wake between 135˚ and 270˚, before falling as the effects of the wake takes hold once again. The periodic nature begins to smooth out as the distance between the two increases, a consequence of the diverging wake and the wind velocity recovering, but this also reduces the peak torque value when outside of the wake. Despite the recovery in the wake the torque produced does not quite reach that of the ideal case even at its peak, something that the $C_p$ curves suggested.

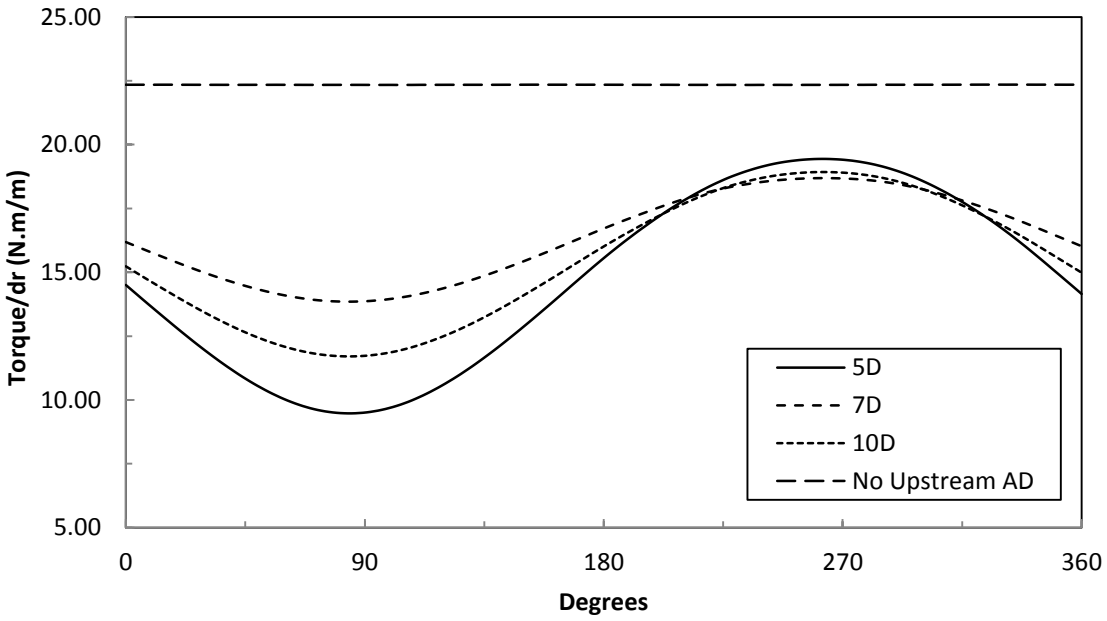


**Figure 5.16 Torque plot for position r/R=0.7 on a single blade throughout one rotation for 0.5D offset AD.**

Two wind turbines interacting when offset by half a diameter are less detrimental to performance and increasing the distance can mitigate this. The overall performance improvements from larger distances between wind turbines are smaller compared to the aligned case, because of the diverging wake. While the wake is recovering with distance, more of the rotor sees it. This problem becomes more evident when wind turbines are offset by one diameter.

### 5.3.3 Actuator Disc Offset One Diameter with Full Rotor

An inevitable outcome of wind farms in the UK is that some form of interaction between turbines is going occur, even when visually it doesn't appear that the wake would have any effect. Figure 5.17 shows the wake interaction when two wind turbines are offset by one diameter. The effect is similar to that found in the previous case, but is overall far less damaging to the wind as seen by the second rotor. Noticeably, the further downstream the turbine is placed the more of the wake it sees, which impedes on potential energy yield. The wake behind both wind turbines is much wider than that

seen in the other cases, but it has also recovered more with increased mixing with the freestream flow.

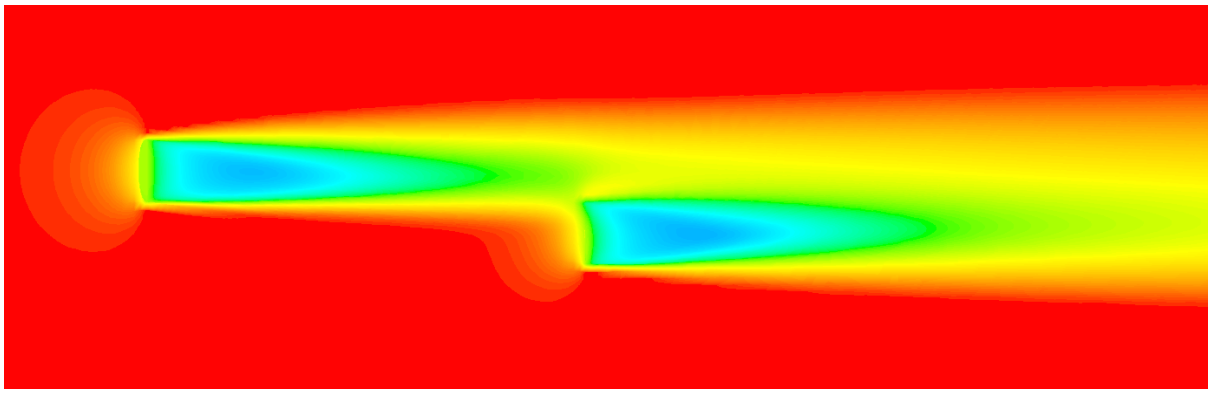

**Figure 5.17 Velocity magnitude contour plot of a wind turbine wake interaction between two wind turbines 7D apart and offset by one diameter using the actuator disc technique (Red = 10 $ms^{-1}$ and Blue = 4 $ms^{-1}$).**

The $C_p$ curves (Figure 5.18) show a vast improvement when compared to the other cases, but still does not match that of the undisturbed situation. Unlike previous layouts the leading edge suction peak is seen to fall as the distance between the turbines increase for the blade furthest away from the wake. The improvement seen for the blade closer to the wake due to wake recovery is outweighed by the worsening curve for the blade away from the wake. This is the result of a diverging wake and as the wake increases in width the percentage that the second rotor is affected it by also increases. At 10D the differences in the curves are much smaller, but the overall enclosed area falls. The minor changes in wind speed due to the diverging wake equate to approximately a 2% loss in performance for a doubling in distance between turbines. This is an important result, because it allows for wind turbines that are in relatively close proximity to one another to outperform that of more spread out layouts. However, it still should be a matter of priority to reduce interactions to zero as and when possible.

The pressure contour plot (Figure 5.19) displays the minor changes in pressure along the surface of the blade, significantly towards the tip, at which point the greatest

amount of time is spent in the disturbed airflow of the wake. It is also clear the blades are not performing as well as in the ideal case, with less negative pressure distributed along its length. Ultimately, the overall ability for the blade to produce lift is reduced and, thus, the torque production is lowered.

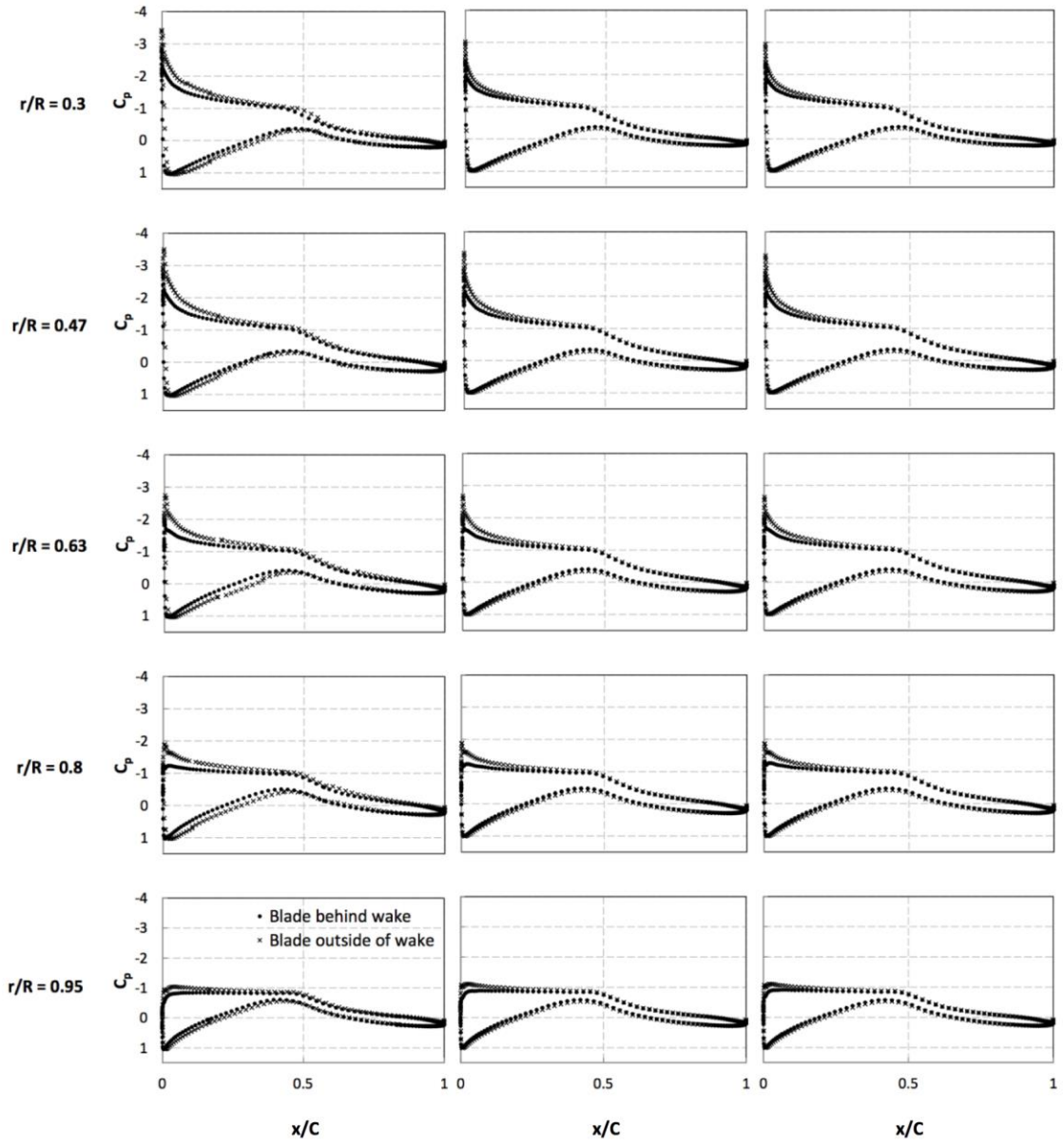


**Figure 5.18 $C_p$ plots along the blade at five radial distances for cases: 1D offset AD at 5D upstream of rotor (left), 1D offset AD at 7D upstream of rotor (middle), and 1D offset AD at 10D upstream of rotor (right) – all versus no upstream AD or rotor.**

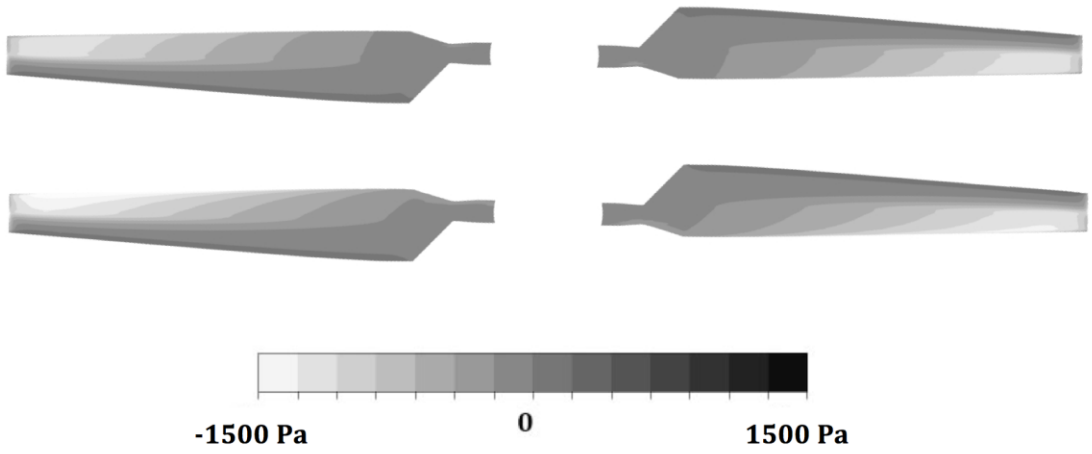


**Figure 5.19 Pressure contour plots on the suction surface of the blades for cases: No upstream AD (top). Rotor 7D downstream 1D offset AD (bottom) - out of wake (left) and behind the wake (right).**

For this case the torque production is similar to that of the ideal setup as revealed in Figure 5.20. Reiterating the results from the CP data and $C_p$ curves, the second wind turbine performs best at 5D, it can be seen that while at 90° the torque production is at its lowest, the recovery to the ideal level is far quicker than that of the increased distances. The flattening effect occurs for 7D and 10D, where the diverging wake is mixing more with the surrounding airflow and, therefore, lowering the peak wind speed. The consequence of these results is interesting as it is counterintuitive to what is expected from turbine-turbine interactions. It also allows for wind turbines in larger wind farms to be placed in closer proximity to one another when such conditions arise. The increased yield is dependent on the correct flow direction as it could also result in increased wake interactions if prevailing wind directions change.

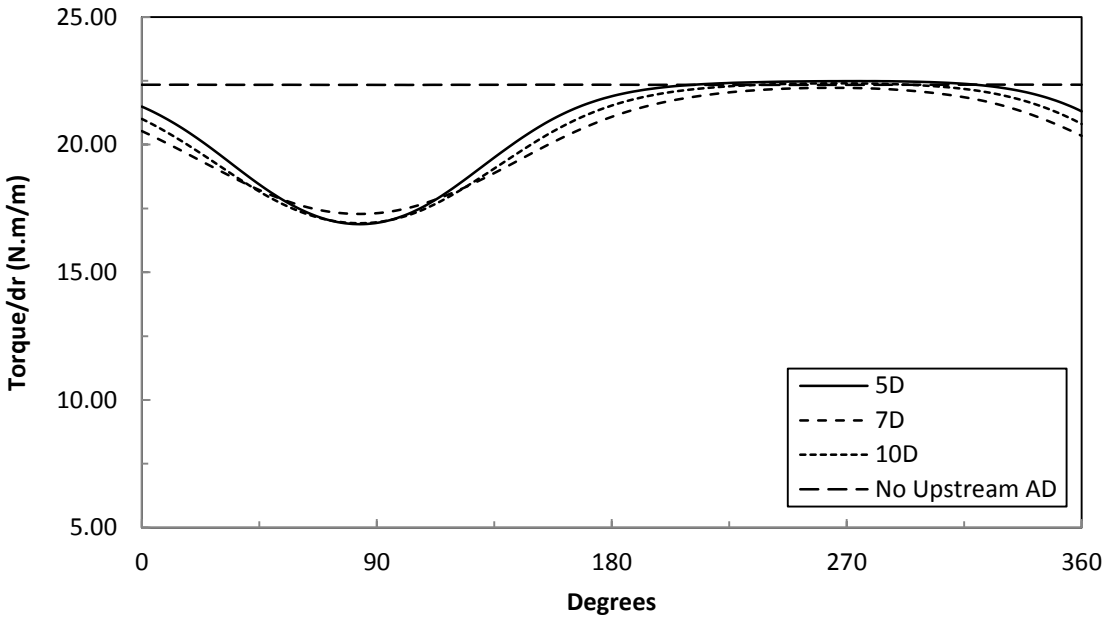


Figure 5.20 Torque plot for position r/R=0.7 on a single blade throughout one rotation for 1D offset AD.

Thus far the interactions of only two wind turbines has been analysed. It is often the case that a third row of turbines will be present in a wind farm and it important to understand how the aerodynamics of two upstream rotors can affect the performance.

### 5.3.4 Two Actuator Discs Upstream of Full Rotor

Increasing the number of rows of wind turbines in wind farms increases the complexity of optimising layout due to the higher probability of wake interactions occurring. However, in a column of wind turbines, the third row shows a slight improvement when compared to that in the second row for aligned and offset by one diameter cases; but there is a fall in performance when offset by half a diameter. The biggest change is seen for the aligned case, where for a separation of 7D the CP of the third wind turbine increases by 9% from the second. The coefficient of pressure, $C_p$, curves in Figure 5.21 show how the different layouts affect the aerodynamics around the blade. By comparing the fully aligned case and the ideal, the drop in performance is noticeably less than the second wind turbine at a distance of 7D (Figure 5.10). The

change in the leading edge suction peak is also less, especially in the upper two-thirds of the blade, which yields a larger enclosed area. The reason for this can be explained by the available power in the wind as illustrated in Figure 5.22, the airflow is able to recover more after the second wind turbine given the same distance, even once the drop in velocity upstream of the rotor due to blockage is taken into account.

For the offset by half a diameter case, the overall enclosed area is not much larger than that of the aligned case. There is a small improvement as the blade rotates out of the wake, especially in the upper half of the blade. However, in comparison to $C_p$ curves for the same separation (Figure 5.14) there is a noticeable drop in overall lift the blade is able to produce. This is due to the width of the accumulated wakes dropping the wind speed across the whole rotor. Moving to a one diameter offset, the improvements are significant; by this point the wake has mixed out enough that the velocity across the whole rotor is similar. The curves for when the blade is in and out of the wake are comparable, with the bigger disparities occurring towards the tip. When the distance is 7D apart between wind turbines, the third one is only performing 7% less than the ideal case. This is important because it illustrates that a wind farm with wind turbines that are precisely sited can all perform near maximum output.

The torque plot shown in Figure 5.23 depicts the torque along a point on the blade through a single rotation for all cases at distances of 7D. Immediately it is clear the performance gains of the third wind turbine over the second for the aligned and offset by 1D cases, which further iterates the differences in CP described in the beginning of Section 5.3. When the three rotors are offset by one diameter, the third reaches a similarly lower torque production at 90°, however it increases sooner and the peak goes slightly above that of the ideal case. This is the result of mixing of airflow from both the

upstream wind turbines and the surrounding freestream wind. The drop in overall torque production for when the rotors are offset by half a diameter is due to when the blade is in the wake, it finds itself in the area of largest velocity deficit.

By comparing three rows of wind turbines in various layouts an enhanced picture is provided for performance gains and losses in a wind farm. It is important that the second row of wind turbines is optimised so that the separation from the first is enough the wake does not diminish performance drastically. Improvement is seen in the third row, and by optimising the second row all wind turbines thereafter will see increased performance; the basis of which can be used for designing future wind developments.

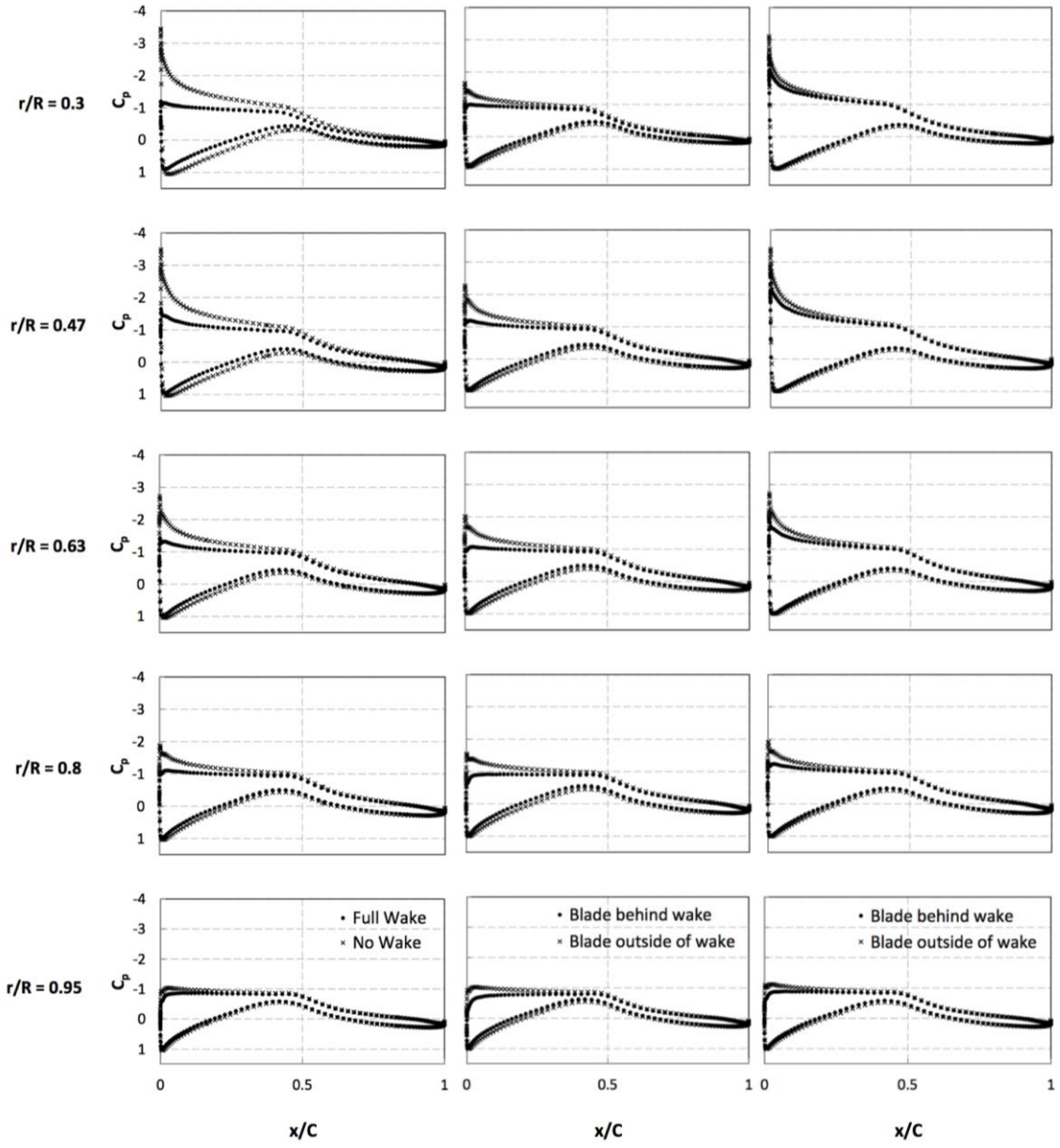


**Figure 5.21 $C_p$ plots along the blade at five radial distances for cases: Aligned AD at 2x 7D upstream of rotor versus no upstream AD of rotor (left), 0.5D offset AD at 2x 7D upstream of rotor (middle) and, 1D offset AD at 2x 7D upstream of rotor (right).**

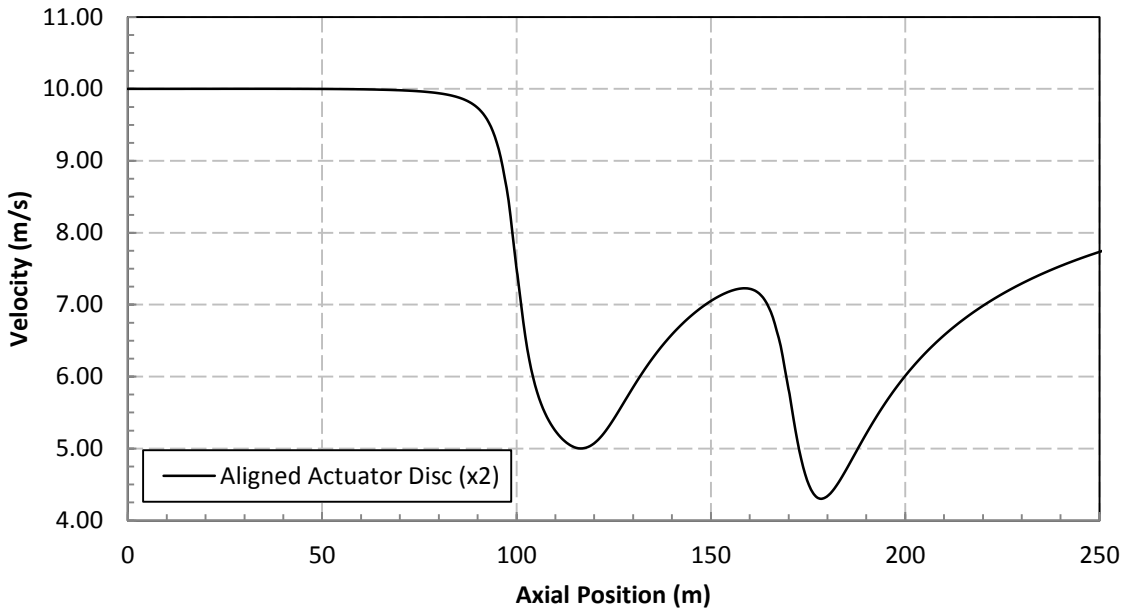


Figure 5.22 The wake recovering behind two fully aligned actuator discs.

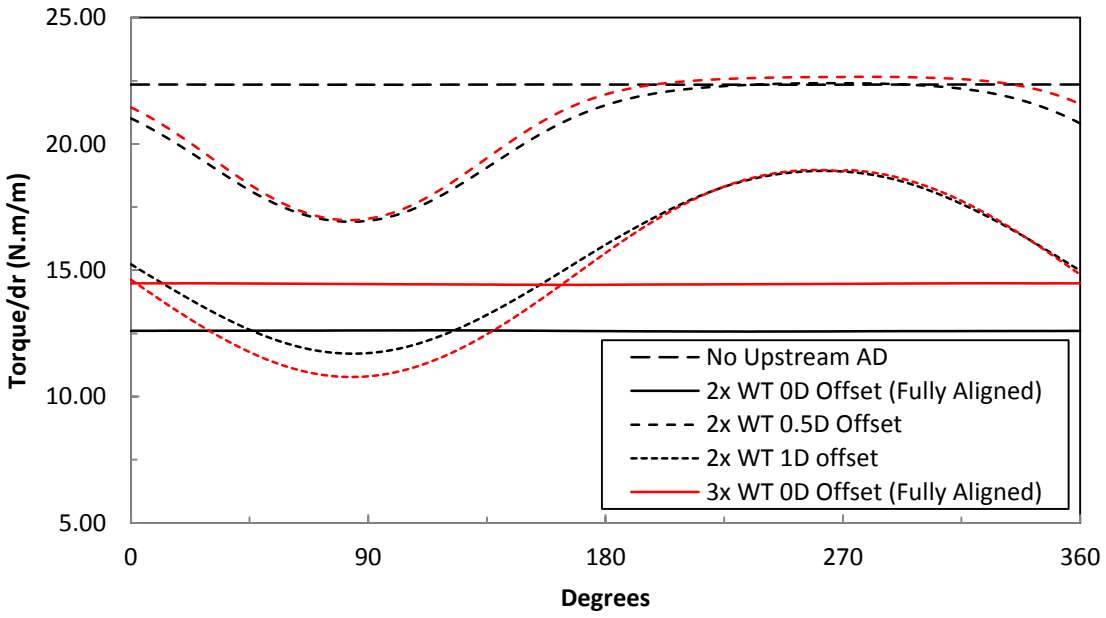


Figure 5.23 Torque plot for position r/R=0.7 on a single blade throughout one rotation comparing the second and third turbine in row at 7D apart.

## 5.4 Summary

Numerical simulations have been carried out to investigate a set of reference cases and the effects of turbine-turbine interactions over a range of offset positions and downstream distances, using a new novel methodology developed through this thesis.

An ideal case was used for comparison and it was found that two wind turbines aligned at their centres yield the largest drop in performance. As the downstream distance increases, the wake from the first wind turbine recovers and becomes less detrimental when interacting. Offsetting the second wind turbine by half a diameter shows an improvement, and once again, increasing downstream distance is also beneficial. When the turbines are offset by one diameter, an increase in distance between the two results in a fall in performance because the diverging wake outweighs the recovery experienced. Adding a third wind turbine shows improvement when compared to the second row for the cases where all three turbines are aligned at their centre and offset by one diameter to the rotor upstream.

The next chapter seeks to apply the findings from the reference simulations to provide suggestions for improving a current wind farm called Blackstone Edge in the form of a case study.

# 6 CASE STUDY: BLACKSTONE EDGE

## 6.1 Introduction

In the previous chapter a novel hybrid methodology of combining actuator disc theory and high fidelity wind turbine rotor simulations was applied to a set of reference cases. The result of which yielded an understanding of how the location of interacting wind turbines can be detrimental to the energy yield of a wind farm, which in turn affects the economic viability. In this chapter the simulation methods are used for a case study of a wind farm called Blackstone Edge. This will be used to assess the current energy yield of the wind farm and then using an engineering approach, consider and evaluate alternate layouts, the number, and the size of individual wind turbines. Toward the end of the chapter an annual energy yield analysis for all the suggestions made has been carried out to quantify the potential improvements offered.

Blackstone Edge is a wind farm that was developed by E.ON but is now owned and operated by a relatively small renewable energy developer, Infinis. The wind farm

consists of three 2.5 MW Nordex N80 wind turbines, that have an 80 m rotor diameter, a hub height of 60 m and, a height to tip of 100 m. The wind farm is located on a small farm in the North of England, in close proximity to the Peak District National Park.

Figure 6.1 is taken from the design and access statement submitted by E.ON to Barnsley Metropolitan Borough Council [93] and depicts the location of each wind turbine within the boundaries of the farm for which it is placed. The numbers found for each wind turbine in this figure will be used going forward in the following format, Wind Turbine 1 is known as WT1, and so forth. Of the three wind turbines, WT1 is at the highest elevation and both WT2 and WT3 are lower than this point by 18 m and 4 m, respectively. The environmental constraints for the allotted plot of land are shown in Figure 6.2, the details and consequences of which will be discussed in the next chapter where the planning implications of the wind development are analysed. The remainder of this chapter will focus on the modelling and engineering analysis.

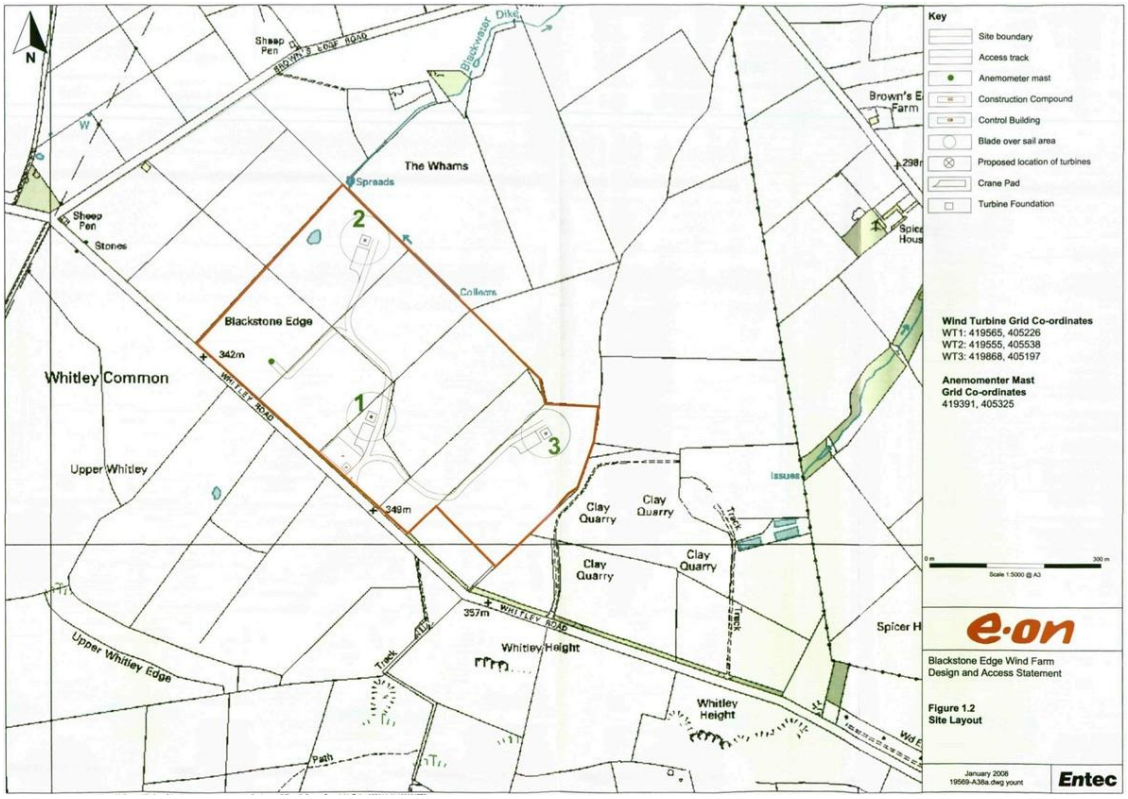


**Figure 6.1 Blackstone Edge wind farm site layout from the design and access statement, from** [111].

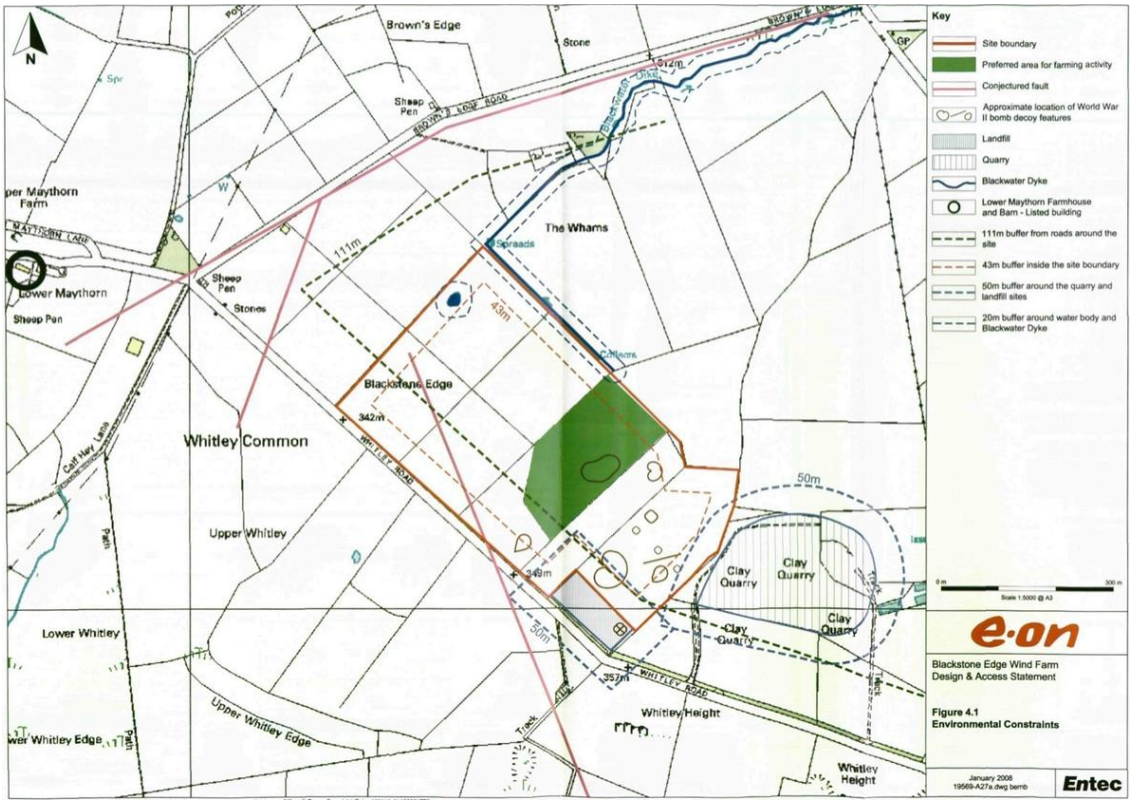


**Figure 6.2 Blackstone Edge wind farm environmental constraints from the design and access statement, from** [111].

As mentioned above, 2.5 MW Nordex N80 wind turbine are used, the power curve for which is found in Figure 6.3. This particular wind turbine has a cut-in wind speed of approximately 3 $ms^{-1}$ and a cut-out wind speed of 25 $ms^{-1}$, which is regulated by altering rotor blade pitch angle [112]. The maximum CP occurs with a wind speed of approximately 8 $ms^{-1}$, which as described in the next section is similar to that found on site.

For the purposes of this case study the author has used the same NREL rotor model as used in previous chapters, and employed the scaling techniques described in Section 4.6. The reason for this is that the purpose of the case study is to compare the effects on energy yield that layout and wind turbine size has, rather than the aerodynamic characteristic changes between different turbine models. There would also be very little gained from developing a new turbine model for this study and time constraints deemed it unnecessary. By producing a normalised comparison, where the current energy yield of the wind farms equal to unity, then a percentage gain in improvement can be calculated for the suggestions laid out. Therefore, it should be understood that the results laid out in the remainder of this chapter do not reflect or simulate the current or suggested replacements for the wind turbines found on Blackstone Edge, but rather show a representation of potential differences between suggestions.

It should be noted that when an actuator disc is used for the purposes of simulating interactions between wind turbines, the diameter and CP is matched for those conditions.

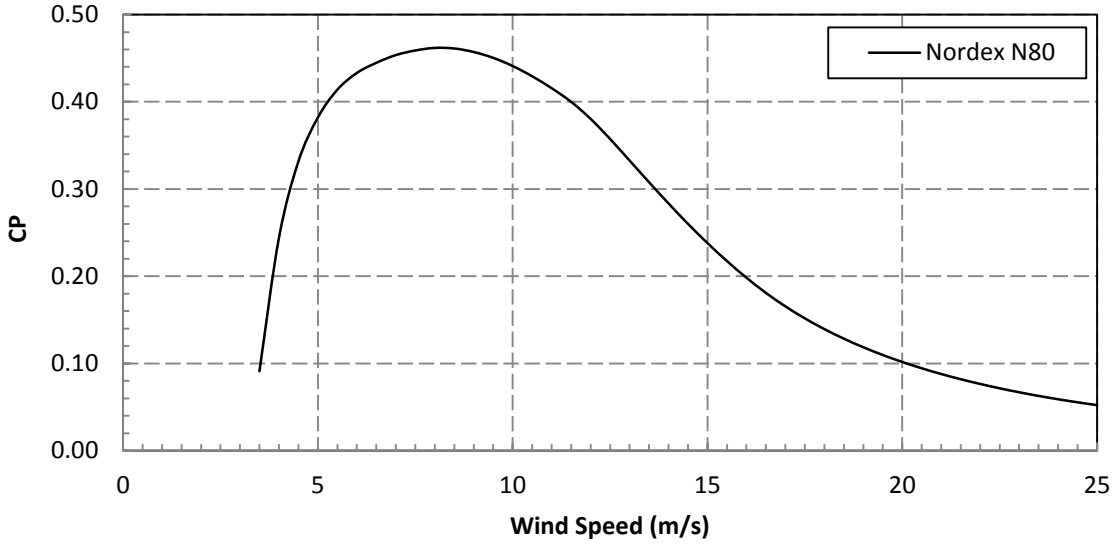


**Figure 6.3 Power curve for a Nordex N80 wind turbine, from** [112].

In order to carry out the case study that follows, background information on the wind farm in situ must first be presented. Figure 6.4 gives the normalised power output for each individual wind turbine for the year October 2013 – October 2014 and the mean wind direction for the corresponding months. Like most wind energy developments in the UK, peak power production occurs during the winter months with a fall in summer following the wind speed. However, the data for Blackstone Edge does not reveal when exactly each turbine is producing power or whether any were down due to maintenance. This is because the information is of commercial interest and, therefore, not all the data required for a complete analysis has been provided and what has been given is normalised. Fortunately, it does provide enough information to begin to make suggestions on potential improvements. Table 6.1 shows the normalised total power production for the three wind turbines found on Blackstone Edge wind farm, given that WT1 performed best by producing the highest amount of energy yield, WT2 yielded 4.82% less and WT3 8.50% less.

Table 6.1 Normalised total power production for the three wind turbines found on Blackstone Edge wind farm for the year October 2013 – October 2014.

| Wind Turbine | Normalised Power Production | Difference from WT1 (%) |
|---|---|---|
| **WT1** | 1 | 0 |
| **WT2** | 0.952 | 4.82 |
| **WT3** | 0.915 | 8.50 |

There are also drops in the overall power when the average prevailing wind is from a southerly direction, likely due to the effects the terrain and elevation change has on the wind turbine's ability to take advantage of the energy in the wind. Determining the productivity of a wind farm based on monthly totals and averaged data will not provide the complete picture of the effects that layout and terrain have on the wind farm.

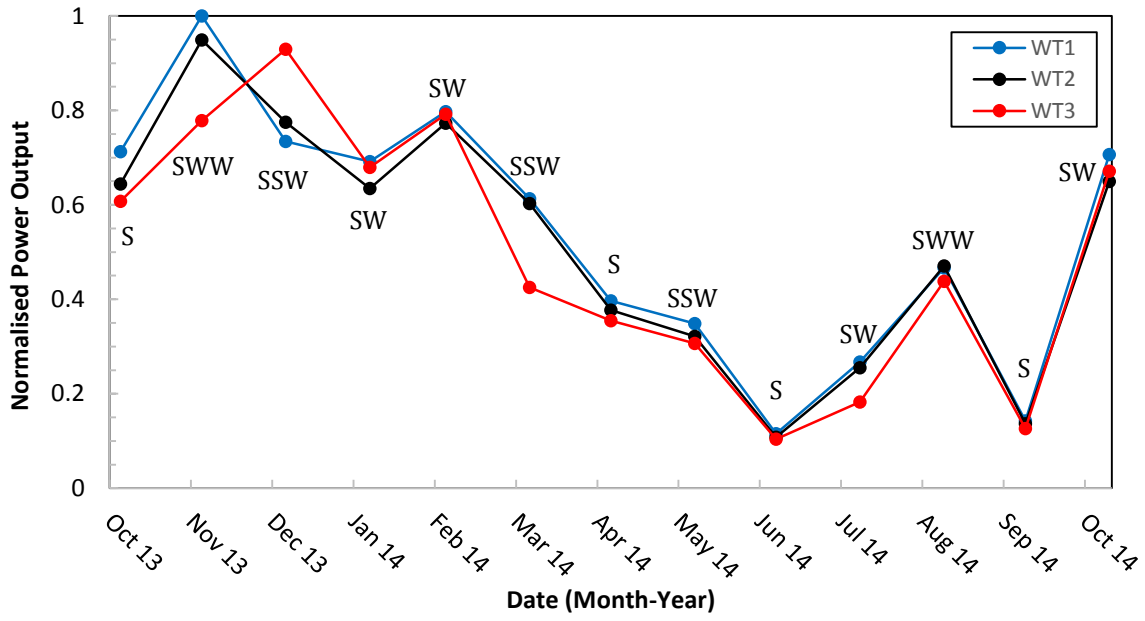


Figure 6.4 Normalised power production for the three wind turbines on the Blackstone Edge wind farm and mean wind direction for each given month, where S = South and W = West.

For the plots throughout the case study Figure 6.5 shall be used as reference for the relative position during a single rotation.

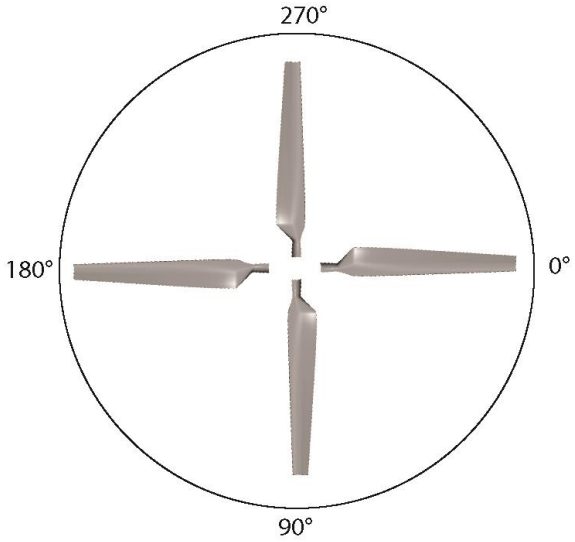


**Figure 6.5 Relative position of a single turbine blade relative to the ABL, with 90° closest to the ground.**

## 6.2 Ideal Case: Constant Inlet vs. ABL Inlet

The atmospheric boundary layer (ABL) results in a profile that shows a rise in velocity as the distance from the ground increases. The NOABL Wind Map provides a 1 km square resolution of localised wind speeds at heights of 10 m, 25 m, and 45 m [113], which when used with Equation (2.8) yields the plot shown in Figure 6.6. In this graph the extrapolated ABL is shown with the velocity profile replicated in Ansys Fluent as well as a constant inlet velocity boundary layer condition, which yields this boundary layer profile at the location of the wind turbine.

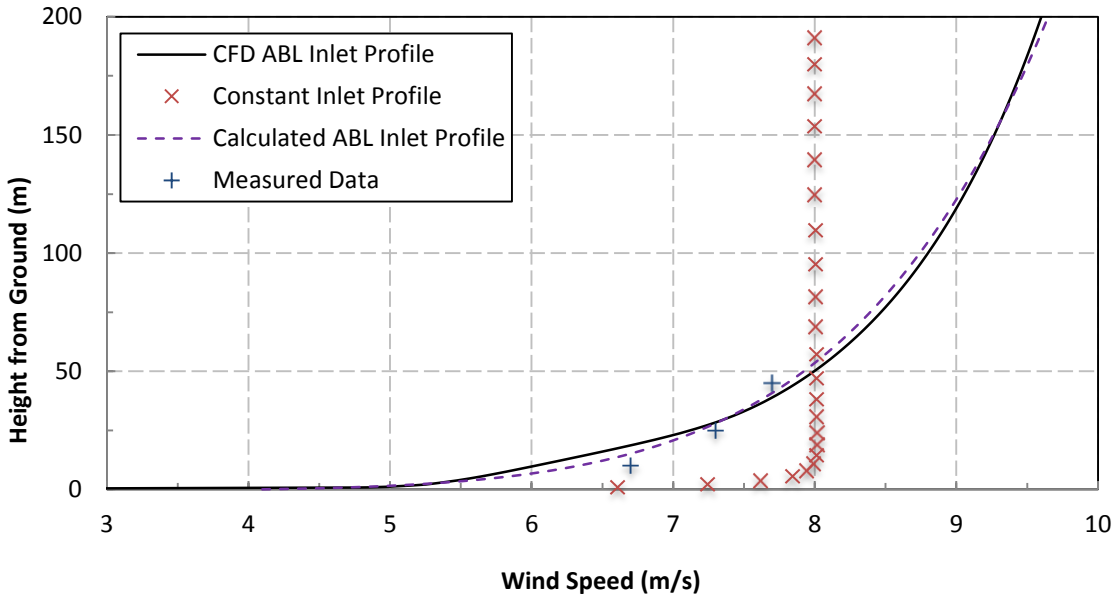


**Figure 6.6 Velocity profile with a constant inlet versus an ABL inlet calculated using measured speeds from NOABL Wind Map** [113].

A constant and ABL velocity inlet profile will alter how the wind turbine reacts due to the changing aerodynamics, which in turn effects power production. A constant inlet speed of 8 $ms^{-1}$ was chosen because it is approximately the average wind speed across the diameter of the rotor for this ABL profile. The CP for the wind turbine simulated in the ABL is 0.31 compared to a CP of 0.29 from a constant inlet. This increase in performance is due to the increased wind speeds experienced in the upper half of the rotation. Increased velocities in the upper half of the rotor contribute disproportionately to energy when compared to the reduced wind speeds in the lower half, the result is that within the swept area the integrated available energy is larger when compared to the constant inlet case. Higher velocity allows for a more optimal AoA to occur as the blade is closer to achieving the ideal TSR. This result is illustrated in Figure 6.7 where the $C_p$ along one of the blades from both cases when at 270˚, i.e. at the top of a rotation, is shown. The turbine in the ABL experiences higher wind speeds at the top of the rotor blade rotation (270˚) and thus results in a slightly larger leading

edge suction peak (where there is an initial high velocity followed by a deceleration) compared to when the blade is in the lower end of the ABL. In the upper two-thirds of the blade the incoming wind is up to 1 $ms^{-1}$ faster than that seen on the same location for a constant inlet speed. The stagnation point and the overall shape of the pressure recovery remain the same, with the overall integrated pressure-surface distance area changing as a result of the leading edge suction peak. The opposite will occur as the blades rotate 180˚ because there is less available kinetic energy in the lower end of the ABL. However, in general the increased performance that variation in the ABL offers is enough to see gains in power production.

The blade sees a maximum and minimum wind velocity as it rotates through the top and then bottom of a full circle. The pressure contours along the suction surface of the blades for both velocity inlet profiles are depicted in Figure 6.8. As expected, regardless of the point within the rotation, the constant inlet case shows no difference. However, for the ABL case when the blade is at the top of the rotation there is a slight increased region of negative pressure, this drops considerably 180˚ later. For this blade the difference due to location within the ABL is effectively the same as experiencing changing inlet speeds that varies up to 2.7 $ms^{-1}$ during each rotation. Compared with the constant inlet blade, at the bottom of the ABL the regions of negative pressure are far less, with the opposite occurring at the top of the rotation.

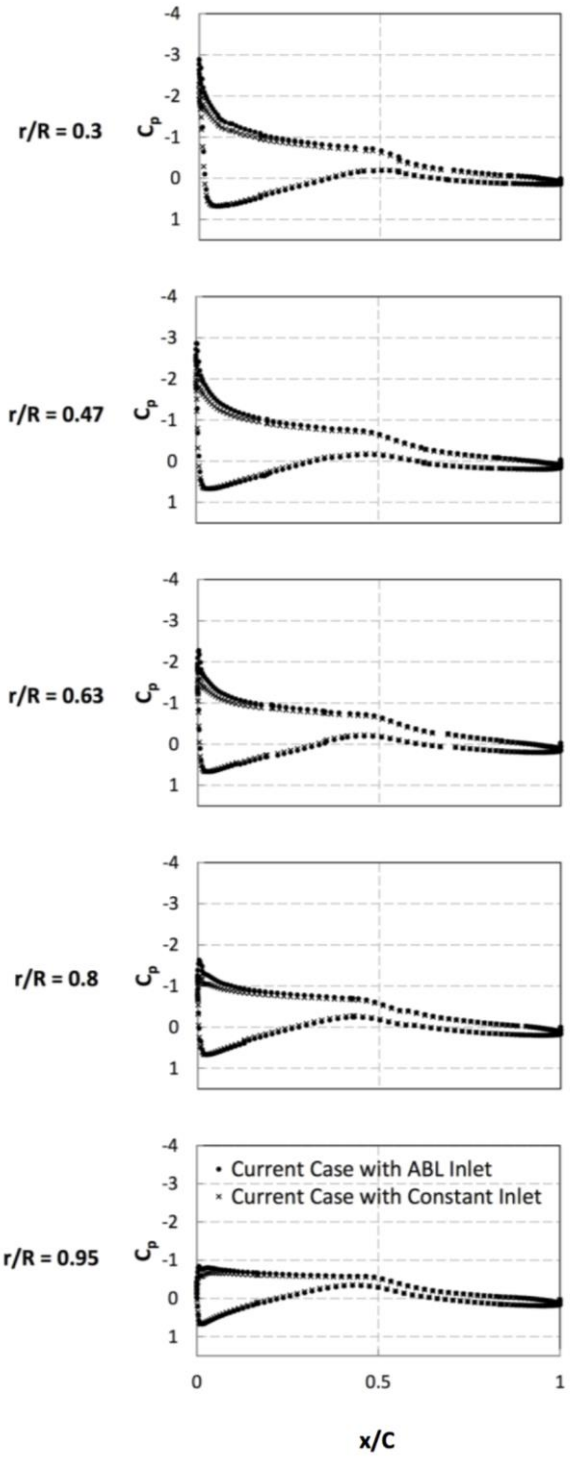


**Figure 6.7 $C_p$ plots along the blade at five radial distances for an ideal case at Blackstone Edge Wind Farm comparing a constant and ABL inlet velocity profile.**

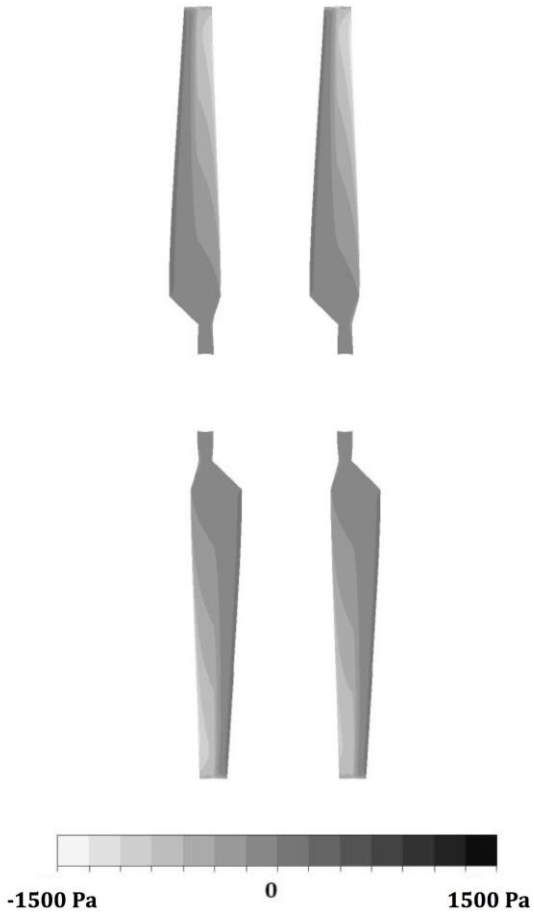


**Figure 6.8 Pressure contour plots on the suction surface of an ideal case at Blackstone Edge Wind Farm comparing a constant (left) and ABL (right) inlet velocity profile.**

An overall result of the blade rotating through the ABL is that it experiences a periodic change in torque production, as shown in Figure 6.9. The torque produced over a rotation varies from a minimum a little over 8,000 N.m to a peak of above 12,000 N.m, which is linked to the amount of lift the blade is able to produce from an optimal relative AoA. In the upper part of the ABL there is more available kinetic energy from higher wind speeds, which as described by Equation (4.9) has a cubic relationship with power production. While the increase in velocity actually reduces the optimal AoA, therefore decreasing lift, the small gain in velocity outweighs this and produces more torque. Therefore, the small increase in velocity goes a long way in terms of performance.

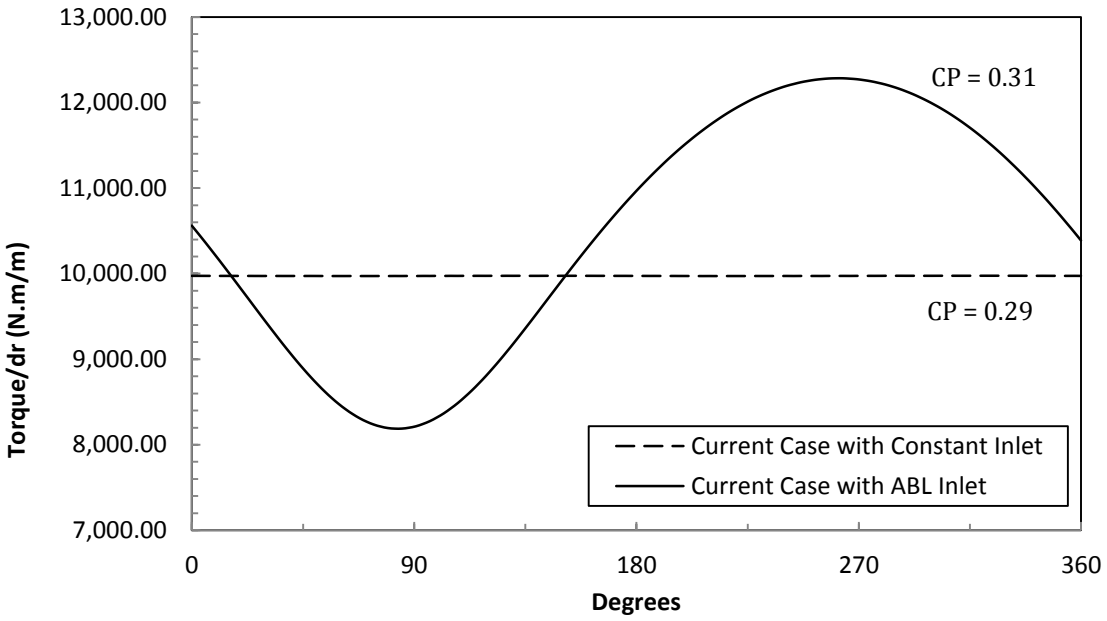


**Figure 6.9 Torque plot for position r/R=0.7 on a single blade throughout one rotation for an ideal case at Blackstone Edge Wind Farm comparing a constant and ABL inlet velocity profile.**

Given that the simulations now take into account the effects of the ABL, further cases can be investigated. This begins with the effects of terrain and layout of the wind farm.

## 6.3 Proposed Wind Farm Variations

By applying knowledge gained from the set of reference cases and an understanding of aerodynamic effects of terrain and the ABL, the following sections set out proposed changes to the wind farm found at Blackstone Edge. The intention is that by changing the position of a single wind turbine, increasing the hub height, or replacing three turbines with two larger ones, it can have a dramatic effect on the economic viability of a wind farm. At this stage, the proposed variations are solely based on maximising energy yield and either use the existing wind turbines found on site or other models that Nordex manufacture. Chapter 7 looks into the wider context of the implications that the suggestions made would have on the planning process for such a wind development and how current policy limits approval for such changes.

### 6.3.1 Terrain and Layout

One of the fundamental issues of wind farms in the UK is the compromise between visual amenity, environmental constraints, and layout. This plays a crucial role in the placement of individual wind turbines, not only on the landscape, but also with regards to one another. As mentioned in the previous section there is an elevation drop of 18 m from the south to the north side of the farm. The current layout means that this can be detrimental when prevailing wind direction is either southerly or northerly. For example, a southerly wind direction effectively produces a hill between WT1 and WT2 that results in a drop in velocity, and therefore, the energy in the wind is reduced. This reduction of energy in the wind is because the descent down the hill decelerates the air flow [46], which means the blades have less available kinetic energy to extract. There is a potential for flow separation off the hill to also occur because adverse pressure gradients may form along a decline in the slope, although this is unlikely because the change in curvature along the elevation is not sudden enough. If the situation is reversed and there is a northerly wind direction (while this does not happen often, as discussed by Porté-Agel et al. [36] all wind direction should be considered), because WT1 is higher up, when the air flow has reached the turbine it will have been accelerated slightly by the increase in elevation. This increased wind speed will yield higher power production, however, WT2 will have not seen this benefit in its current location. Moving the wind turbines toward the Southern side of the wind farm will have a profound effect, but this could lead to detrimental turbine-turbine interactions.

If the prevailing wind direction is Westerly, then the wake from WT1 has a negative effect on WT3. When rotated to face west, the distance between the two is only 3.75D. At this point in the wake the velocity is at its lowest (Figure 6.10), and with over

two-thirds of the rotor in the wake it renders WT3 almost redundant, yielding a 10.6:1 drop in power when compared to wake free inlet. Figure 6.11 and Figure 6.12 further illustrate the interaction; here the velocity streamlines are shown, behind WT1 the majority of the airflow is reduced considerably and has little time to recover before hitting WT3. There is also a drop of 4 m in elevation between WT1 and WT3, which further reduces the usefulness of the latter.

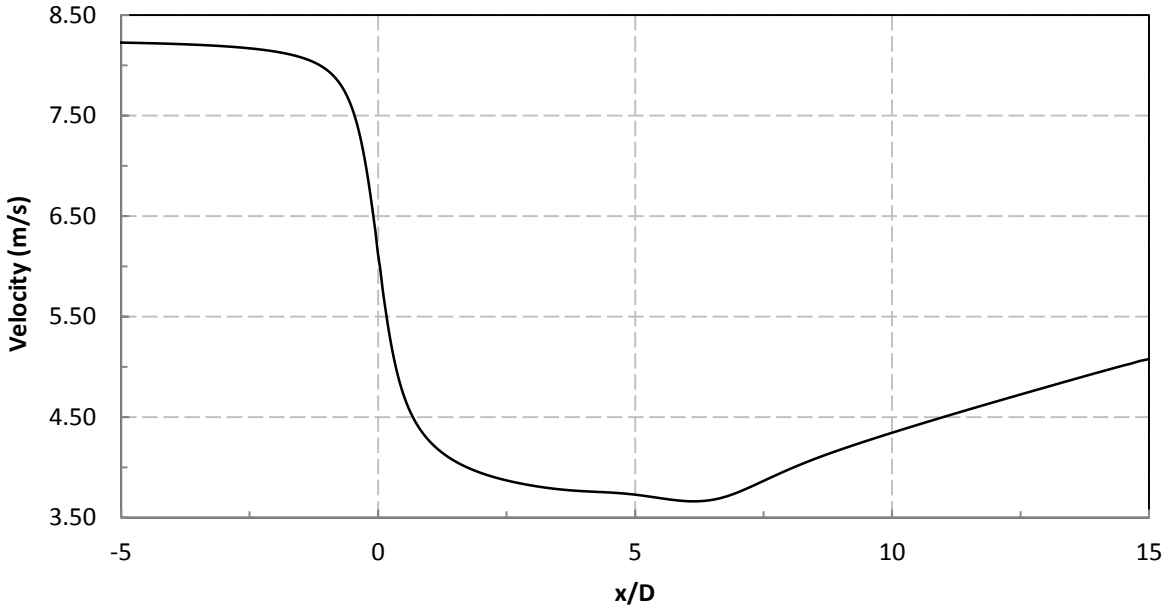


**Figure 6.10 The wake recovery behind an 80 m actuator disc.**

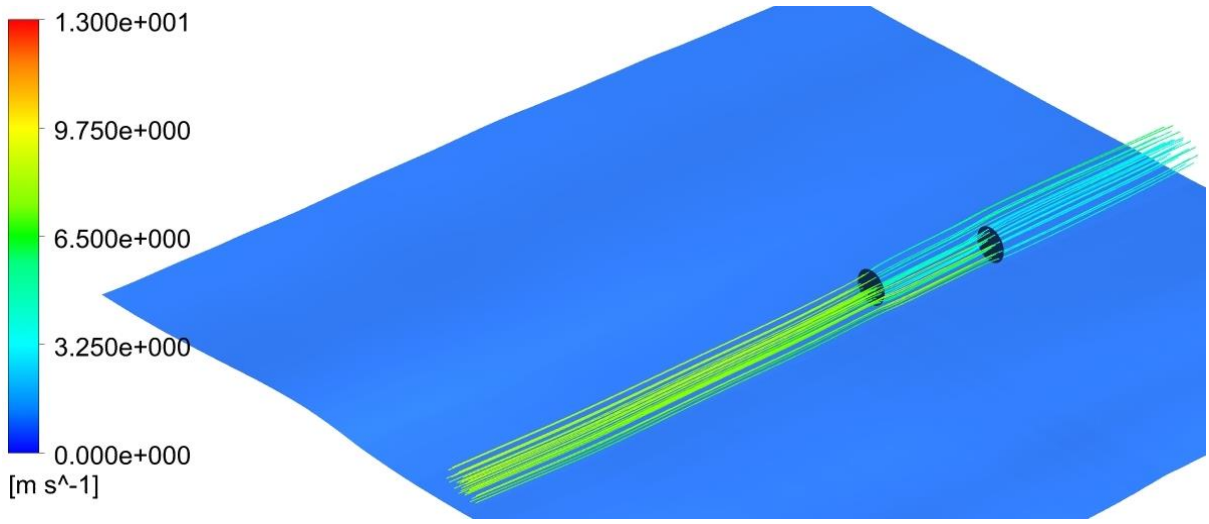


Figure 6.11 Velocity streamline plot of the interaction between WT1 (left) and WT3 (right).

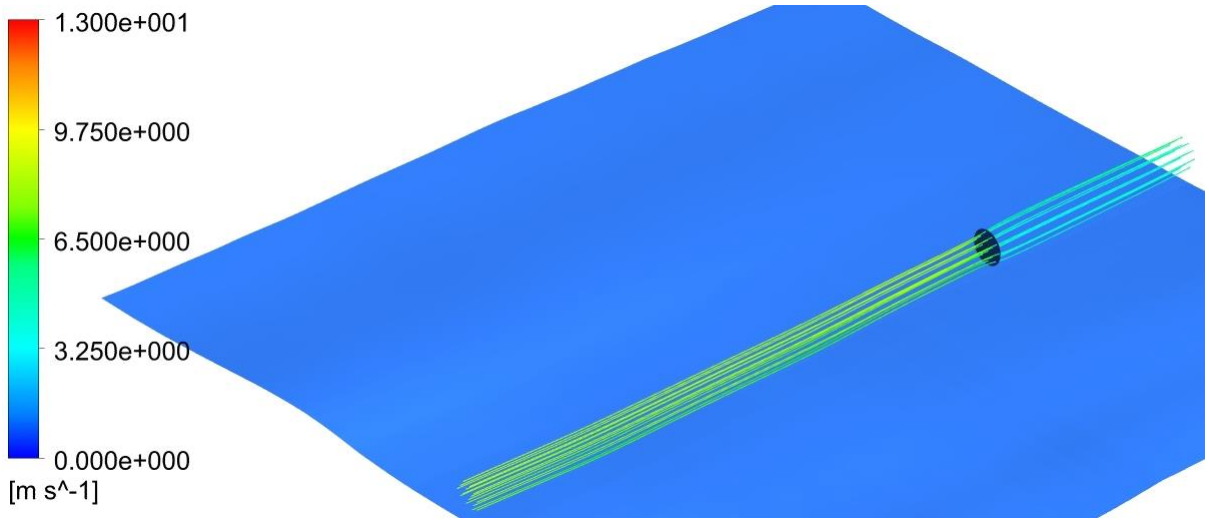


Figure 6.12 Velocity streamline plot of WT3 with WT1 relocated.

Due to the velocity deficit in the wake, the $C_p$ around the blade (Figure 6.13) especially toward the hub, which is in the centre of the wake throughout a whole rotation, the leading edge suction peak completely flattens into the positive region. This is because the relative wind direction at these velocities is closer to the true direction and, therefore, the AoA is far from ideal. The change in AoA moves the stagnation point around the blade, and the flow over the blade is causing it to generate less lift and

underperform. For this $C_p$ curve, the blade is in between the worst and best part of the wake for this layout. The pressure recovery along the chord barely reaches below zero, resulting in the area between the curves being greatly reduced which points to there being far less lift being produced. Toward the tip of the blade, which experiences the least time in the low velocity wake region during a rotation, the differences between the ideal case and the current layout is far less, which means that the tip generally performs significantly better..

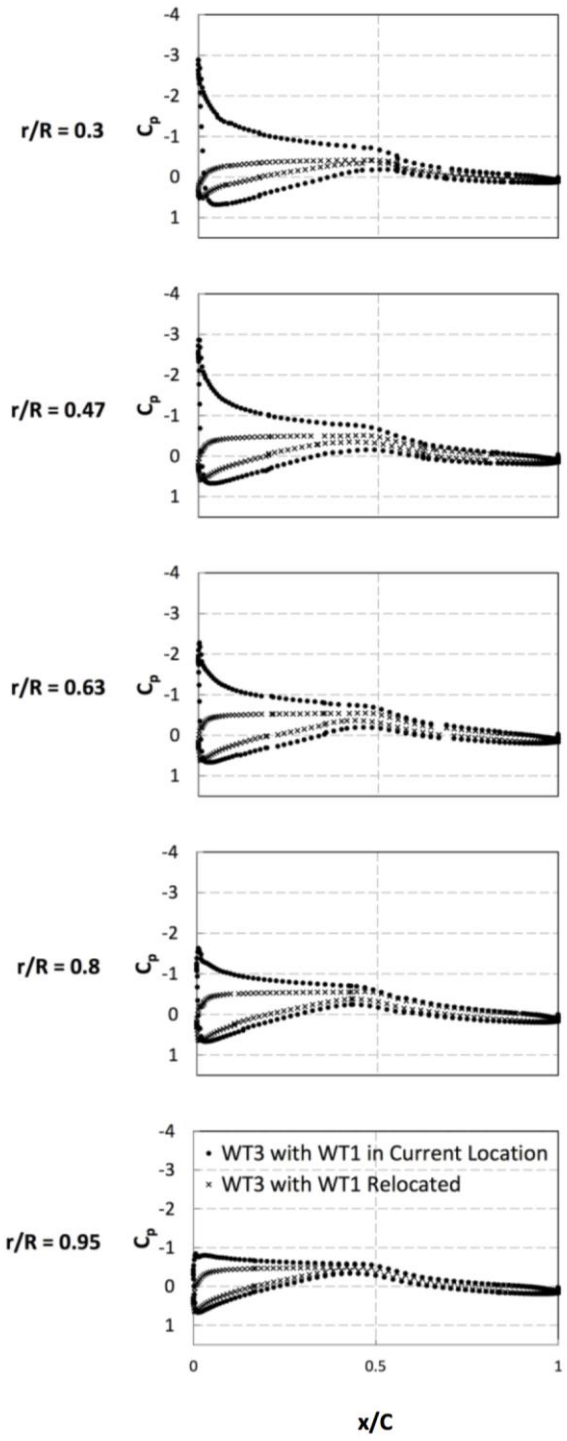


**Figure 6.13 $C_p$ plots along the blade at five radial distances for WT3 with WT1 in current location and relocated.**

The pressure contour plots are shown in Figure 6.14, the region of negative pressure toward the hub is almost non-existent, and the improvement toward the tip is

small. For the contour plot the blades are positioned at the top and bottom of the rotation, which while poor, it is not in the worst part of the wake.

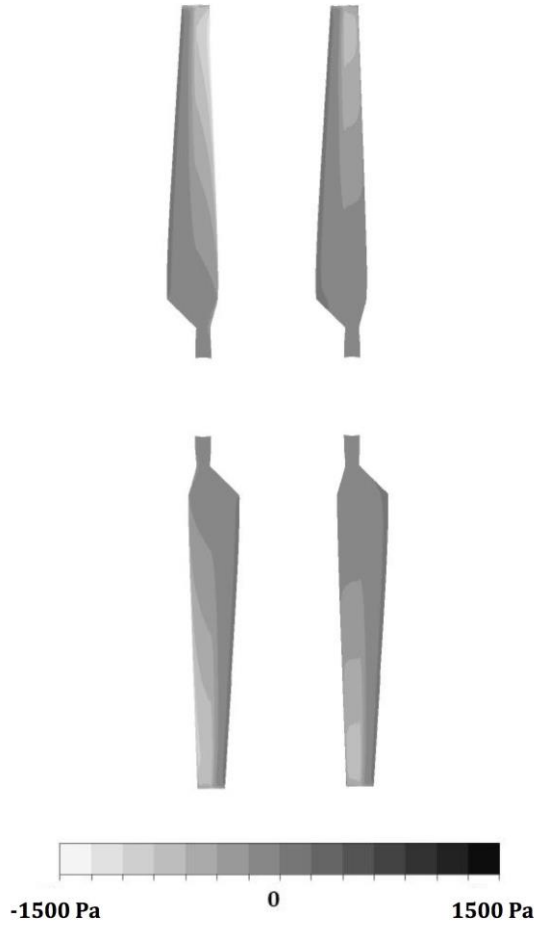


**Figure 6.14 Pressure contour plots on the suction surface for WT3 with WT1 relocated (left) and in current location (right).**

The wake deficit is so harmful that the ability of the wind turbine to produce power in the region of the maximum wake results in nearly no torque (Figure 6.15). The velocity in the lower end of the ABL exaggerates this, and even the increased velocity at the top end of the ABL has little effect in overcoming the detrimental feature of the wake. The peak torque is when the blade rotates out of the wake at 180˚. The corresponding overall CP reflects the inability for the wind turbine to be viable, with a drop from 0.31 to 0.09.

Fortunately, as the average power production suggests (Figure 6.4) WT3 is actually viable in comparison to the other wind turbines, however, it does tend to underperform. The prevailing wind in the UK tends to come from the west and for Blackstone Edge it varies mostly between this and a southerly direction. Had WT3 been located towards the edge of the plot on the south side, the interactions between it and WT1 would have been largely mitigated. Doing so would also have allowed WT2 to be placed further south, therefore, higher on the slope and increasing the average wind speeds it experiences. These suggestions are illustrated in Figure 6.16.

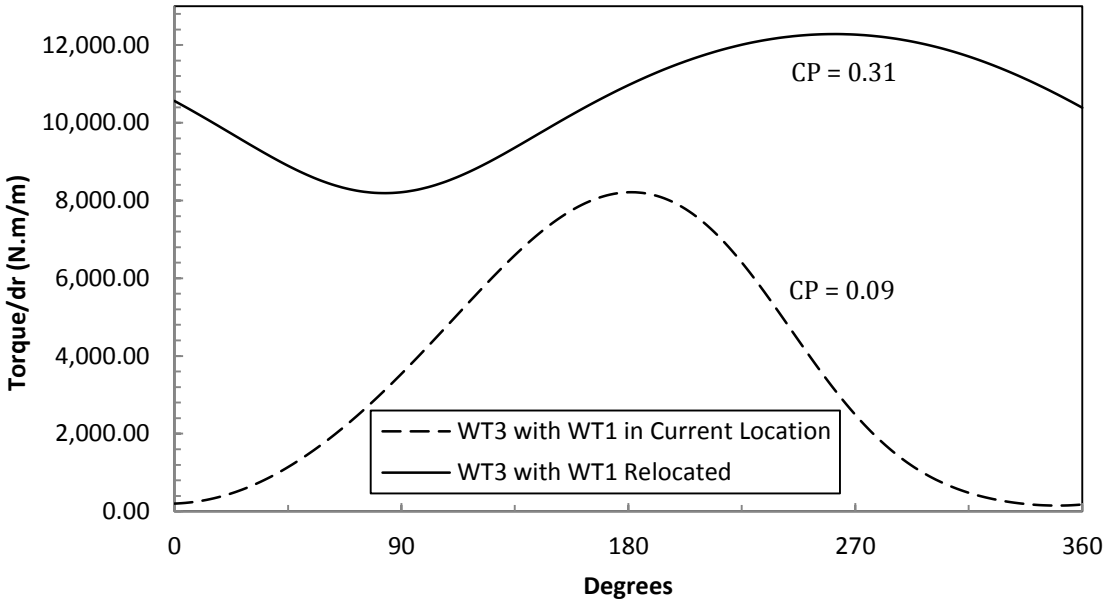


**Figure 6.15 Torque plot for position r/R=0.7 on a single blade throughout one rotation for WT3 with WT1 in current location and relocated.**

An analysis in Section 6.4 puts in to perspective the potential improvements that suggested changes to layout may have on annual energy yield.

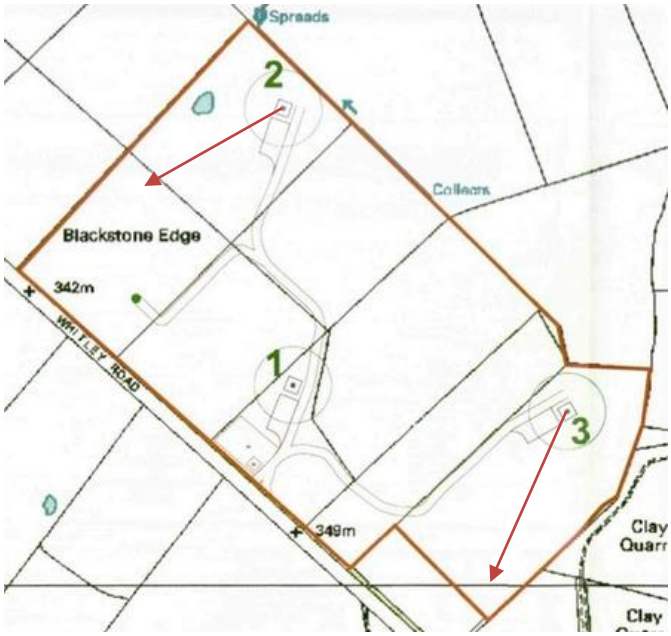


Figure 6.16 Suggested relocation of WT1 and WT3.

### 6.3.2 Hub Height

An increase in the height from the ground yields higher wind speeds within the ABL, naturally, this lends itself to wind turbines with taller hub heights. This aspect of the case study looks at how using the same wind turbine at different heights can be beneficial for performance. The models chosen are of those currently supplied by Nordex, these include the currently used hub height of 60 m, as well as 80 m and 100 m.

Figure 6.15 is a plot of $C_p$ around a single blade for the three hub heights; the blade is positioned at the top of its rotation where the velocity in the wind is highest. At this point the differences between the cases are small, with a slight change in leading edge suction peaks with increased hub height. The differences are small due to the already ideal conditions the blade is rotating in and thus, optimal AoA and TSR.

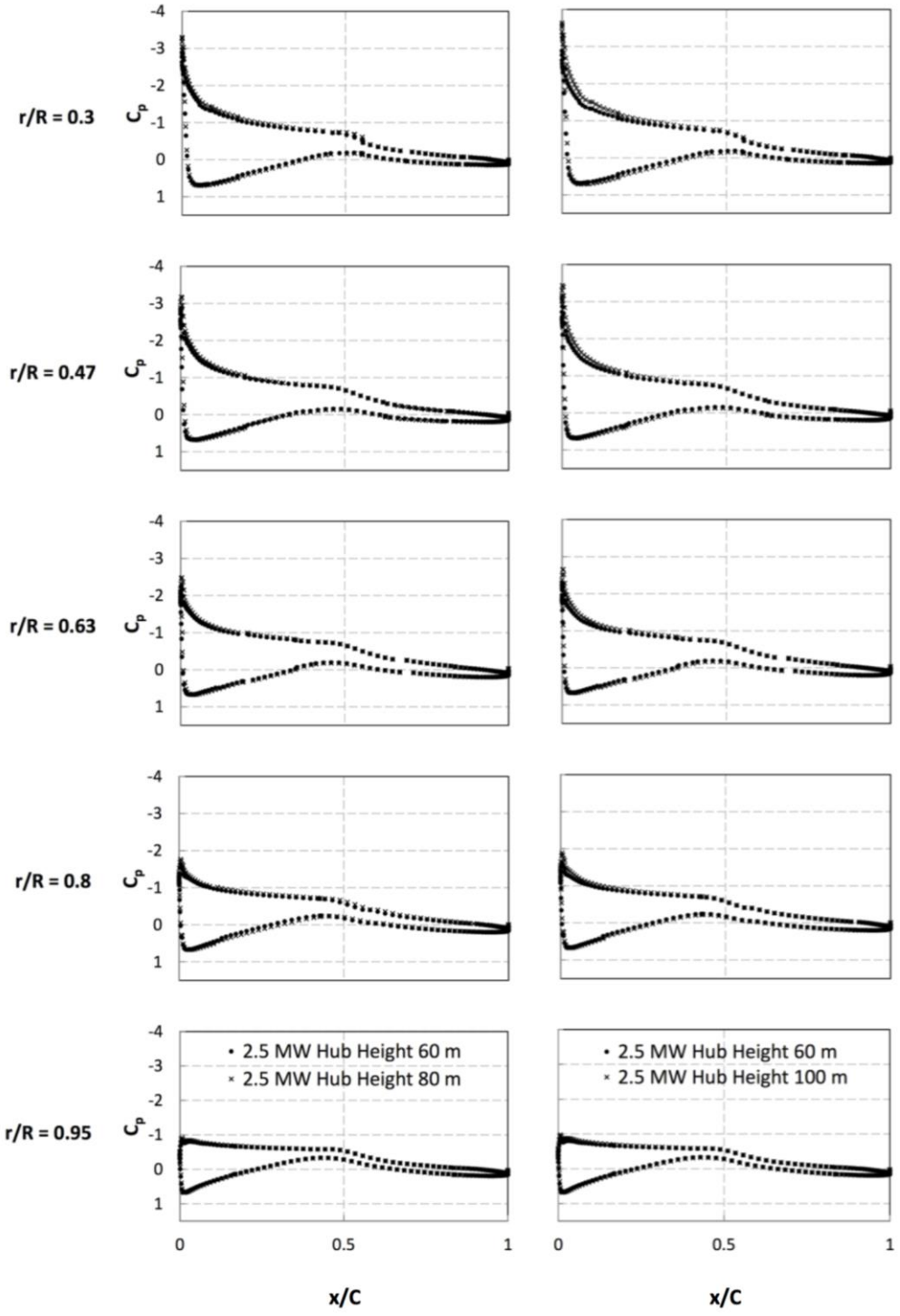


**Figure 6.17 $C_p$ plots along the blade at five radial distances for cases: a hub height of 60 m versus 80 m (left) and, a hub height of 60 m versus 100 m (right).**

Further analysis with the pressure contour plots (Figure 6.18) reflects the same minor changes. However, in the lower half of the rotation, where the change in velocity

varies more (as shown in Figure 6.6), it is evident that this is where the hub height increase has the greatest effect. The regions of negative pressure for the blade while in bottom end of the ABL is smaller for the lower hub heights; the increase is especially significant when comparisons are made between hub heights of 60 m and 100 m along the length of the blade.

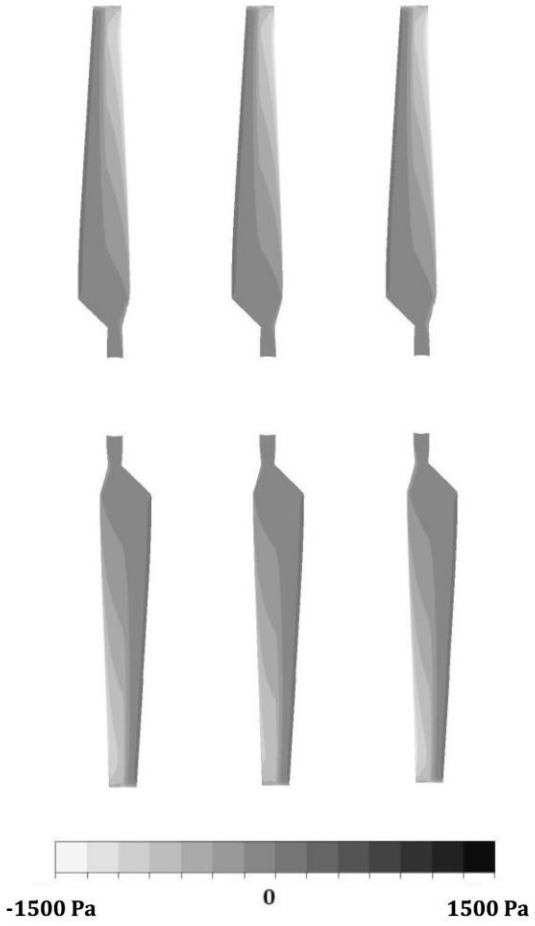


**Figure 6.18 Pressure contour plots on the suction surface for a hub height of 60 m (left), 80 m (middle) and, 100 m (right).**

Noticeably, despite little change in $C_p$ around the blade, because there is more kinetic energy in the wind higher in the ABL power output will also increase. This is the result of higher velocities, which due to a cubic relationship to power means increased performance. Looking at the torque through a single rotation (Figure 6.19) for 100 m

hub height, the periodic curve begins to flatten out more compared with the 60 m case. By adding 40 m to the hub height, the minimum torque produced is on par with the maximum of the lower wind turbine. The average torque production per rotation for: 60 m is $1.05 \times 10^4$ N.m, 80 m is $1.18 \times 10^4$ N.m, and 100 m is $1.28 \times 10^4$ N.m. Overall, there is a maximum increase of 18%. The CP values for each hub height are also similar; showing that efficiency of each does not change a huge amount, which reflects the pressure plots.

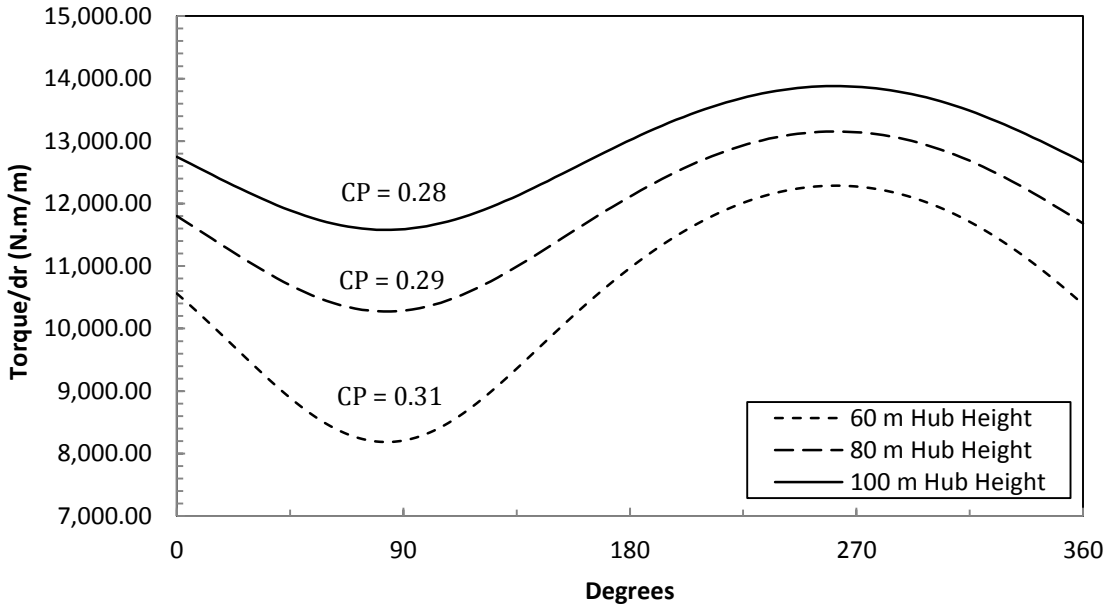


**Figure 6.19 Torque plot for position r/R=0.7 on a single blade throughout one rotation for hub heights of 60 m, 80 m and, 100 m.**

It is clearly shown that even when using exactly the same model of wind turbine that increasing the height has a profound effect on energy production. This change could also be used in conjunction with relocating the turbines to more optimal positions on the terrain.

### 6.3.3 Repowering

As wind farms come to the end of their life cycle and technology advances, so does the ability for newer replacement wind turbines to increase in size, location, and

efficiency. While Blackstone Edge only began generating power in 2013 and, therefore, uses relatively new wind turbines, there is a case for reducing the number of wind turbines from three to two. There are a number of advantages for using fewer wind turbine, for example the capital cost of buying and installing is often less per MW, maintenance requirements are reduced, and simply there are fewer wind turbines disturbing the landscape, which as described throughout Chapter 3 and research carried out by the WindNet [114] research group plays a vital role in gaining planning permission. Placement of wind turbines is also made easier, as it is less likely to result in turbine-turbine interactions for the same plot of land. However, to reproduce the amount of power there is a need for much larger rotors that have their own visual impact problems. The wind turbines chosen for the case study are again those that Nordex currently manufacture, both are rated at 3 MW, have a rotor diameter of 116.8 m, and either have a hub height of 91 m or 120 m.

$C_p$ plots (Figure 6.20) immediately reveal the effects of larger rotors higher in the ABL. For simulating the different wind turbines models, again the same NREL turbine blade has been and scaled to size, as discussed in Section 4.6. However, a result of this is that the aerofoil shape is unlikely to be optimised for the given relative velocity and resulting angle of attack. However, comparisons can still be drawn that make clear that large rotor areas increase performance and thus the energy yield. While the suction peak is reduced when comparing the 2.5 MW and 3 MW wind turbines, there is increased negative pressure over the chord of each blade and pressure recovery happens further down the chord. Toward the tip of the blade, the 3 MW wind turbines have a larger leading edge suction peak, with both curves in the negative pressure region. All of the above results in a far larger integrated area yielding greater lift and

increased torque. The pressure contour plots (Figure 6.21) reflect the larger regions of negative pressure for the 3 MW wind turbines. This is occurring down along the blade as well as around it, with minor improvements with an increased hub height.

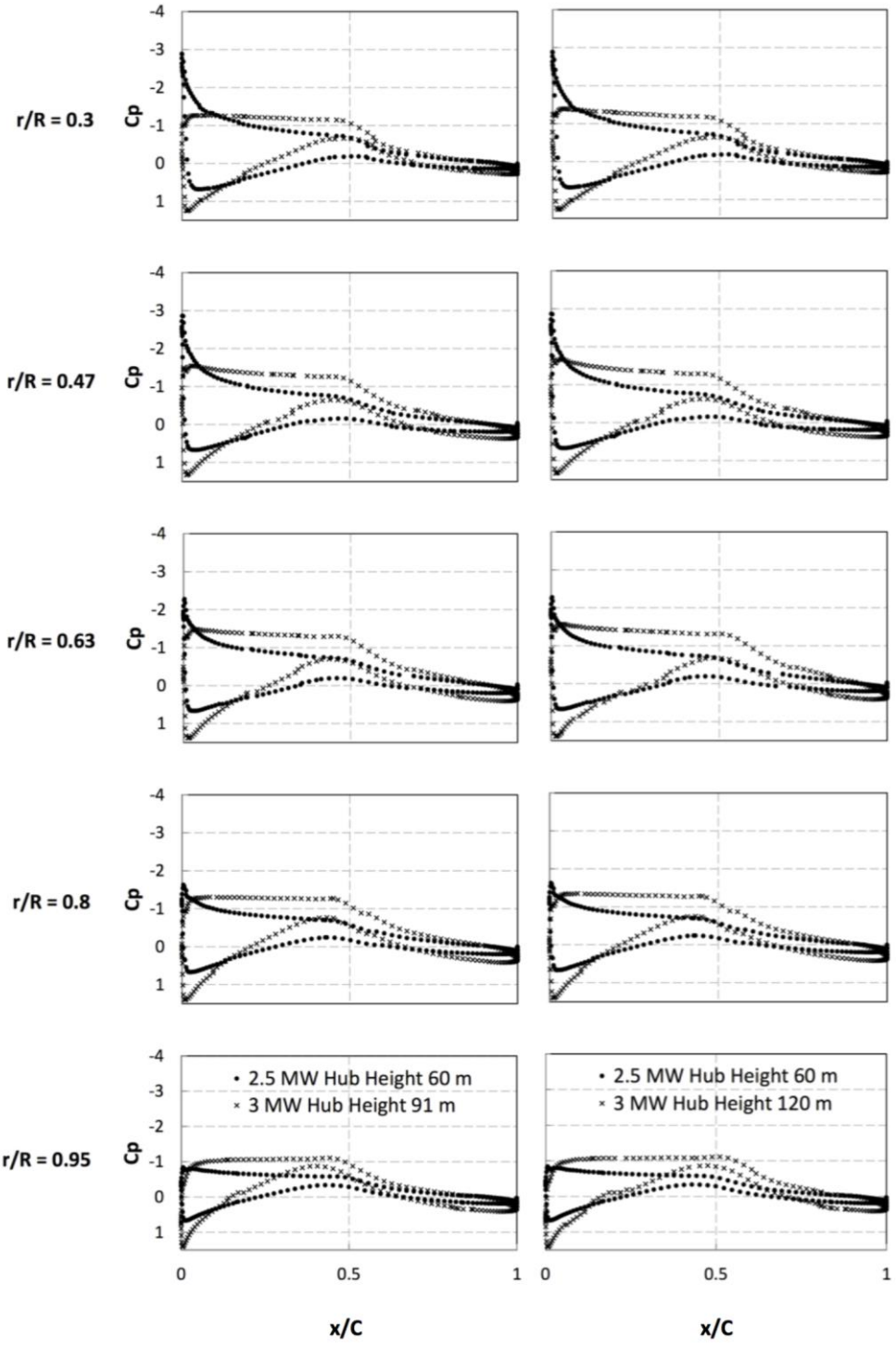


**Figure 6.20 $C_p$ plots along the blade at five radial distances for cases: 2.5 MW at 60 m versus 3 MW at 91 m (left) and, 2.5 MW at 60 m versus 3 MW at 120 m (right).**

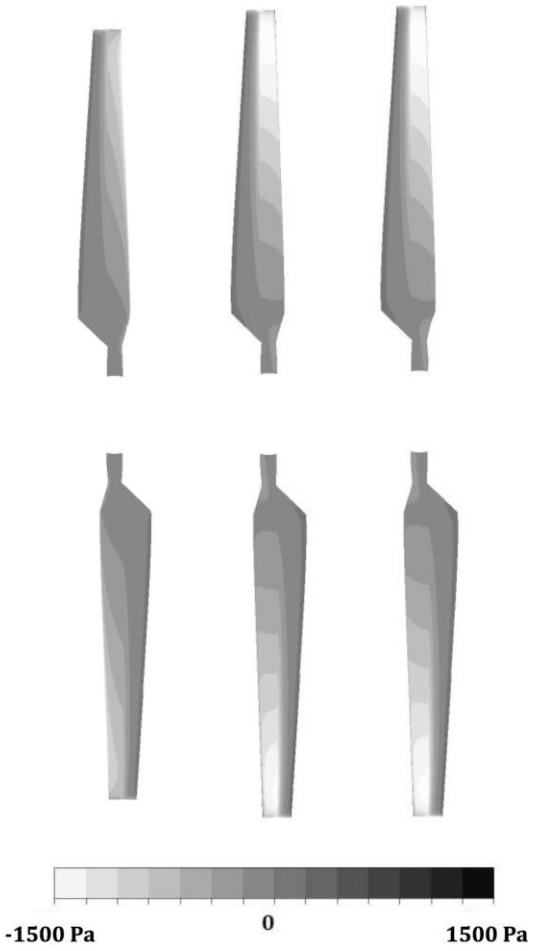


**Figure 6.21 Pressure contour plots on the suction surface for 2.5 MW at 60 m (left), 3 MW at 91 m (middle) and, 3 MW at 120 m (right). Not to scale.**

The torque produced by the larger wind turbines is shown to increase compared to the current installation (Figure 6.22). With the higher hub heights there are fewer periodic fluctuations experienced by the blade due to the nature of the ABL. The average torque production per rotation for each case is: 2.5 MW 60 m is $1.05 \times 10^4$ N.m, 3 MW 91 m is $1.61 \times 10^4$ N.m, and 3 MW 120 m is $1.79 \times 10^4$ N.m. A wind farm consisting of three 2.5 MW wind turbines results in an average torque production per rotation of $3.15 \times 10^4$ N.m. Replacing this with two 3 MW wind turbines can produce more power at $3.22 \times 10^4$ N.m or $3.57 \times 10^4$ N.m, depending on the hub height. Again there is little difference in CP values, which is understandable given that CP is determined by swept

area and the wind energy per unit area, which will all change with different rotor diameters in an ABL. The real changes, as expected, come from the larger swept area that the longer blades offer.

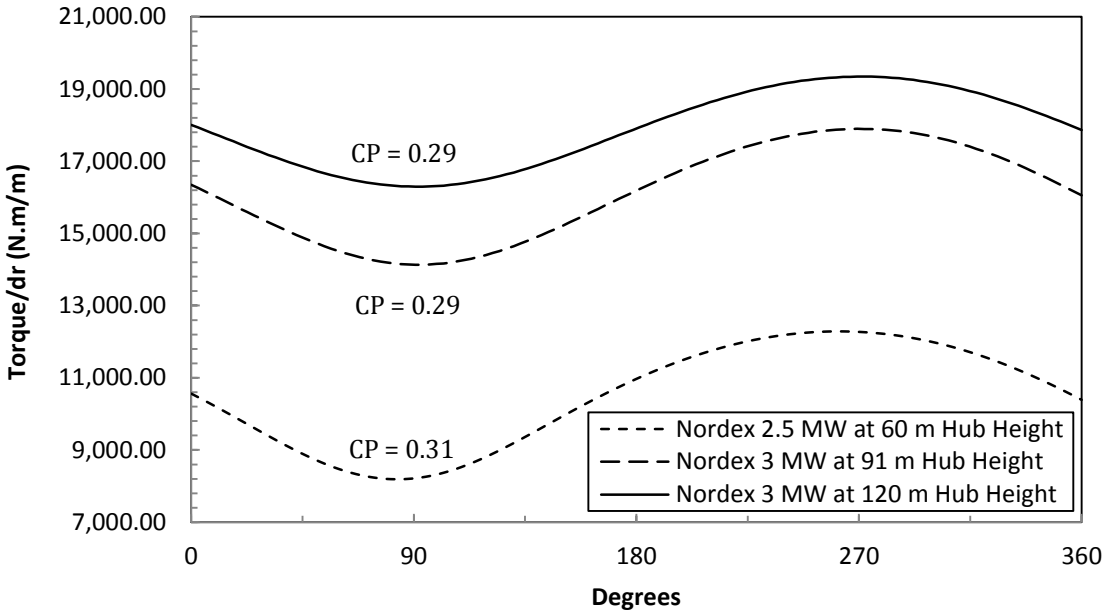


**Figure 6.22 Torque plot for position r/R=0.7 on a single blade throughout one rotation for a 2.5 MW wind turbine at a 60 m hub height and, a 3MW wind turbine at hub heights of 91 m and 120 m.**

The previous suggestions for change have used pre-existing wind turbines in different positions or heights, but by introducing fewer and larger rotors can actually improve power production by up to 12%. The underlying advantage is that placement can be easily optimised and wind conditions, be it direction or speed, are more likely to be in favour with less physical impact on the landscape.

## 6.4 Energy Yield Analysis

An energy yield analysis has been carried out to quantify how relocating the wind turbines or increasing hub height or changing the model entirely effects the viability of Blackstone Edge wind farm. Using normalised site data for the year October 2013 - October 2014, estimations based on performance data discussed

throughout this chapter are applied in order to make comparisons. Table 6.2 provides the total improvement that each suggested case yields in terms of power production over the course of a year. As discussed throughout this chapter, increasing the hub height or repowering the site entirely can have a significant effect on the wind farms ability to perform. The improvement gained from relocating wind turbines is more difficult to determine as there are a number factors that have to be taken into consideration. These include the effect that the wind direction has as a result of placement on the terrain, i.e. losses in wind speed because of elevation drops, wind direction and, turbine-turbine interactions.

**Table 6.2 Total percentage improvement of suggested wind farm cases over current layout.**

| Wind Farm Case | Normalised Power Production | Improvement Over Current Layout (%) |
|---|---|---|
| **Current** | 1 | 0 |
| **Relocating WT2 and WT3** | 1.03 | 3 |
| **Increase Hub Height to 80 m** | 1.11 | 11 |
| **Increase Hub Height to 120 m** | 1.18 | 18 |
| **Repower – 3 MW Hub Height 91 m** | 1.04 | 4 |
| **Repower – 3 MW Hub Height 120 m** | 1.14 | 14 |

As was discussed in Section 6.1 and is shown again in Table 6.3, the performance of both WT2 and WT3 suffered with a southerly wind direction. By bringing forward these two wind turbines so the drop in elevation along the terrain is less when compared to WT1, as well as mitigating any wake interactions between WT1 and WT3, an overall improvement is seen (Table 6.4). WT2 sees the largest improvement as a result of this change as the elevation drop in the current layout is 18 m, and in some months it is predicted that for the same conditions that WT2 would outperform WT1. In general WT3 sees minor differences, except during the periods where the wind direction is

more westerly, because of wake interactions from WT1 have a detrimental effect on performance. In some months WT3 is able to perform on par or slightly better than the benchmark of WT1.

**Table 6.3 Energy yield for each wind turbine for the year October 2013 – October 2014. Each wind turbine has been normalised against WT1 for that month and the average wind direction per month is shown. *WD = wind direction.**

| | Month/Year | | | | | | | | | | | | |
|---|---|---|---|---|---|---|---|---|---|---|---|---|---|
| | **10/ 13** | **11/ 13** | **12/ 13** | **1/ 14** | **2/ 14** | **3/ 14** | **4/ 14** | **5/ 14** | **6/ 14** | **7/ 14** | **8/ 14** | **9/ 14** | **10/ 14** |
| **WT1** | 1.00 | 1.00 | 1.00 | 1.00 | 1.00 | 1.00 | 1.00 | 1.00 | 1.00 | 1.00 | 1.00 | 1.00 | 1.00 |
| **WT2** | 0.90 | 0.95 | 1.05 | 0.92 | 0.97 | 0.98 | 0.95 | 0.92 | 0.94 | 0.95 | 1.01 | 0.96 | 0.92 |
| **WT3** | 0.85 | 0.78 | 1.27 | 0.98 | 0.99 | 0.69 | 0.89 | 0.88 | 0.90 | 0.68 | 0.94 | 0.88 | 0.95 |
| **WD*** | S | SWW | SSW | SW | SW | SSW | S | SSW | S | SW | SWW | S | SW |

**Table 6.4 Normalised improvement against WT1 with relocation of WT2 and WT3.**

| | Month/Year | | | | | | | | | | | | |
|---|---|---|---|---|---|---|---|---|---|---|---|---|---|
| | **10/ 13** | **11/ 13** | **12/ 13** | **1/ 14** | **2/ 14** | **3/ 14** | **4/ 14** | **5/ 14** | **6/ 14** | **7/ 14** | **8/ 14** | **9/ 14** | **10/ 14** |
| **WT1** | 1.00 | 1.00 | 1.00 | 1.00 | 1.00 | 1.00 | 1.00 | 1.00 | 1.00 | 1.00 | 1.00 | 1.00 | 1.00 |
| **WT2** | 0.95 | 1.00 | 1.11 | 0.96 | 1.02 | 1.03 | 1.00 | 0.97 | 0.98 | 1.00 | 1.06 | 1.01 | 0.97 |
| **WT3** | 0.90 | 0.82 | 1.30 | 1.01 | 1.02 | 0.71 | 0.94 | 0.90 | 0.95 | 0.70 | 0.99 | 0.93 | 0.97 |

The improvements from the increase in hub height are easier to quantify as discussed throughout Section 6.3.2, the improvements on a monthly basis for both increases are shown in Table 6.4 and Table 6.5. WT1 is used as a benchmark, therefore, there is a consistent improvement across the year. However, the increase in hub height effectively negates the effects of the drop in elevation that is seen by WT2 as it is now on level or outperforming WT1 in the current situation. Again, WT3 is still struggling to perform as well as the other two wind turbines, but the benefit is still seen with an

increase in energy yield similar to the current WT2. The same pattern is seen with a further increase in hub height to 100 m, but with an overall improvement as expected.

**Table 6.5 Normalised improvement against current WT1 with increased hub height to 80 m.**

| | Month/Year | | | | | | | | | | | | |
|---|---|---|---|---|---|---|---|---|---|---|---|---|---|
| | **10/ 13** | **11/ 13** | **12/ 13** | **1/ 14** | **2/ 14** | **3/ 14** | **4/ 14** | **5/ 14** | **6/ 14** | **7/ 14** | **8/ 14** | **9/ 14** | **10/ 14** |
| **WT1** | 1.11 | 1.11 | 1.11 | 1.11 | 1.11 | 1.11 | 1.11 | 1.11 | 1.11 | 1.11 | 1.11 | 1.11 | 1.11 |
| **WT2** | 1.00 | 1.05 | 1.17 | 1.02 | 1.08 | 1.09 | 1.06 | 1.02 | 1.04 | 1.06 | 1.12 | 1.06 | 1.02 |
| **WT3** | 0.95 | 0.86 | 1.40 | 1.09 | 1.10 | 0.77 | 0.99 | 0.98 | 1.00 | 0.76 | 1.04 | 0.98 | 1.05 |

**Table 6.6 Normalised improvement against current WT1 with increased hub height to 100 m.**

| | Month/Year | | | | | | | | | | | | |
|---|---|---|---|---|---|---|---|---|---|---|---|---|---|
| | **10/ 13** | **11/ 13** | **12/ 13** | **1/ 14** | **2/ 14** | **3/ 14** | **4/ 14** | **5/ 14** | **6/ 14** | **7/ 14** | **8/ 14** | **9/ 14** | **10/ 14** |
| **WT1** | 1.18 | 1.18 | 1.18 | 1.18 | 1.18 | 1.18 | 1.18 | 1.18 | 1.18 | 1.18 | 1.18 | 1.18 | 1.18 |
| **WT2** | 1.07 | 1.12 | 1.24 | 1.08 | 1.14 | 1.16 | 1.12 | 1.09 | 1.10 | 1.13 | 1.19 | 1.13 | 1.08 |
| **WT3** | 1.01 | 0.92 | 1.49 | 1.16 | 1.17 | 0.82 | 1.06 | 1.04 | 1.07 | 0.81 | 1.11 | 1.04 | 1.12 |

Repowering Blackstone Edge wind farm is possible by replacing the three wind turbines that currently inhabit the site with two much larger ones. For this energy yield analysis an assumption that the wind turbine placement would take advantage of the land in a way that interaction between wind turbines is non-existent and the effects of terrain are reduced, i.e. placement of turbines are at higher elevations than currently found with WT2. In the case of Table 6.7 and Table 6.8 the improvements have been normalised against the WT1 and WT2 data from the current layout. While each wind turbine individually is outperforming a single one from the current array, because of reduced numbers the total increase in energy yield is less dramatic.

**Table 6.7 Normalised improvement against current WT1 and WT2 for 3 MW wind turbine with hub height of 91 m.**

| | Month/Year | | | | | | | | | | | | |
|---|---|---|---|---|---|---|---|---|---|---|---|---|---|
| | **10/13** | **11/13** | **12/13** | **1/14** | **2/14** | **3/14** | **4/14** | **5/14** | **6/14** | **7/14** | **8/14** | **9/14** | **10/14** |
| **WT1** | 1.53 | 1.53 | 1.53 | 1.53 | 1.53 | 1.53 | 1.53 | 1.53 | 1.53 | 1.53 | 1.53 | 1.53 | 1.53 |
| **WT2** | 1.39 | 1.46 | 1.62 | 1.41 | 1.49 | 1.51 | 1.46 | 1.41 | 1.43 | 1.46 | 1.54 | 1.47 | 1.41 |

**Table 6.8 Normalised improvement against current WT1 and WT2 for 3 MW wind turbine with hub height of 120 m.**

| | Month/Year | | | | | | | | | | | | |
|---|---|---|---|---|---|---|---|---|---|---|---|---|---|
| | **10/13** | **11/13** | **12/13** | **1/14** | **2/14** | **3/14** | **4/14** | **5/14** | **6/14** | **7/14** | **8/14** | **9/14** | **10/14** |
| **WT1** | 1.68 | 1.68 | 1.68 | 1.68 | 1.68 | 1.68 | 1.68 | 1.68 | 1.68 | 1.68 | 1.68 | 1.68 | 1.68 |
| **WT2** | 1.52 | 1.59 | 1.77 | 1.54 | 1.63 | 1.65 | 1.60 | 1.55 | 1.57 | 1.60 | 1.69 | 1.61 | 1.54 |

The energy yield analysis reveals that the biggest gain in power production is from doubling the hub height, however, as will be discussed in the next Chapter this is likely to effect the visual impact aspect of the planning application. Relocating WT2 and WT3 will also come with planning issues, but public opposition is not going to be one as the visual impact will be mostly the same. A 3% gain in energy yield over a year does not at first appear significant, but it equates to over 600 MWh/year or £55,000.

## 6.5 Summary

The case study analysed in this chapter has applied techniques developed in thesis to inform siting decisions that could improve the energy yield of the Blackstone Edge wind farm. It has been shown that optimising layout on the terrain and with regards to individual wind turbines can have a subtle, but important effect to the efficiency of the wind farm. Increasing the hub height of all the turbines so that the rotor is experiencing

increased wind speeds, and thus producing more power is a relatively simple and effective method of improvement. Finally, by replacing three wind turbines, with two larger and taller ones can reduce costs and increase yield. The potential improvements are vital as it provides an understanding that there is opportunity for land-use to be appropriately utilised and may also open up currently discounted sites. However, as mentioned throughout this thesis, planning policy does not place energy yield at the top of the priority list. The implications that these suggestions have on developers, planners and the general public, as well as the affects it could have on policy change will be discussed in the next chapter.

# 7 DISCUSSION: WIND DEVELOPMENT IMPLICATIONS

## 7.1 Introduction

In the previous chapter proposed variations of Blackstone Edge wind farm were modelled using the techniques developed in the thesis. The case study set out to improve the energy yield of the wind farm above all other considerations, effectively ignoring other potential impacts such as visual, noise, and environmental. In this chapter the design and access statement [111] and environmental statement [115] that both accompany the planning application is analysed and the planning implications of the suggested improvements are discussed.

## 7.2 Wind Development Implications

The developer's design and access statement explains how the wind farm design was reached, and how any requirements and potential adverse impacts have been addressed. Another important document is the environmental statement, from the planners, and sometimes the publics, point of view the environmental statement is

heavily relied upon for decision-making as it provides an appraisal of the potential environmental effects associated with this wind energy development and where by necessary the proposed mitigation measures. It is also worth noting that for Blackstone Edge the design and access statement and the environmental statement are 48 pages and 284 pages in length, respectively. Blackstone Edge wind farm is located between two other wind developments, Royd Moor (Figure 7.1) that is due to be decommissioned in 2018 and, Hazelhead, which was granted planning permission shortly before Blackstone Edge.

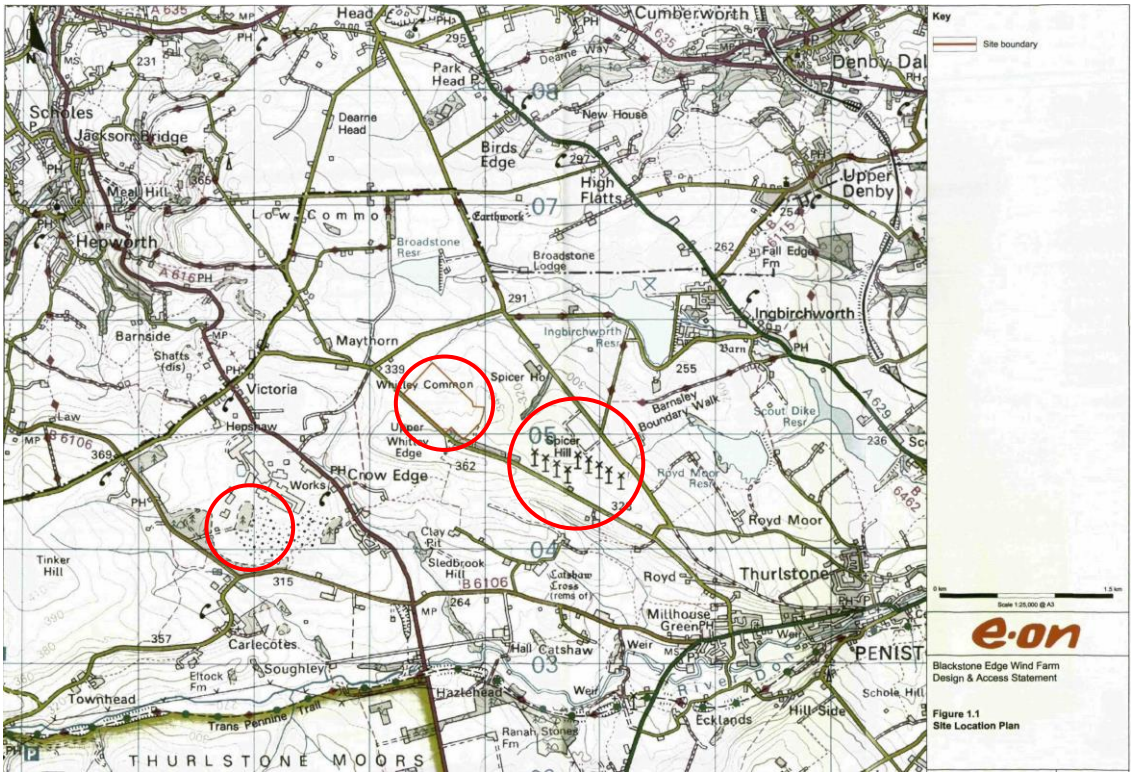


**Figure 7.1 Blackstone Edge wind farm site location plan from the design and access statement, from** [111].

### 7.2.1 Developers

At the time of writing, Infinis owns and operates Blackstone Edge wind farm, however the initial planning application was submitted by and approval awarded to E.ON Energy. The current planning process requires a detailed design and access

statement from wind energy developers when applying for permission. When gaining planning consent developers are required to show conformity with development plan policies, environmental regulation, and any other material considerations relevant to the application.

**Site Selection**

The sites available in Barnsley local authority area are limited as illustrated in Figure 7.2. Choice of sites is constrained by a 600 m housing buffer between wind turbines and houses, as well as nature reserves and parks where there is a presumption against wind turbine development. The methodology employed for site selection puts local environmental considerations at the forefront for both selection and site design, as demonstrated by ensuring sufficient buffer zones from all relevant constraints (Figure 7.3). The wind turbine relocation suggested in the case study (Figure 6.16) would immediately be prevented because of the impact on World War II bomb decoy features and the oversailing (the turbine blades cannot go over site boundaries) 43 m buffer inside the site boundary. The site itself was identified because the landowner approached E.ON as the land was only used for grazing purposes.

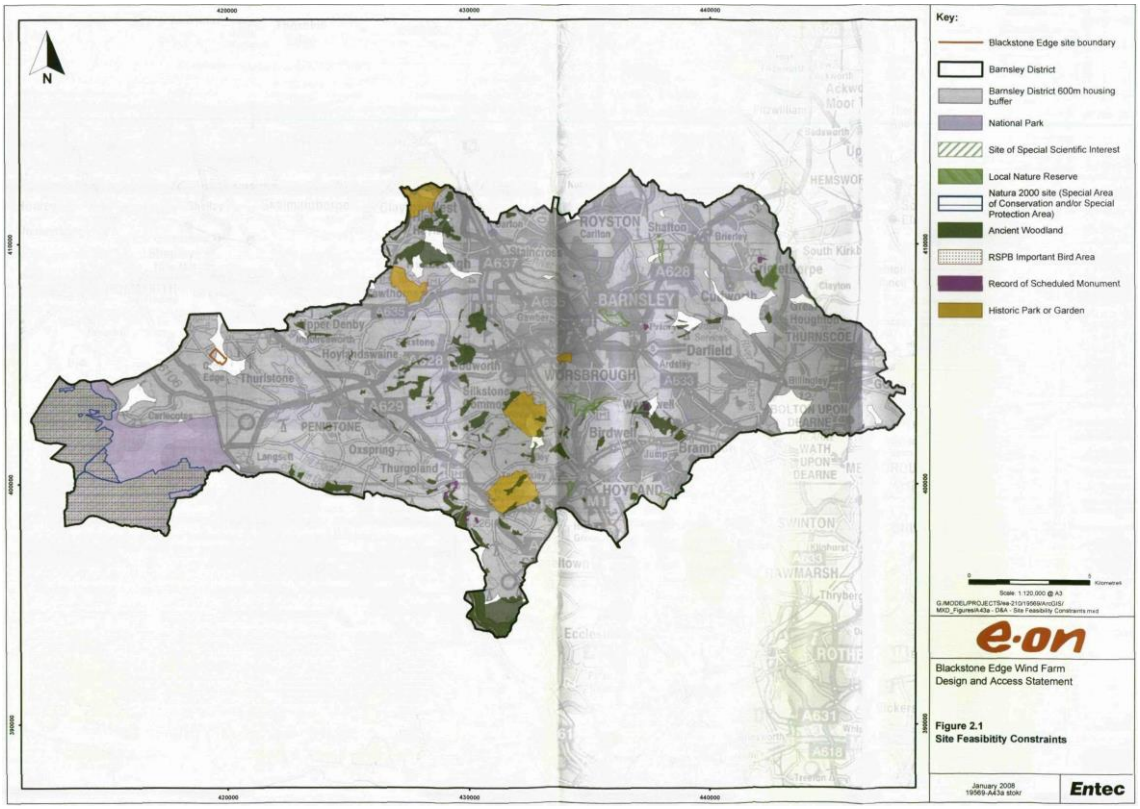


**Figure 7.2 Barnsley site feasibility constrains from the design and access statement, from** [111].

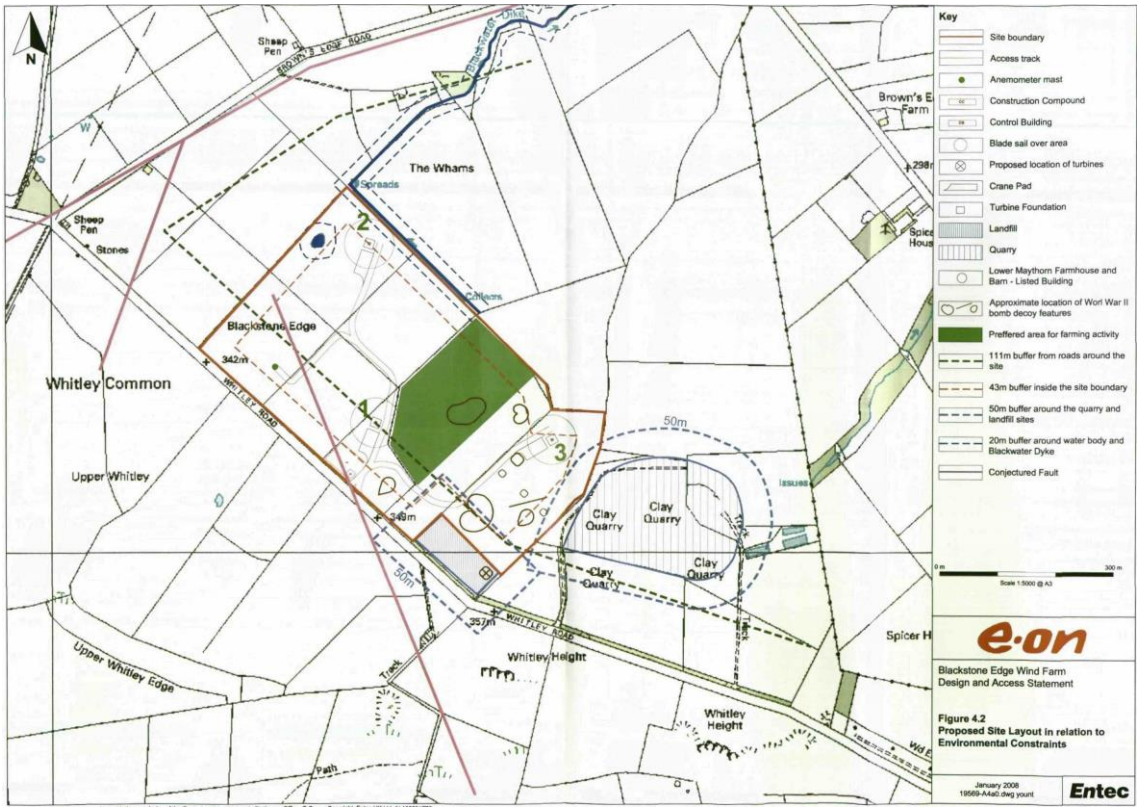


**Figure 7.3 Blackstone Edge wind farm site layout and environmental constraints from the design and access statement, from** [111].

**Design**

Visual amenity is the most important aspect in the determination of wind developments and by carrying out a design consultation it can help the developer identify and resolve any design issues prior to the application. E.ON distributed 3173 newsletters to local residents and held a public exhibition. The wind turbines were in part chosen because of how 'comfortably' they fit into the landscape with regards to the scale and character of the site [115]. For the same reason, it was also concluded to be appropriate to use a similar height to tip as the wind turbines from at the time recently consented Hazelhead wind farm. Another notable justification for choosing this height and size wind turbine is because it is comparable to other existing and approved wind farms in the UK.

**Development**

The development section of the design and access statement is centred on the construction of the wind farm and includes a section about decommissioning the site. This process occurs at the end of the life-cycle of a wind development, normally 25 years and it is an important statement in the planning application as currently all wind farms are temporary installations. At this point, the developer may choose to apply for alternative options such as repowering or extending the site. This is something that the UK industry is now approaching as the first wind farms, including the nearby Royd Moor, are coming to the end of their service lives. It could be argued that developments are required or are at least offered the ability to repower a wind farm with relative ease given the limited land available in the UK, particularly given restricting government policy for onshore wind developments [11].

**Access**

A major limitation to wind developments is access to the proposed site. As already discussed, feasible sites are limited because of buffer distances from residential areas. A result of this is that suitable locations tend to be away from the larger, main roads. Figure 7.4 shows part of the highway accessing planning for transporting wind turbine components. A wind turbine tower is made up from multiple parts; therefore, an increase in hub height as suggested in the case study would not affect the ability for delivery onto site. However, there is an increased difficulty of access if the wind farm were repowered using larger rotors. A wind turbine blade is a single component and is transported in its complete form; a key reason for this is structural integrity and optimising aerodynamics by having no joints along the length of the blade. Currently, each blade is 40 m in length and increasing this to over 58 m as suggested would rule out the site for access reasons.

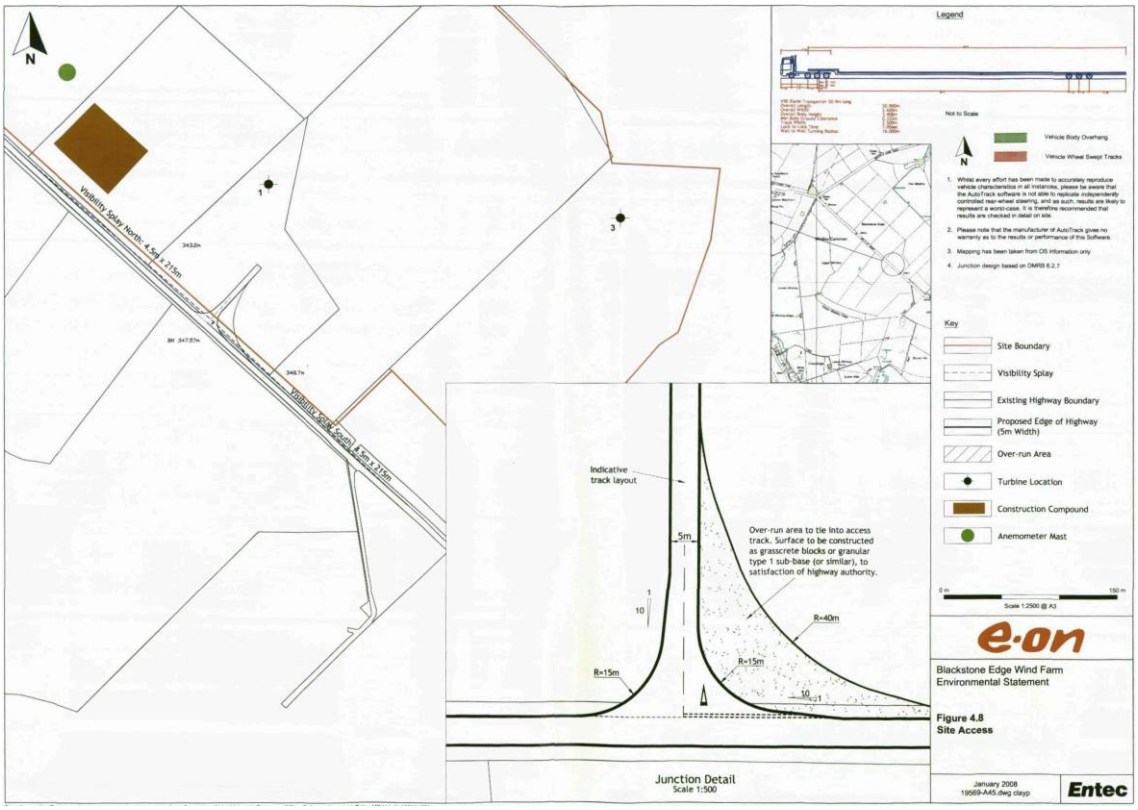


**Figure 7.4 Blackstone Edge wind farm highway access plan from the design and access statement, from** [111].

### 7.2.2 Land-Use Planning

The role of land use regulation is to weigh up the benefits and negative impacts of the development in accordance with planning law and policy guidance, taking into account the perspective of various interests, including developers and residents. Decision making is on a case by case basis and requires detailed assessments of site applications based on UK law and policy for land-use planning controls. For certain kinds of developments, such as wind energy, there is an EU requirement for Environmental Impact Analysis (EIA). The preface to the EIA Statement supplied by E.ON energy reiterates that the site is on farmland, within the Yorkshire Southern Pennine Fringe, between the Peak District moorland and the urban fringes of Barnsley and Huddersfield. The key topics covered in the EIA report are landscape and visual,

noise, ecology, cultural heritage, radar and communications, shadow flicker, socio-economics and community, public safety, and the planning policy context.

As discussed earlier in the thesis, the potential energy yield from a site is now a material consideration [83] in planning decisions. However, contribution of renewable energy generation is a weaker material consideration that impacts on amenity or ecology and it will not outweigh those considerations.

**Planning and Renewables Policy**

In December 2004 the Government Office for Yorkshire and Humber and the Yorkshire and Humber Assembly published a report titled, "Planning for Renewable Energy Targets in Yorkshire and Humber" [116]. In the report two scenarios were developed, the first was potential renewable energy targets for 2010 and the second for 2021. Table 7.1 gives the wind energy targets for each sub region in South Yorkshire for 2010, although there is no change for Barnsley in the 2021 target.

**Table 7.1 South Yorkshire wind energy potential for 2010, from** [116].

| Sub Region | Local Authority | Wind (MW) |
|---|---|---|
| South Yorkshire | Barnsley | 15 |
| | Doncaster | 10 |
| | Rotherham | 10 |
| | Sheffield | 10 |
| | **Total** | **45** |

The implication of this energy target along with the National Planning Policy Framework (NPPF) [83] is that the planning process should be actively encouraging and supporting renewable energy projects. A pro-renewables decision might have allowed for taller hub heights to maximise the potential of the site. However, decision making is

not solely or mainly about maximising renewable energy generation (or developer profit), but about weighing up the positive and negative impacts of development.

**Environmental Impact Assessment**

The EIA for this development is extensive and covers a broad range of topics and for the purpose of this discussion only the implicated issues from the case study will be covered. As discussed in Section 3.2.2, in the original planning application the local authority imposed a maximum noise level that limited the potential energy yield from the wind turbines; the limit was eventually increased accounting for this [93]. If fewer but larger wind turbines were used, as suggested in the case study, the noise characteristics will change. Increasing blade length means that the rotational speed required is less to maintain the optimal tip speed ratio, thus lowering the frequency of the aerodynamic noise produced. However, the decibel level may increase and this would be of issue for planners. The visual impact is the main constraint for wind turbine height and size, as increasing the hub height will result in a higher visual impact to surrounding communities. As the design and access statement suggests (see above) the turbines for Blackstone Edge were selected to minimise landscape impact. It is difficult for a developer to predict the planning response to larger wind turbines, but it is likely that the development would have been rejected with such a design despite the increase in energy yield. Relocating the wind turbines as per the case study suggestion will be limited by the perimeter buffer zone, which will require increasing if larger wind turbines are used. This buffer is imposed to prevent oversailing of the blade, because even though the wind turbine tower would still be located within the site boundaries, the blades could span the buffer.

### 7.2.3 The General Public

E.ON held pre-application consultation with the affected parties. While E.ON do not explicitly say what feedback was offered through consultation, it is said to be useful [115]. Figure 7.5 illustrates the visual impact of Blackstone Edge wind farm by showing the areas where wind turbines and the number of which are visible.

Even though there are only three wind turbines on the site, relocation would have implications for visual impact. The biggest change to both power production and how the wind farm is perceived by the general public would come as a result of repowering i.e. replacing the current three turbines with two larger ones (as discussed in Section 6.3.3). As the case study revealed, this particular design would increase the potential energy yield from the wind farm.

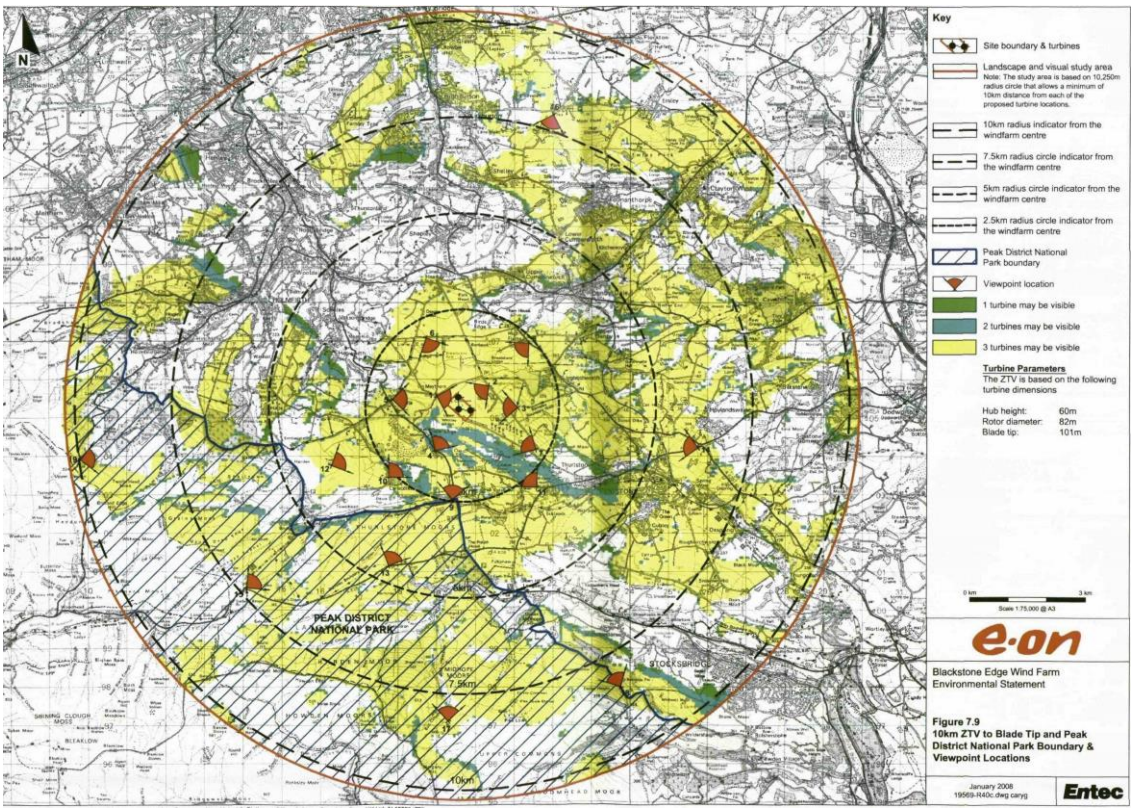


**Figure 7.5 Blackstone Edge wind farm viewpoint locations from the design and access statement, from** [111].

## 7.3 Summary

The need to tackle climate change through renewable energy generation is explicitly stated in UK energy policy with clear targets laid out and local authorities have the power help dictate the development and use of renewable energy. However, onshore wind turbines have not been strongly supported by the UK in national planning policy. Looking beyond national policy support, the research carried out in this thesis has highlighted the difficulties for developers working in a system where there is very little flexibility to reposition wind turbines after permission is granted. In that context predictive modelling could make an important contribution to maximising the energy value of sites where planning permission is likely to be granted.

This chapter has put into context the engineering approach of wind farm design by discussing the implications is has on the three groups involved in renewable projects: developers, local planning authorities responsible for determining planning applications, and the general public. The research aims of this investigation were to determine how wind farm design and location affects the potential energy yield. Detailed CFD simulations illustrated how detrimental wind turbine wake interactions can affect the power output. It was also demonstrated that by altering the layout slightly or increasing the hub heights can be hugely beneficial for energy generation.

# 8 CONCLUSIONS AND RECOMMENDATIONS

## 8.1 Introduction

The energy yield impacts of wind farm design and location has been investigated using experimental and numerical engineering techniques along with studying the planning regime and energy policy. The project was motivated by the challenges faced by onshore wind developments in the UK. This is particularly important in a context of tight regulation and limited scope to alter the design and location of wind turbines after the granting of planning consent. The dimensions of the relationship between planning consent and wind turbine placement has had limited coverage previously. Engineering research on optimising wind turbine performance has been separate from considerations of the process of bringing forward wind turbine developments. A multidisciplinary approach was employed, allowing for a holistic understanding of the subject. To frame the question an analysis of the UK planning consent regime from the 'engineering perspective' of energy yield was carried out, along with a comparison with

how Denmark and Scotland tackle the same problems. The study draws on energy policy analysis, interactions with a wind energy developer, and interviews with local planning officers in England and Scotland.

Switching to the engineering methods, a technique by which the far wake region of a wind turbine can be replicated both experimentally and numerically known as actuator disc theory was used. The method was validated using current literature, wind tunnel experiments, and CFD modelling and simulations. A new hybrid technique that combines actuator disc modelling with a full rotor model was produced to allow for more time and computationally efficient yet detailed analysis of turbine-turbine wake interactions and its effect on wind turbine performance.

The novel hybrid method was used to run a set of reference cases where by the wake produced by an actuator disc is applied as the inlet boundary condition of the full rotor model. Analysis of distances of 5D, 7D, and 10D and configurations of aligned at their centres, offset by half a diameter, and offset by one diameter was carried out. The introduction of a second actuator disc, therefore, making the full rotor the third wind turbine in a column was also simulated for performance comparison.

The new engineering methodology was applied to a case study wind farm using the various techniques developed throughout the thesis. The real-world modelling examined whether and to what extent the techniques would be useful for developers in practice. The implications for developers, planners, and the public from the case study were then discussed. Finally, contributions and potential benefits for energy policy were highlighted.

### 8.1.1 The Practical and Policy Application of Wind Farm Design

An analysis of wind turbine assessment and the planning process was carried out from an engineering point of view. The objective was to understand the implications of planning consent for the design and layout of wind energy developments and how this impacted the potential energy yield from sites. A number of key findings were discovered through the combination of studying energy policy and interviewing planners that specialise in renewable energy projects. While UK energy policy acknowledges the need to tackle climate change through sustainable energy developments, maximising energy yield does not carry much weight in decision making because other material considerations related to amenity and environmental protection are more important in local and national policy. It was shown that developers often having to compromise on wind farm performance because of concerns about the visual and noise impact of development. An overview of the process that wind developers go through in designing a wind farm is given and provides an insight to the challenges met. Comparison with Denmark revealed how national planning policy can support onshore wind. Scotland and Denmark both use land zoning to steer decision making, however, in Scotland this is driven to protect natural heritage rather than maximising energy yield. Denmark also continues to exploit its wind resources by introducing repowering, a process that replaces older wind turbines with fewer, larger and more efficient ones.

### 8.1.2 Actuator Disc Validation: Experimental and Numerical

The actuator disc theory is known for its ability to replicate the far wake region downstream of a wind turbine and has been used extensively in the past. However, from the literature there was a noticeable requirement to validate the numerical simulations with experimental work carried out in the wind tunnel. The experiment used a mesh

disc with a calculated induction factor of 0.34 and measurements were taken downstream at 2D, 4D, 6D, 8D, and 10D, across and either side of the disc. The wind tunnel test section and mesh disc were replicated using CFD, with the boundary conditions set to match the characteristics of the experiment. It was shown that overall the two sets of data matched well, although there were small discrepancies in wake width and centreline velocities. However, these differences were also noted in past literature and it was determined that while the actuator disc technique and current turbulence modelling is not a perfect way to represent the far wake, it was more than acceptable for the purposes of this thesis.

### 8.1.3 Hybrid Actuator Disc – Full Rotor Method

Using the validated actuator disc methodology and combining it with a full RANS CFD turbine model that had been developed within the same research group, a novel hybrid technique was established. The new method uses the actuator disc to produce a simulation where a velocity profile at any point downstream of the wind turbine can be extracted. This slice of the wake is then used as an inlet boundary condition for the full rotor model, which can be placed in any position relative to the inlet boundary condition to simulate lateral offset positions or change in elevation between the two rotors. A time step study was carried out to ensure that the new method converged in a timely manner and it was revealed that a total of eight turbine rotations was required to achieve periodic convergence due to the asymmetrical nature of the incoming wake found in some wind farm layouts. Testing the hybrid method led to the ability to gain detailed aerodynamic data along the wind turbine blades while in the wake of another without the costly computational power and time normally required to yield such results.

In conjunction with the hybrid method, techniques to simulate the atmospheric boundary layer and to model terrain were also developed for the latter case study. The modelling of terrain used Google Maps to export any site that the database currently holds and import it into ICEM for meshing and adding of actuator discs.

### 8.1.4 Ideal and Reference Cases

A set of simulations using the novel hybrid approach was completed to produce a number of references cases that could be compared with an ideal case. The cases chosen applied distances of 5D, 7D, and 10D apart with the two wind turbines being aligned at their centres, offset by half a diameter, and offset by one diameter. The aim here was not to deal in absolute values, but rather to compare and contrast the differences in performance for a number of layouts. The results showed that when two wind turbines are fully aligned the largest drop in performance is observed. As the distances between the two increases, the wake of the first wind turbine is allowed to recover and becomes less detrimental during interactions. Offsetting the second turbine by half a diameter shows an overall improvement, and once again, increasing the downstream distance is beneficial for performance. Conversely, when the turbines are offset by one diameter, an increase in distance results in a fall in performance. This is caused by the diverging wake which outweighs any recovery experienced. By adding a third wind turbines using the same conditions showed an overall improvement across the board when compared with the second row.

### 8.1.5 Case Study: Blackstone Edge

The case study sought to employ the techniques and knowledge gained from the previous chapters to analyse a wind farm that is currently operational and to provide suggestions to improve energy yield from a solely engineering stand point. By

eliminating constraints usually encountered during the planning process, an exercise of maximising land use and energy yield was carried out. It was illustrated that even by using the same wind turbines, placement on the landscape can mitigate turbine-turbine interactions, generating a potential 3% gain in energy yield over a year, which equates to over 600 MWh/year or £55,000. Further to this, increasing the hub height of all turbines resulted in a potential 18% increase in power output, by simply taking advantage of the increased wind speeds higher up in the atmospheric boundary layer. Repowering the site in order to reduce the three wind turbines to only two by using larger rotors and taller hub heights saw a 12% improvement in energy yield. A combination of the suggestions if applied would have made Blackstone Edge wind farm far more viable as a development.

### 8.1.6 Implications and Contributions

The implications of the case study were analysed by discussing whether and how improved modelling of energy yield would have had on the original planning application. Energy yield is unlikely to influence planning decisions because energy yield in itself is not given weight in decision making. However, it is possible that improved energy modelling can have an impact on choices about where to locate wind turbines, because it can help demonstrate for developers the viability of marginal locations, which are amenable to planning consent but might not be exploited. It is also possible that improved modelling could help to build the support of landowners and residents, either by appealing to concerns about climate change or by demonstrating increased financial returns from the development. The appeal to residents is particularly important because minimising opposition is important in planning decisions. It might be the case that robust information about increased energy yields

may have an impact on planning decisions where consent is likely to be given, but constraints are imposed on location of turbines within a site. Energy yield would not sway a planning application decision if the development is unacceptable in planning terms, but it could have an impact on the detailed conditions applied to design and layout.

## 8.2 Recommendations

The research completed in this thesis is the initial stage in combining the subjects of mechanical engineering and land-use regulation to produce an enhanced understanding of wind farm design and the decision making processes that enable their completion.

The hybrid methodology provides detailed wind turbine performance analysis of wake interactions in a time frame that is shorter than current techniques. However, there are still areas where the modelling techniques could be taken a step further to maximise land-use through understanding the finer details of wind turbine placement. As discussed in Chapter 6, a 3% gain in energy yield can equate to a significant increase in both power and income generation. It is possible to develop the method further by employing a similar technique of simulating the far wake region, but downstream of a high fidelity wind turbine model. By applying such a velocity field as the inlet of another rotor would allow for the smaller disturbances in the flow, such as tip vortices, to be resolved and studied. The overall simulation time relative to that experienced through the hybrid methodology developed in this thesis would increase, however, compared to other techniques a saving in computational cost and time could still be achieved. There is potential for the added advantage of it also being applied to other areas such as the structural design of wind turbine blades.

The incoming wind velocity was also kept constant during the running of simulations, while there was variations in height to replicate the ABL, there was no variation over time. In reality, wind turbines experience velocities that fluctuate with time and when simulating wind speeds an average is used from a time period of approximately 10 minutes. The benefit would be a fundamental understanding of how fluctuations effect energy yield, as well as providing considerations of the structural aspect of wind turbine blades under varying wind loads and also the noise it generates.

In addition to the engineering aspect, the thesis has raised questions about the use of the techniques by developers within the planning process. Further case studies on a range of locations and wind farms should be carried out to determine the practical application of the methods developed in this thesis. This would be continued through a follow up study on how the detailed modelling of wind turbine performance affects the attitudes and behaviour of developers, residents, and regulators in relation to wind farm developments. Thereby providing a deeper understanding of how improved informed decision making through enhanced public engagement could help optimise wind farms.

The thesis has also highlighted that it is becoming increasingly difficult to develop onshore wind farms in new locations in the UK, especially with the new government's proposed limitations for onshore wind. As the first operational wind turbines reach the end of their life-cycle, the prospect of extending existing developments and/or repowering them is an increasingly viable option. However, it cannot be assumed that replacing or extending existing wind farms will face less opposition because the site has already been developed. Intensifying an existing site can be just as controversial as a new development, especially if it further increases impacts on visual and noise amenity.

By researching the feasibility and acceptability of such options for the UK then wind farms could continue the growth of renewable energy and energy security.

# REFERENCES


[1] "Where does the UK's electricity come from?," *Good Energy*, 2012. [Online]. Available: http://www.goodenergy.co.uk/blog/articles/2012/11/16/where-does-the-uk-s-electricity-come-from. [Accessed: 26-Mar-2015].

[2] DECC, "UK Renewable Energy Roadmap," 2011.

[3] T. J. Price, "James Blyth - Britain's first modern wind power pioneer," *Wind Eng.*, vol. 29, no. 3, pp. 191–200, 2005.

[4] R. W. Righter, *Wind Energy in America: A History*. University of Oklahoma Press, 1996.

[5] M. O. L. Hansen, *Aerodynamics of Wind Turbines*, Secon. London: Earthscan, 2008.

[6] V. L. Okulov and G. A. M. van Kuik, "The Betz–Joukowsky limit: on the contribution to rotor aerodynamics by the British, German and Russian scientific schools," *Wind Energy*, vol. 15, pp. 335–344, 2012.

[7] ENERGY.GOV, "The Inside of a Wind Turbine," 2015. [Online]. Available: http://energy.gov/eere/wind/inside-wind-turbine-0. [Accessed: 27-Mar-2015].

[8] REN21, "Renewable 2014 Global Status Report," 2014.

[9] D. Sturge, A. While, and R. Howell, "Engineering and energy yield: The missing dimension of wind turbine assessment," *Energy Policy*, vol. 65, pp. 245–250, Feb. 2014.

[10] BERR, "Onshore Wind Energy Planning Conditions Guidance Note," 2007.

[11] C. Barclay, "Consents for Wind Farms - Onshore," 2012.

[12] C. Barclay, "Wind Farms - Distance from housing," 2012.

[13] G. Sterzinger, F. Beck, and D. Kostiuk, "The Effect of Wind Development on Local Property Values," 2003.

[14] S. Ring and B. Webb, "Wind farm noise and private nuisance: a return to common sense," *J. Plan. Environ. Law*, pp. 1–7, 2012.

[15] T. Gjestland, "Background noise levels in Europe," 2008.

[16] National Wind Coordinating Collaborative, "Wind Turbine Interactions with Birds, Bats, and their Habitats: A Summary of Research Results and Priority Questions," 2010.

[17] K. Galbraith, "Ice-Tossing Turbines: Myth or Hazard?," *The New York Times*, 2008. [Online]. Available: http://green.blogs.nytimes.com/2008/12/09/ice-tossing-turbines-myth-or-hazard/.

[18] "Kirklees Council suspends turbine planning applications after blades fly off windmills," *Huddersfield Examiner*, 2013. [Online]. Available: http://www.examiner.co.uk/news/west-yorkshire-news/kirklees-council-suspends-turbine-planning-4961463.

[19] C. Smith, "Fires are major cause of wind farm failure, according to new research," *Imperial College London News*, 2014. [Online]. Available:

http://www3.imperial.ac.uk/newsandeventspggrp/imperialcollege/newssummary/news_17-7-2014-8-56-10.

[20] D. W. Colby, R. Dobie, G. Leventhhall, D. M. Lipscomb, R. J. McCunney, M. T. Seilo, and B. Sondergaard, "Wind Turbine Sound and Health Effects An Expert Panel Review," 2009.

[21] H. Babinsky, "How do wings work?," *Phys. Educ.*, vol. 6, no. 38, pp. 497–503, 2003.

[22] "Drag." [Online]. Available: http://www.pilotfriend.com/training/flight_training/aero/drag.htm. [Accessed: 01-Jul-2015].

[23] O. Reynolds, "An investigation into the circumstances which determine whether the motion of water shall be direct or sinous, and the law of resistance in parallel channels," *Philos. Trans. R. Soc.*, vol. 174, pp. 935–982, 1883.

[24] A. Betz, "Das Maximum der theoretisch moglichen Ausnutzung des Windes durch Windmotoren," *Zeitschrift für das gesamte Turbinenwes.*, no. 26, pp. 307–309, 1920.

[25] L. J. Vermeer, J. N. Sørensen, and A. Crespo, "Wind turbine wake aerodynamics," *Prog. Aerosp. Sci.*, vol. 39, pp. 467–510, Aug. 2003.

[26] M. O. L. Hansen and H. Aagaard Madsen, "Review Paper on Wind Turbine Aerodynamics," *J. Fluids Eng.*, vol. 133, p. 114001, 2011.

[27] P. Gipe, *Wind Power*, 2nd ed. Chelsea Green Publishing, 2004.

[28] M. Raghen and A. M. Ragheb, *Fundamental and Advanced Topics in Wind Power*. INTECH, 2011.

[29] S. J. Schreck and M. C. Robinson, "Horizontal Axis Wind Turbine Blade Aerodynamics in Experiments and Modeling," *IEEE Trans. Energy Convers.*, vol. 22, no. 1, pp. 61–70, 2007.

[30] J. W. Larsen, S. R. K. Nielsen, and S. Krenk, "Dynamic stall model for wind turbine airfoils," *J. Fluids Struct.*, vol. 23, no. 7, pp. 959–982, Oct. 2007.

[31] B. Sanderse, "Aerodynamics of wind turbine wakes Literature review," Energy research Centre of the Netherlands, 2009.

[32] A. Zervos and A. Huberson Hemon, "Three-dimensional free wake calculation of wind turbine wakes," *J. Wind Eng. Ind. Aerodyn.*, vol. 27, no. 1–3, pp. 65–76, 1988.

[33] C. Montavon, I. Jones, C. Staples, C. Strachan, and I. Gutierrez, "Practical Issues in the Use of CFD for Modelling Wind Farms," in *European Wind Energy Conference*, 2009.

[34] L. P. Chamorro, R. E. A. Arndt, and F. Sotiropoulos, "Turbulent Flow Properties Around a Staggered Wind Farm," *Boundary-Layer Meteorol.*, vol. 141, pp. 349–367, Aug. 2011.

[35] L. P. Chamorro, R. E. A. Arndt, and F. Sotiropoulos, "Reynolds number dependence of turbulence statistics in the wake of wind turbines," *Wind Energy*, vol. 15, pp. 733–742, 2012.

[36] F. Porté-Agel, Y.-T. Wu, and C.-H. Chen, "A Numerical Study of the Effects of Wind Direction on Turbine Wakes and Power Losses in a Large Wind Farm," *Energies*, vol. 6, no. 10, pp. 5297–5313, Oct. 2013.

[37] Vattenfall, "Horns Rev 1 Offshore Wind Farm." [Online]. Available: http://corporate.vattenfall.dk/globalassets/danmark/om_os/horns_rev/hornsrevbroschureuk.pdf. [Accessed: 08-Aug-2015].

[38] R. J. A. M. Stevens, D. F. Gayme, and C. Meneveau, "Large eddy simulation studies of the effects of alignment and wind farm length," *J. Renew. Sustain. Energy*, vol. 6, no. 2, Mar. 2014.

[39] E. Son, S. Lee, B. Hwang, and S. Lee, "Characteristics of turbine spacing in a wind farm using an optimal design process," *Renew. Energy*, vol. 65, pp. 245–249, May 2014.

[40] S. McTavish, D. Feszty, and F. Nitzsche, "A study of the performance benefits of closely-spaced lateral wind farm configurations," *Renew. Energy*, vol. 59, pp. 128–135, 2013.

[41] S. Wharton and J. K. Lundquist, "Assessing atmospheric stability and its impacts on rotor-disk wind characteristics at an onshore wind farm," *Wind Energy*, vol. 15, pp. 525–546, 2012.

[42] N. Sezer-uzol and O. Uzol, "Effect of steady and transient wind shear on the wake structure and performance of a horizontal axis wind," *Wind Energy*, vol. 16, pp. 1–17, 2013.

[43] W. Zhang, C. D. Markfort, and F. Porté-Agel, "Wind-Turbine Wakes in a Convective Boundary Layer: A Wind-Tunnel Study," *Boundary-Layer Meteorol.*, Jul. 2012.

[44] J. Meyers and C. Meneveau, "Optimal turbine spacing in fully developed wind farm boundary layers," *Wind Energy*, vol. 15, pp. 305–317, 2012.

[45] P. Carpenter and N. Locke, "Investigation of wind speeds over multiple two-dimensional hills," *J. Wind Eng. Ind. Aerodyn.*, vol. 83, pp. 109–120, 1999.

[46] K. Røkenes and P. Krogstad, "Wind Tunnel Simulation of Terrain Effects on Wind Farm Siting," *Wind Energy*, vol. 12, pp. 391–410, 2009.

[47] X. Yang, K. B. Howard, M. Guala, and F. Sotiropoulos, "Effects of a three-dimensional hill on the wake characteristics of a model wind turbine," *Phys. Fluids*, vol. 27, p. 025103, 2015.

[48] W. D. Lubitz and B. R. White, "Wind-tunnel and field investigation of the effect of local wind direction on speed-up over hills," *J. Wind Eng. Ind. Aerodyn.*, vol. 95, no. 8, pp. 639–661, Aug. 2007.

[49] A. El Kasmi and C. Masson, "Turbulence modeling of atmospheric boundary layer flow over complex terrain: a comparison of models at wind tunnel and full scale," *Wind Energy*, vol. 13, pp. 689–704, 2010.

[50] A. Makridis and J. Chick, "Validation of a CFD model of wind turbine wakes with terrain effects," *J. Wind Eng. Ind. Aerodyn.*, vol. 123, pp. 12–29, Dec. 2013.

[51] R. van Haaren and V. Fthenakis, "GIS-based wind farm site selection using spatial multi-criteria analysis (SMCA): Evaluating the case for New York State," *Renew. Sustain. Energy Rev.*, vol. 15, no. 7, pp. 3332–3340, 2011.

[52] J. R. Janke, "Multicriteria GIS modeling of wind and solar farms in Colorado," *Renew. Energy*, vol. 35, no. 10, pp. 2228–2234, 2010.

[53] S. Grassi, S. Junghans, and M. Raubal, "Assessment of the wake effect on the

energy production of onshore wind farms using GIS," *Appl. Energy*, Jun. 2014.

[54] S. M. J. Baban and T. Parry, "Developing and applying a GIS-assisted approach to locating wind farms in the UK," *Renew. Energy*, vol. 24, pp. 59–71, 2001.

[55] H. Glauert, "Airplane Propellers," *Aerodyn. Theory*, pp. 169–360, 1935.

[56] R. Malki, I. Masters, A. J. Williams, and T. Nick Croft, "Planning tidal stream turbine array layouts using a coupled blade element momentum – computational fluid dynamics model," *Renew. Energy*, vol. 63, pp. 46–54, Mar. 2014.

[57] P. Réthoré, P. Van Der Laan, N. Troldborg, F. Zahle, and N. N. Sørensen, "Verification and validation of an actuator disc model," *Wind Energy*, 2014.

[58] G. España, S. Aubrun, S. Loyer, and P. Devinant, "Spatial study of the wake meandering using modelled wind turbines in a wind tunnel," *Wind Energy*, vol. 14, pp. 923–937, 2011.

[59] R. Mikkelsen, "Actuator Disc Methods Applied to Wind Turbines," Technical University of Denmark, 2003.

[60] R. B. Cal, J. Lebrón, L. Castillo, H. S. Kang, and C. Meneveau, "Experimental study of the horizontally averaged flow structure in a model wind-turbine array boundary layer," *J. Renew. Sustain. Energy*, vol. 2, p. 013106, 2010.

[61] S. Aubrun, P. Devinant, and G. Espana, "Physical modelling of the far wake from wind turbines. Application to wind turbine interactions," in *European Wind Energy Conference*, 2007.

[62] B. Sanderse, S. P. van der Pijl, and B. Koren, "Review of computational fluid dynamics for wind turbine wake aerodynamics," *Wind Energy*, vol. 14, pp. 799–819, 2011.

[63] J. N. Sørensen and A. Myken, "Unsteady actuator disc model for horizontal axis wind turbines," *J. Wind Eng. Ind. Aerodyn.*, vol. 39, pp. 139–149, Jan. 1992.

[64] F. Castellani and A. Vignaroli, "An application of the actuator disc model for wind turbine wakes calculations," *Appl. Energy*, vol. 101, pp. 432–440, Jun. 2013.

[65] G. Crasto, A. R. Gravdahl, F. Castellani, and E. Piccioni, "Wake Modeling with the Actuator Disc Concept," *Energy Procedia*, vol. 24, pp. 385–392, Jan. 2012.

[66] N. Troldborg, J. N. Sørensen, and R. Mikkelsen, "Actuator Line Simulation of Wake of Wind Turbine Operating in Turbulent Inflow," *J. Phys. Conf. Ser.*, vol. 75, p. 012063, Jul. 2007.

[67] M. Shives and C. Crawford, "Mesh and load distribution requirements for actuator line CFD simulations," *Wind Energy*, 2012.

[68] J. N. Sørensen and W. Z. Shen, "Numerical Modeling of Wind Turbine Wakes," *J. Fluids Eng.*, vol. 124, pp. 393–399, 2002.

[69] W. Z. Shen, J. H. Zhang, and J. N. Sørensen, "The Actuator Surface Model: A New Navier–Stokes Based Model for Rotor Computations," *J. Sol. Energy Eng.*, vol. 131, p. 011002, 2009.

[70] R. C. Storey, S. E. Norris, and J. E. Cater, "An actuator sector method for efficient transient wind turbine simulation," *Wind Energy*, vol. 18, pp. 699–711, 2015.

[71] A. Bechmann, N. N. Sørensen, and F. Zahle, "CFD simulations of the MEXICO rotor," *Wind Energy*, vol. 14, pp. 677–689, 2011.

[72] P. Weihing, K. Meister, C. Schulz, T. Lutz, and E. Krämer, "CFD Simulations on Interference Effects between Offshore Wind Turbines," *J. Phys. Conf. Ser.*, vol. 524, p. 012143, Jun. 2014.

[73] P.-E. Réthoré, N. N. Sørensen, A. Bechmann, and F. Zhale, "Study of the atmospheric wake turbulence of a CFD actuator disc model," in *European Wind Energy Conference*, 2009.

[74] A. Bechmann and N. N. Sørensen, "Hybrid RANS/LES applied to complex terrain," *Wind Energy*, vol. 14, pp. 225–237, 2011.

[75] D. Cabezón, E. Migoya, and A. Crespo, "Comparison of turbulence models for the computational fluid dynamics simulation of wind turbine wakes in the atmospheric boundary layer," *Wind Energy*, vol. 14, pp. 909–921, 2011.

[76] E. S. Politis, J. Prospathopoulos, D. Cabezon, K. S. Hansen, P. K. Chaviaropoulos, and R. J. Barthelmie, "Modeling wake effects in large wind farms in complex terrain: the problem, the methods and the issues," *Wind Energy*, vol. 15, pp. 161–182, 2012.

[77] C. A. Montavon, G. Ryan, C. B. Allen, P. Housley, C. J. Staples, and I. P. Jones, "Comparison of Meshing Approaches and RANS Turbulence Models Performance for Flows Over Complex Terrain," in *European Wind Energy Conference*, 2010, no. Figure 2.

[78] D. Mehta, A. H. van Zuijlen, B. Koren, J. G. Holierhoek, and H. Bijl, "Large Eddy Simulation of wind farm aerodynamics: A review," *J. Wind Eng. Ind. Aerodyn.*, vol. 133, pp. 1–17, Oct. 2014.

[79] DECC, "New Feed-in Tariff levels for large-scale solar and anaerobic digestion announcecd today," 2011. [Online]. Available: https://www.gov.uk/government/news/new-feed-in-tariff-levels-for-large-scale-solar-and-anaerobic-digestion-announcecd-today. [Accessed: 22-May-2013].

[80] G. Ellis, R. Cowell, C. Warren, P. Strachan, J. Szarka, R. Hadwin, P. Miner, M. Wolsink, and A. Nadaï, "Planning Theory & Practice Wind Power: Is There A 'Planning Problem'?," *Plan. Theory Pract.*, vol. 10, no. 4, pp. 521–547, 2009.

[81] M. B. Gerrard, "Climate Change and the Environmental Impact Review Process," *Nat. Resour. Environ.*, vol. 22, no. 3, pp. 20–24, 2008.

[82] P. H. Selman, "Learning to Love the Landscapes of Carbon-Neutrality," *Landsc. Res.*, vol. 35, no. 2, pp. 157–171, 2010.

[83] DCLG, "National Planning Policy Framework," 2012.

[84] P. Wintour, "Energy minister John Hayes switches to No 10 role in surprise reshuffle," 2013. [Online]. Available: http://www.guardian.co.uk/politics/2013/mar/28/energy-minister-john-hayes-no10. [Accessed: 22-May-2013].

[85] R. Stevenson, "Environmental Impact Assessment for Wind farms," 2006.

[86] P. Fraser, "Report on Danish Wind Energy Planning & Development," 2002.

[87] S. Chowdhury, J. Zhang, A. Messac, and L. Castillo, "Unrestricted wind farm layout optimization (UWFLO): Investigating key factors influencing the maximum power generation," *Renew. Energy*, vol. 38, pp. 16–30, Feb. 2012.

[88] J. S. González, Á. G. G. Rodríguez, J. C. Mora, M. Burgos Payán, and J. R. Santos, "Overall design optimization of wind farms," *Renew. Energy*, vol. 36, pp. 1973–1982, Jul. 2011.

[89] W. Husien, W. El-Osta, and E. Dekam, "Effect of the wake behind wind rotor on optimum energy output of wind farms," *Renew. Energy*, vol. 49, pp. 128–132, Jan. 2013.

[90] M. Magnusson and A.-S. Smedman, "Air flow behind wind turbines," *J. Wind Eng. Ind. Aerodyn.*, vol. 80, pp. 169–189, Mar. 1999.

[91] I. Troen and E. L. Petersen, *European Wind Atlas*. Commission of the European Communities and Risø National Laboratories, 1989.

[92] DE&C, "Wind Power as a Source of Renewable Energy," 2012.

[93] BC, "Report of the Assistant Director Planning and Transportation to the Planning Regulatory Board," 2009.

[94] BC, "Report of the Assistant Director Planning and Regulatory Services to the Planning Regulatory Board," 2012.

[95] ODPM, "Planning for Renewable Energy A Companion Guide to PPS22," 2004.

[96] LGL, "High Court judge quashes policy on wind turbine separation distances," *Local Government Lawyer*, 2013. [Online]. Available: http://www.localgovernmentlawyer.co.uk/index.php?option=com_content&view=article&id=13870:high-court-judge-quashes-policy-on-wind-turbine-separation-distances&catid=63&Itemid=31. [Accessed: 10-Jun-2013].

[97] SNH, "Strategic locational guidance for onshore wind farms in respect of the natural heritage," 2009.

[98] N. I. Meyer, "Learning from Wind Energy Policy in the EU: Lessons from Denmark, Sweden and Spain," *Eur. Environ.*, vol. 17, pp. 347–362, Sep. 2007.

[99] K. Sperling, F. Hvelplund, and B. V. Mathiesen, "Evaluation of wind power planning in Denmark – Towards an integrated perspective," *Energy*, vol. 35, pp. 5443–5454, Dec. 2010.

[100] S. Ivanell, J. N. Sørensen, R. Mikkelsen, and D. Henningson, "Analysis of Numerically Generated Wake Structures," *Wind Energy*, vol. 12, pp. 63–80, 2009.

[101] J. Whale, C. . Anderson, R. Bareiss, and S. Wagner, "An experimental and numerical study of the vortex structure in the wake of a wind turbine," *J. Wind Eng. Ind. Aerodyn.*, vol. 84, no. 1, pp. 1–21, Jan. 2000.

[102] L. A. M. Danao, "The Influence of Unsteady Wind on the Performance and Aerodynamics of Vertical Axis Wind Turbines," The University of Sheffield, 2012.

[103] ANSYS, "ANSYS Fluent 12.0 User's Guide," 2009.

[104] D. Cabezón, J. Sanz, I. Marti, and A. Crespo, "CFD modelling of the interaction between the Surface Boundary Layer and rotor wake. Comparison of results obtained with different turbulence models and mesh strategies," *Eur. Wind Energy Conf.*, 2009.

[105] ANSYS, "ANSYS Fluent 12.0 Theory Guide," 2009.

[106] D. Sobotta, "The Influence of the Aerodynamics of Small Scale Horizontal Axis Wind Turbines on Turbine Starting using CFD," The Univeristy of Sheffield, 2014.

[107] NREL, "NREL Turbine Specifications," 2000. [Online]. Available: http://wind.nrel.gov/amestest/. [Accessed: 19-Nov-2013].

[108] M. M. Hand, D. A. Simms, L. J. Fingersh, D. W. Jager, J. R. Cotrell, S. Schreck, and S. M. Larwood, "Unsteady Aerodynamics Experiment Phase VI: Wind Tunnel Test Configurations and Available Data Campaigns," 2001.

[109] D. Sturge, D. Sobotta, R. Howell, A. While, and J. Lou, "A hybrid actuator disc - Full rotor CFD methodology for modelling the effects of wind turbine wake interactions on performance," *Renew. Energy*, vol. 80, pp. 525–537, 2015.

[110] S. Al-Yahyai, Y. Charabi, A. Gastli, and A. Al-Badi, "Wind farm land suitability indexing using multi-criteria analysis," *Renew. Energy*, vol. 44, pp. 80–87, Aug. 2012.

[111] E.ON, "Blackstone Edge Wind Farm Design and Access Statement," 2008.

[112] Nordex, "Power Curves Nordex N80/2500," 2010.

[113] "NOABL Wind Map," 2015. [Online]. Available: http://www.rensmart.com/Weather/BERR. [Accessed: 26-Feb-2015].

[114] C. R. Jones, E. Lange, J. Kang, A. Tsuchiya, R. Howell, R. J. Crisp, J. Steel, K. Meade, F. Qu, D. Sturge, and A. Bray, "WindNet: Improving the impact assessment of wind power projects," *AIMS energy*, vol. 2, no. 4, pp. 461–484, 2014.

[115] E.ON, "Blackstone Edge Wind Farm Environmental Statement Volume 1: EIA Assessments," 2008.

[116] Y&HA+GOYH, "Planning for Renewable Energy Targets in Yorkshire and Humber," 2004. [Online]. Available: http://www.lgyh.gov.uk/dnlds/Planning for Renewable Energy Targets Vol 2.pdf. [Accessed: 01-Apr-2015].